

**EUROPEAN SCHOOL OF MOLECULAR MEDICINE**  
**NAPLES**  
**UNIVERSITA' DEGLI STUDI DI NAPOLI "FEDERICO II"**  
**Ph.D. in Molecular Medicine –Cycle XXII**

**Human Genetics**



**Human aldolase C:  
gene transcriptional regulation and protein functional role**

**Tutor:**

Prof. Francesco Salvatore

**Internal Supervisor:**

Prof. Margherita Ruoppolo

**External Supervisor:**

Prof. Dean Richard Tolan

**Coordinator:**

Prof. Francesco Salvatore

**Ph.D. student:**

Dr. Laura Serio

**Academic Year: 2009-2010**

## **INDEX**

<b>ABSTRACT</b>	p. 5
<b>1. INTRODUCTION</b>	
1.1 Aldolase A, B and C genes	p. 7
1.2 Aldolase C gene structure in mammals	p. 8
1.3 Aldolase C gene structure in inferior organisms	p. 9
1.4 Human aldolase C gene promoter: in vivo and in vitro studies on transcriptional regulation	p. 10
1.5 Aldolase C: messenger and protein expression in mammalian Central Nervous System (CNS)	p.19
1.6 Aims	p.26
<b>2. MATERIALS AND METHODS</b>	
2.1 Materials	p.27
2.2 Generation of reporter constructs and site-directed mutagenesis	p.28
2.3 Cell cultures	p.29
2.4 Transient transfection and CAT assay	p.29
2.5 Nuclear extracts and Electro Mobility Shift Assays	p.31
2.6 Chromatin Immunoprecipitation (X-ChIP)	p.31
2.7 Western Blot	p.35
2.8 Immunofluorescence assays	p.36
2.9 Cloning and vectors preparation for microinjection and production of transgenic mice lines	p.37
2.10 Generation and identification of transgenic mice	p.39

2.11 $\beta$ -galactosidase assay	p.40
2.12 Immunohistochemistry	p.40
2.13 RNA extraction, Reverse Transcription Polymerase Chain Reaction (RT-PCR)	p.41
2.14 Real-Time Quantitative PCR (RT-qPCR)	p.42
2.15 Site-directed Mutagenesis by PCR	p.44
2.16 Cloning and expression of chimeric aldolase A/C and C/A genes	p.50
2.17 Affinity chromatography and recombinant aldolases purification	p.51
2.18 Steady-state Kinetics	p.52
2.19 Preparation of construct for aldolase C - conditional knockout	p.53
2.20 From electroporation of ES cells to microinjection into mouse blastocysts: chimera mouse	p.53
2.21 Screening of F1 mice by PCR	p.54

### **3. RESULTS**

#### **3.1 Transcriptional regulation of human aldolase C gene during NGF-induced neuronal differentiation in PC12 cells**

3.1.1 Analysis of aldolase C messenger expression during NGF-induced neuronal differentiation	p.56
3.1.2 Identification of human aldolase C gene promoter region responsive to NGF	p.59
3.1.3 Identification of a transcriptional factor binding in the distal promoter region of human aldolase C gene responsive to NGF	p.62
3.1.4 Identification of USF1 as transcriptional factor binding to the distal region of human aldolase C gene promoter responsive to NGF treatment by chromatin immunoprecipitation (CHIP) assay	p.64

3.1.5 Functional analysis of USF1 binding to element E in distal region of human aldolase C gene promoter	p.67
3.1.6 Subcellular localization of USF1 in PC12 cells treated with NGF	p.69
<b>3.2 Transcriptional regulation of human aldolase C gene during development in transgenic mice</b>	
3.2.1 Expression analysis of endogenous aldolase C and LacZ transgene messengers in pAldC-2500-LacZ transgenic mice during development	p.73
3.2.2 Identification of human aldolase C gene promoter region(s) regulating $\beta$ -galactosidase activity in restricted areas of adult transgenic mice CNS	p.78
3.2.3 Expression analysis of endogenous aldolase C and recombinant $\beta$ -galactosidase proteins in brain and cerebellar sections of transgenic mice	p.84
3.2.4 Expression analysis of LacZ transgene messenger in adult pAldC-1580-LacZ, pAldC-1464-LacZ and pAldC-2336-LacZ transgenic mice	p.89
<b>3.3 Functional role of recombinant aldolases</b>	
3.3.1 Production of aldolase chimers	p.92
3.3.2 Evaluation of kinetic parameters of chimeric aldolases A/C and C/A	p.95
<b>3.4 Aldolase C Knockout mice</b>	
3.4.1 Screening of chimeric mice	p.99
<b>4. DISCUSSION</b>	p.102
<b>5. REFERENCES</b>	p.110

## ABSTRACT

Aldolase C is the brain-specific aldolase isoenzyme. In the human brain, aldolase C messenger and protein are expressed in a stripe-like pattern in the Purkinje cells of the cerebellum, in the inferior olives and in the Goll and Burdach nuclei of the posterior horn in the spinal cord. Notwithstanding numerous studies have been conducted on aldolase C transcriptional regulation, promoter regions governing brain- and cell-specific expression in human are not yet precisely known.

We analysed transcriptional regulation of human aldolase C gene through *in vitro* and *in vivo* systems. We previously demonstrated that cAMP increased human aldolase C gene expression in PC12 cells through NGFI-B binding to element D in the distal promoter region of the gene. Here we demonstrate that NGF up-regulates human aldolase C gene expression in PC12 cells. We identified the element E in the distal promoter region as responsive to NGF treatment and demonstrated that USF1 binds to this region thus mediating transcriptional up-regulation. We also analyzed the transcriptional regulation of the human aldolase C gene using transgenic mice as *in vivo* model. We found that the construct pAldC2500-LacZ, containing the cis-elements A, B, C, D and E in the promoter region, was able to direct specific, high levels AldC/LacZ hybrid messenger expression in the brain of transgenic mice, as well as stripe-like expression in the Purkinje cells of the cerebellum. Construct pAldC1500-LacZ, containing elements A, B and C in the proximal promoter region, plus element D of the distal region, was able to direct low levels brain-specific AldC/LacZ and also the stripe-like expression in the Purkinje cell layer. Here we analysed three new transgenic mice lines carrying constructs containing different deleted promoter regions of human aldolase C gene fused to LacZ reporter gene, in order to further point out the role of distal and proximal regions in governing brain-specific and stripe-like expression *in vivo*. Our results indicate that proximal region contains all the elements

required for low-levels, stripe-like expression of aldolase C in the cerebellar Purkinje cell layer; the distal region is responsible for high-levels, stripe-like expression in the cerebellum and in distinct brain areas.

The second part of this thesis focuses on the functional role(s) of aldolase C protein. To improve our knowledge on the canonical glycolytic role of aldolase C, linking isozyme structure with function, we produced recombinant aldolases by swapping Isozymes Specific Residues (ISRs) from aldolase A to C and viceversa and we analysed their kinetic properties. Finally, to shed light on the putative additional functions we have long intended aldolase C exert, we started a project aimed to the production of a conditional aldolase C knockout mouse.

## 1. INTRODUCTION

### 1.1 Aldolase A, B and C genes

The glycolytic enzyme fructose-1,6-bisphosphate aldolase catalyzes the aldol fission of fructose-1,6-bisphosphate (FBP) to dihydroxyacetone phosphate (DHAP) and glyceraldehyde- 3-phosphate (G3P) (1, 2).

There are two distinct classes of aldolase: class I aldolases, which are present in animals and higher plants and that use covalent catalysis through a Schiff based intermediate; and class II aldolases, which are present in most bacteria and fungi and that require divalent metal cations as cofactor. The aldolase in mammals belongs to class I enzymes (1, 2).

In mammals there are three different isoforms of aldolase, which are encoded by three different genes, aldolase A (AldoA), aldolase B (AldoB) and aldolase C (AldoC), located, in humans, on chromosome 16 (AldoA), 9 (AldoB) and 17 (AldoC) (3-6).

About 67% nucleotide sequence identity has been found between aldolase A and aldolase C, 63% between aldolase C and B and 68% between A and B. The non-coding sequences don't show any significant sequence identity (2,7-9).

These genes derive from a duplication of one ancestral gene and produce three different proteins with a high sequence identity, especially in the N-terminus. The C-terminal portion of the proteins makes the difference in terms of catalytic and antigenic properties (7, 10).

Aldolase A is ubiquitous but is predominantly expressed in muscle and red blood cells. Mutations in this gene have been associated to haemolytic anaemia and myopathy (3, 11, 12).

Aldolase B is involved in the exogenous fructose utilization pathway in the liver; mutations in this gene cause fructose-intolerance, a hereditary disorder (1, 5, 13-15).

Aldolase C is selectively expressed in adult mammalian brain, particularly in CA3 hippocampal neurons, in pontine and cerebellar olives, in Goll and Burdach nuclei, in the posterior horn of spinal cord, and overall in the Purkinje cells of cerebellum (16).

The expression of the three proteins is regulated during mammals development. In fetal tissues aldolase A is the predominant isoform together with the aldolase C. After the birth, aldolase A levels decrease to almost disappear in the liver, where aldolase B becomes the predominant isoform, and continues to be expressed in all other tissues (2, 5, 7-9, 17, 18). Aldolase C rapidly decreases in all tissues except for the brain, where it reaches maximal expression levels in the adult.

The aminoacidic sequences of the mammalian isozymes are highly conserved, exhibiting 81% sequence identity between aldolases A and C (19). Aldolase B is slightly more divergent with ~70% sequence identity to both aldolases A and C (20). Consistent with this sequence similarity, isozymes A and C exhibit comparable kinetic properties. Aldolases A and C have evolved to perform the glycolytic reaction, FBP cleavage, more efficiently than aldolase B as demonstrated by a 20–30-fold higher  $k_{cat}$  (10, 21). Conversely, aldolase B cleaves F1P three times more efficiently than aldolase A or C (10). In addition, aldolases B and C demonstrate a 10-fold lower  $K_m$  for glyceraldehyde 3-phosphate and dihydroxyacetone phosphate, implying that they have evolved to perform the gluconeogenic reaction, FBP synthesis, more efficiently than aldolase A (22).

## 1.2 Aldolase C gene structure in mammals

The aldolase C gene is present, in mammals, as a single copy per haploid genome and it is localized on chromosome 17 in humans. It spans 5198 bp, is shorter than the aldolase A and B genes and consists of nine exons: the first is a non-coding exon; the second contains 12 bp of the 5'-noncoding region versus 20 bp in the aldolase A gene and 10 bp in the aldolase B gene. The coding region is constituted by 1092 bp (364 aa); length and position



of coding exons are conserved in human aldolase A and B genes. A consensus polyadenylation signal is present in exon IX. In addition, in the human aldolase C gene, all the introns after exon I are shorter than those of human aldolase A and B genes (3, 4, 19, 20, 23, 24).

Aldolase C gene is present on chromosome 10 of rat and on chromosome 11 of mouse. Both are constituted by the same number of exons of the homologous human gene and show a first non-coding exon of different length.

Nucleotide sequence of aldolase C gene coding region is conserved among species, exhibiting 96% sequence identity between human and rat and 98% sequence identity between human and mouse (17).

### **1.3 Aldolase C gene in inferior organisms**

Aldolase C is highly conserved among species and during the evolution. It is expressed not only in mammals like mouse, rat, rabbit and human as an independent gene, but also in inferior organisms like lower vertebrates *Xenopus laevis*, *Lampreda* and *Goldfish* and invertebrates *Drosophila melanogaster* and *Caenorhabditis elegans* (2, 6, 8, 9, 17, 25-37).

*Xenopus laevis* shows three different genes, localized on three different chromosomes, coding for aldolase A, B and C. Aldolase C gene structure is very similar to that of human and rat. It is composed by 9 exons and encodes for a 363 aminoacids protein. Aldolase C is expressed since the first embryonal stages and, in the adult, is mainly present in the brain, heart and ovary (25, 26).

*Lampreda* shows two distinct genes coding for two proteins, muscular and non-muscular. The first type shows intermediate characteristics between superior vertebrates aldolase A and C and is expressed in skeletal muscle, heart and brain. The second type is equivalent to aldolase B of superior vertebrates and is mainly expressed in the liver (28, 29).

*Goldfish* shows one independent gene coding for a brain-specific enzyme that seems to be

very similar to aldolases A and C of vertebrates rather than aldolase B. *Goldfish* aldolase and human aldolase A, B and C exhibit 83%, 68% and 85% sequence identity, respectively (30).

In invertebrates there are two types of aldolase: neuronal and non-neuronal, which originate from a single gene by alternative splicing. The three different aldolase isoforms ( $4\alpha$ ,  $4\beta$  and  $4\gamma$ ) described in *Drosophila melanogaster* arise from a single gene by alternative splicing of the last exon (exon 4) at the 3'-end (32). In the invertebrate *Caenorhabditis elegans*, two different coding sequences (cds) have been described: Ce-1 which shows 60% sequence identity with aldolase B and encodes for a non-neuronal aldolase mainly expressed in the gut and pharynx; and Ce-2, which shows about 70% sequence identity with vertebrate aldolases A and C and is expressed in neural and muscular tissues (neuronal aldolase) (37, 38).

The high conservation of aldolase C gene during the evolution and its expression limited to specific tissues in which aldolase A is co-expressed, suggest the hypothesis of an additive role beside that of glycolytic enzyme.

#### **1.4 Human aldolase C gene promoter: *in vivo* and *in vitro* studies on transcriptional regulation**

Like other brain-specific genes, aldolase C lacks a normal TATA box and a CAAT box is present far upstream from its expected position. Multiple transcriptional start sites are present in the proximal promoter segment with a major one located -1340 bp upstream from the methionine initiation codon. Furthermore, a 100 bp GC-rich region is present just upstream from the major transcriptional start site in the mouse, human and rat aldolase C genes (8, 29, 39, 40-42).

Two promoter regions are required for complete aldolase C gene expression in cell lines and in transgenic mice (39-42, 43, 44). In the human aldolase C gene promoter, the

proximal region, spanning from -164 bp to the major transcriptional start site (+1), has high sequence identity with the same region of the mouse and rat genes (69%). In this region three *cis*-acting elements, called A, B and C, have been characterized (40) (see Fig.1, panel A). Elements A and B are GC-rich sequences constituted by overlapping motifs that bind Sp1 or Sp1-like transcriptional factors and/or members of the Krox20/Krox24 family when challenged *in vitro* with nuclear extracts from neuroblastoma cell lines (SKNBE), rat pheochromocytoma cells (PC12) or from rat brain (40, 41, 43, 44). The A and B elements in the proximal gene promoter are required to direct low-level, neuronal-specific expression of human aldolase C-CAT chimeric constructs *in vitro*, as we demonstrated in SKNBE and PC12 cells (40, 43, 44). These elements are also required to direct low-level, neuronal specific expression of rat aldolase C-CAT chimeric constructs *in vitro* and *in vivo* (45-48). Like elements A and B, element C also binds Sp1 proteins but it seems redundant, being not required for transcriptional activation of the human and rat genes *in vitro* (39-41) (see Fig. 1, panel A).

The distal promoter region of the human aldolase C gene spans from -164 to -1200 bp with respect to the major transcriptional start site. This region differs among human, rat and mouse aldolase C genes (about 23% sequence identity between rat and human genes). Different *cis*-elements of this region have been characterized through *in vitro* and *in vivo* studies, using cell lines and transgenic mice brain (41, 43, 44, 48-51). The human aldolase C gene distal promoter region, similarly to rat gene, has been split into two functionally different regions: a more proximal distal region and a far distal region. The more proximal distal region (of about 236 bp), spanning from -164 to -400 bp, contains elements that increase by 2.5-fold the transcription of chimeric aldolase C-CAT construct in SKNBE cell line with respect to constructs lacking this region (43, 50) In this region, our group characterized the "element D" (-203/-196 bp) (see Fig. 1, panel A) containing the AGGTCA motif (43, 44, 50). We demonstrated that this element binds the transcriptional

activator NGFI-B, a member of a thyroid/steroid/retinoid nuclear receptor gene family (52, 53). The binding of NGFI-B to the distal promoter region of the human aldolase C gene up-regulates the transcription of chimeric aldolase C-CAT constructs in SKNBE cells and mediates cAMP-induced transcriptional activation of aldolase C mRNA in PC12 cells (43, 44)

The human aldolase C gene is the second gene after mouse 21-OH-ase (54) that has been shown to be activated by NGFI-B. The AGGTCA motif is absent from the rat aldolase C gene distal promoter region. Thus far, there is no evidence of transcriptional activation of mouse or rat aldolase C gene mediated by NGFI-B or cAMP. This supports the hypothesis that the transcriptional regulation of the aldolase C gene differs between human and rat brain (50). Functional studies, conducted on transgenic mice, demonstrated that large genomic fragments (about 5-6 kb) of rat aldolase C gene, are required to direct sustained central nervous system-specific (CNS) expression of the chimeric aldolase C-CAT reporter gene in transgenic mice (45-48). In particular, the distal region of the rat aldolase C gene promoter was found to contain two fragments: an upstream activating sequence (about 0.6 kb) spanning from -115 to -800 bp, and a far upstream activating sequence spanning from -0.8 kb to -5.5 kb (see Fig. 1, panel B). Conserved DNA-binding sequences for the transcriptional brain-specific activators Brn-1 or Brn-2 and Pax-6, belonging to POU homeoproteins, are scattered within the upstream activating sequence. Some of these features are conserved in human aldolase C gene far distal promoter region. The presence of DNA-binding sequences for the neuronal-specific transcriptional activators Brn-1 and/or 2 or other POU homeoproteins are typical features of the promoter regions of many neuronal genes (55-58). The transcription of most of neuronal-specific genes seems to result from a functional synergy between the distal and proximal regulatory elements present in the promoter regions. In fact, like other neuron-specific genes, high levels of expression of rat aldolase C-CAT constructs in transgenic mice brain requires the

synergism between the 0.6 kb fragment, located in the upstream activating sequence of the distal region, the 3.8 kb fragment, located in the far upstream activating sequence, and the proximal promoter region, a fragment of about 115 bp, located just upstream from the major transcriptional start site. (Fig.1, panel B) (51). Analysis of transgenic mice obtained using a larger rat genomic fragment of about 13 kb, containing 6 kb of the 5'-flanking region and 3 kb of the 3'-flanking region and LacZ as gene reporter, demonstrated that this construct contains all the elements sufficient to direct high levels, CNS-specific expression of LacZ (59). In contrast, Walther et al. (60) using a construct containing 1.5 kb of the 5'-flanking region of the mouse aldolase C gene and 500 bp of the 3'-flanking region fused to LacZ reporter gene, demonstrated that LacZ expression was present only in non-neuronal cells, namely astrocytes and pial cells. The same authors, using a larger fragment of the mouse aldolase C gene, containing an additional 3 kb of the 5'-flanking region, identified an enhancer element specific to direct LacZ expression in Purkinje cells in a fragment spanning from -2.7 kb to -3.6 kb in the promoter region (59-61). All these findings suggest that the CNS-specific expression of aldolase C differs between the mouse and rat genes. Moreover, these studies failed to identify the promoter regions involved in the expression of aldolase C in restricted areas of brain.

We conducted an *in vivo* study on transgenic mice in order to identify human aldolase C gene promoter regions involved in brain-specific transcriptional regulation (49, 50). We used two different constructs containing deleted regions of the human promoter:

- pAldC-2500-LacZ, which contains 1.2 kb of the human aldolase C promoter region (complete promoter region analysed so far), the first intron and the second exon up to the methionine (1.3 kb), fused to the methionine of LacZ;
- pAldC-1500-LacZ, which contains 40 bp of the more proximal distal promoter region of the human aldolase C gene, the proximal promoter region (164 bp), the first intron and the second exon up to the methionine (1.3 kb), fused to LacZ.

We found that the construct pAldC-2500-LacZ was able to direct high-level, brain-specific and stripe-like expression of LacZ in adult transgenic mice thereby mimicking the endogenous messenger expression (49, 50) (Fig. 2, A-E).

The construct pAldC-1500-LacZ was able to direct low levels of brain-specific expression of LacZ in transgenic mice (49, 50). This construct, containing a short promoter fragment of human aldolase C gene (164bp), differently from the proximal promoter region of mouse and rat aldolase genes, is able to direct low- levels, stripe-like expression of LacZ in the Purkinje cell layer of the cerebellum (Fig. 2, F-G). Moreover, differently from mouse and rat genes, the fragment spanning from -164 bp to -1200 bp (distal region) is able to direct high levels of LacZ expression in the hippocampal CA3 neurons.

We concluded that the transcriptional regulation of the aldolase C gene in the brain and cerebellum differs among rat, mouse and human genes and that the 2500 bp promoter fragment of human aldolase C gene contains all the elements necessary and sufficient to drive brain-specific, regional-specific and cell-specific expression in transgenic adult mice brain and cerebellum (49, 50).

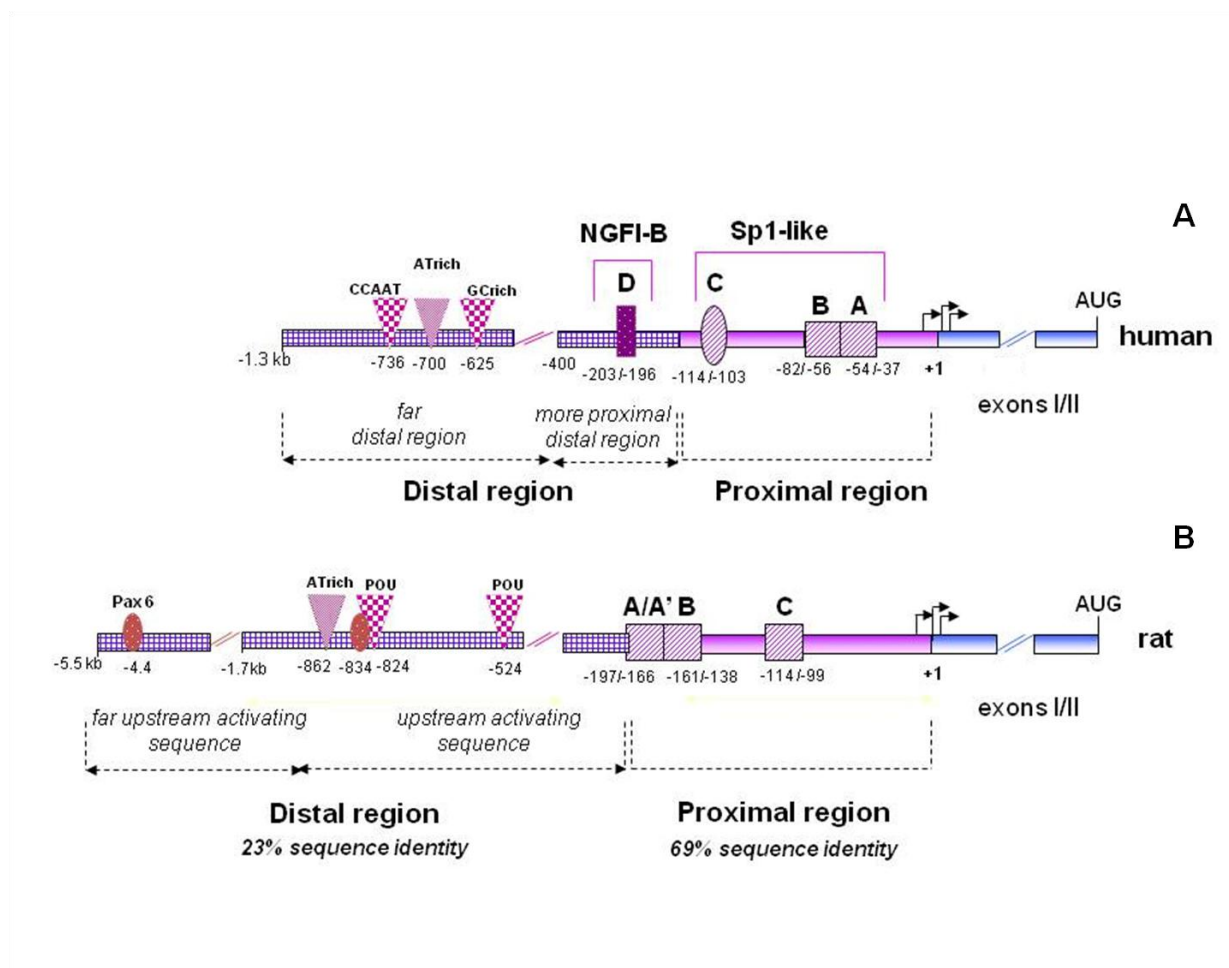


**Figure 1. Organization of the aldolase C gene promoter in human (A) and rat (B):**

(A) Human aldolase C gene promoter. The proximal promoter region is indicated by a dotted line. A, B and C *cis* acting elements are shown to bind Sp1-like factors. The distal region is split into a more proximal distal region and a far distal region as indicated by dotted arrows. In the more proximal distal region, element D is shown to bind NGFI-B factor. In the far distal region the POU binding site, the AT-rich region and the CAAT box are indicated. +1 is the major transcription start site and the arrows indicate the multiple transcriptional start sites. (B) Rat aldolase C gene promoter (51). Rat proximal region is indicated by a dotted line: A/A', B and C *cis* acting elements are boxed. The distal region is split in an upstream activating sequence and a far upstream activating sequence. In the upstream activating sequence, binding sites for POU homeoproteins (namely Brn-1, Brn-2

and Oct-1) are indicated; the AT-rich sequence and a Pax-6 binding-site are also indicated. Another Pax-6 binding-site has been evidenced in the far upstream activating sequence.



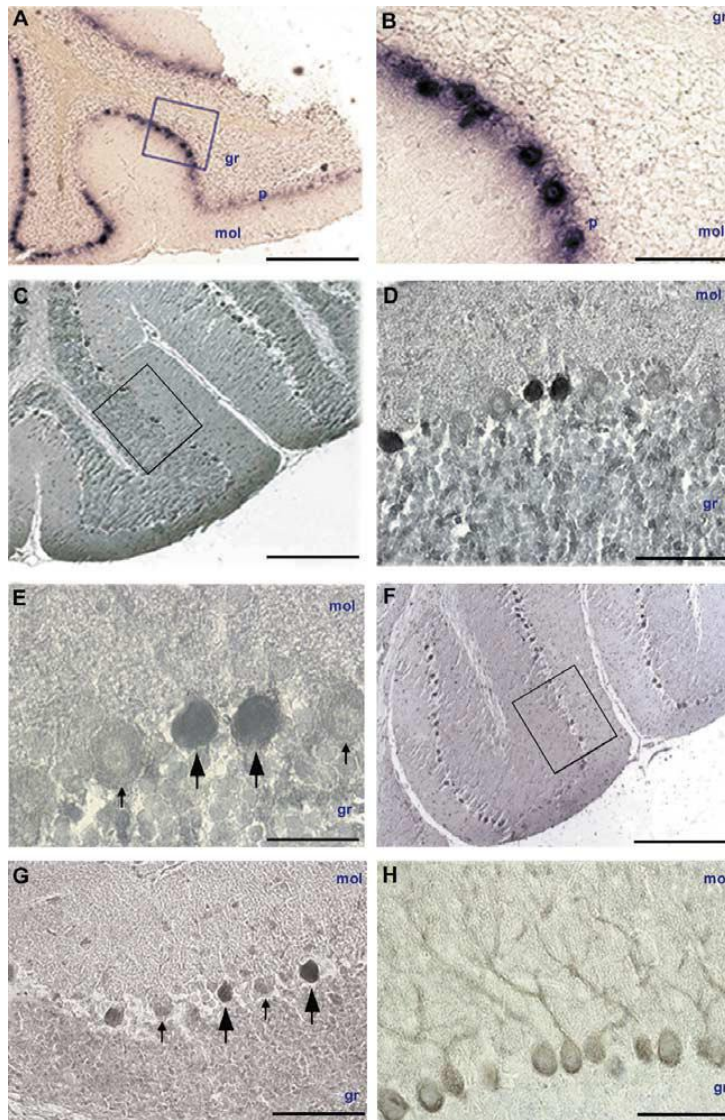


**Figure 2. *In situ* hybridization (A-B) and  $\beta$ -galactosidase ( $\beta$ -gal) (C-G) and calbindin (H) immunostaining on paraffin sagittal cerebellar sections (A-H). (A) *In situ* hybridization with mouse specific aldolase C antisense riboprobe. (B) Higher magnification of the boxed area indicated in (A) showing groups of aldolase C positive Purkinje cells alternating with groups of negative ones. (C) Anti- $\beta$ -gal immunostaining on sections from adult pAldC-2500-LacZ transgenic mice cerebellum. (D, E) Higher magnifications of the boxed area indicated in C: two positive Purkinje cells (thick arrows) surrounded by negative Purkinje cells (thin arrows) are indicated in E. (F) Anti- $\beta$ -gal immunostaining on sections from pAldC-1500-LacZ transgenic mice cerebellum. (G)**

Higher magnification of the boxed area indicated in F: note the clusters of Purkinje cells expressing  $\beta$ -gal (thick arrows) alternating with clusters of  $\beta$ -gal-negative ones (thin arrows). **(H)** Anti-calbindin immunohistochemistry. Staining throughout the Purkinje cell layer shows the integrity of this layer. mol = molecular, p = Purkinje, gr = granular cell layers. Scale bars: A, C, F: 200  $\mu\text{m}$ ; B, D, G, H: 100  $\mu\text{m}$ ; E: 50  $\mu\text{m}$ .

## **1.5 Human aldolase C: messenger and protein expression in mammalian Central Nervous System (CNS)**

The 1.75 kb human aldolase C messenger encodes for a 39.5 kDa protein (364 aminoacids) (8, 9).

The functional enzyme is an hetero/homo-tetramer (160 kDa) selectively expressed in some CNS regions, like the hippocampus, medulla and amygdaloid nuclei with the highest expression level occurring in the cerebellum Purkinje cells.

(1, 2, 62, 63).

During mouse brain development, aldolase C messenger appears in the late embryonal stage (E 15) in all fetal tissues; after birth, it rapidly decreases in all tissues except for the brain, where it reaches maximal expression levels in the adult (64).

In the last years aldolase C protein became the most extensively studied marker for antigenic cerebellar compartmentation (65, 66) being expressed by a subset of Purkinje cells in the cerebellum, thus forming parasagittal stripes that are highly reproducible between individuals and across species.

Although the mammalian cerebellar cortex appears histologically uniform, it is subdivided rostrocaudally and mediolaterally into a complex array of horizontal zones and parasagittal stripes (66-71). This subdivision closely reflects the pattern of afferent and efferent connections linking the cerebellum to the rest of the central nervous system CNS (72, 73).

The cerebellar vermis can be subdivided into four horizontal zones based on differential protein expression: the anterior zone (AZ; lobules I–V), the central zone (CZ; lobules VI–VII), the posterior zone (PZ; lobules VIII–dorsal IX), and the nodular zone (NZ; ventral lobule IX–lobule X) (71, 74, 75). Each horizontal zone is further subdivided into parasagittal stripes.

Aldolase C is expressed in a stripe-like way only in the cerebellar AZ and PZ.

Aldolase C stripes of Purkinje cells are referred to as P1+ to P7+ (numbered in the figure 3 as 1–7 for clarity) (76) from the midline laterally, and the intervening aldolase C – stripes (beige in the figure) are numbered with reference to the neighbouring aldolase C + stripe (Fig. 3) (64, 76).

During mouse brain development, aldolase C protein is not expressed at all until postnatal day 5 (P5), then, from P5-P7 aldolase C is found only in the posterior lobe vermis, with immunoreactive Purkinje cells in lobules X, IX, and VIII but not elsewhere; from P7-P12 most Purkinje cells in the vermis become aldolase C + (initially described in rats by Leclerc et al. 1988) (77); from P12-P15 immunoreactivity also appears in the hemispheres so that almost all Purkinje cells now are aldolase C +; and finally, from P15-P25 aldolase C is gradually suppressed in those Purkinje cells that are negative in the adult until the mature pattern of parasagittal compartments is revealed selectively in lobules I-V and VIII-IX (AZ and PZ) (78, 79).

Stripe-like expression is a common feature of genes selectively expressed in the cerebellum (77, 78). The stripe-like expression of aldolase C in the Purkinje cells of mouse cerebellum was first reported by Anh and Hawkes (64, 80) which called aldolase C "zebrin"; subsequently, our group described the stripe-like expression of the aldolase C mRNA and protein also in the human cerebellum (81).

Our group was able to draw-up a detailed map of aldolase A and aldolase C mRNA and protein expression in different areas of the human brain and cerebellum.

We found that, in human CNS, Aldolase A mRNA, unlike aldolase C, is strongly expressed in all areas of the CNS. Particularly, aldolase A protein is expressed in neurons of the supraorbital gyrus and in neurons from frontal and temporal lobes, in the cytoplasm of pyramidal neurons near Rolando's sulcus. Aldolase C is absent from these areas. In the olives, aldolase A is expressed in neurons of the superior and inferior olives. In the same areas, aldolase C protein is expressed only in the inferior olives and with a stripe-like

distribution in the neuropil. In the cerebellum the aldolase A protein is expressed at low levels throughout the Purkinje cell layer (Fig. 4, A).

Aldolase C protein is expressed in an antero-posterior gradient. It is present in some neurons near Rolando's sulcus and in the neurons near the calcarine scissure in the occipital cortex but is absent from the motoneurons in the supraorbital cortex. Maximum expression occurs in the Purkinje cells of the cerebellum as well as in mouse and rat. Finally, aldolase C stripe-like expression pattern, has been revealed in humans, not only in the Purkinje cells of the cerebellum (Fig. 4, B-D), but also in the inferior olives and in Goll and Burdach nuclei of the posterior horn in the spinal cord (Fig. 4, E-F). Differently from aldolase C, aldolase A, is not expressed in stripes, therefore, stripe-like expression is an aldolase C-specific feature (50, 81). This peculiar stripe-like distribution of aldolase C protein in specific areas of CNS where aldolase A is co-expressed, supports the hypothesis that aldolase C could exert additive functions besides its glycolytic role.

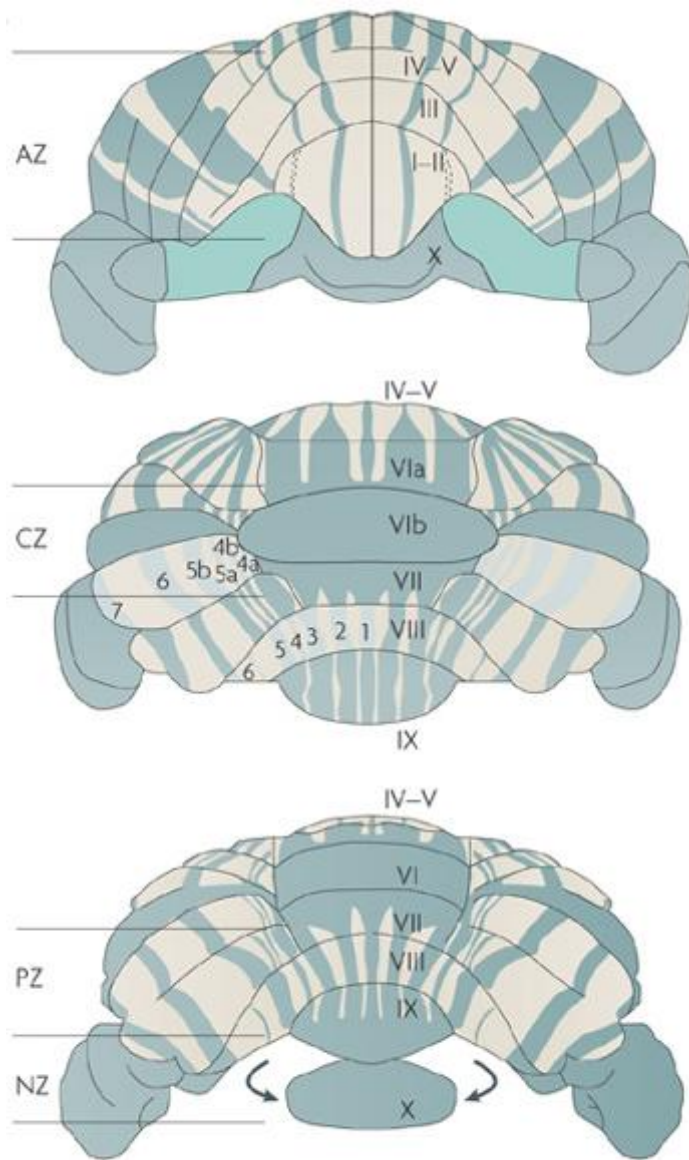


**Figure 3. Aldolase C and cerebellar cortical organization.**

The mouse cerebellar cortex is divided into horizontal zones, and each zone is subdivided into parasagittal stripes. Zones and stripes are clearly seen in the expression pattern of aldolase C. The distribution of Purkinje cells immunoreactive to aldolase C in the cerebellum of the adult mouse, seen from anterior (top panel), dorsal (middle panel) and posterior (bottom panel) views reveals a complex cytoarchitecture comprising four horizontal zones in the vermis and in both hemispheres: the striped anterior zone (AZ) and the posterior zone (PZ) alternate with the uniformly aldolase C immunopositive central

zone (CZ) and nodular zone (NZ; partly reflected out from beneath lobule IX). Aldolase C+ stripes of Purkinje cells are referred to as P1+ to P7+ from the midline laterally, and the intervening negative stripes (beige in the figure) are numbered with reference to the neighbouring (medial) positive stripe. Lobules in the vermis are indicated by Roman numerals.

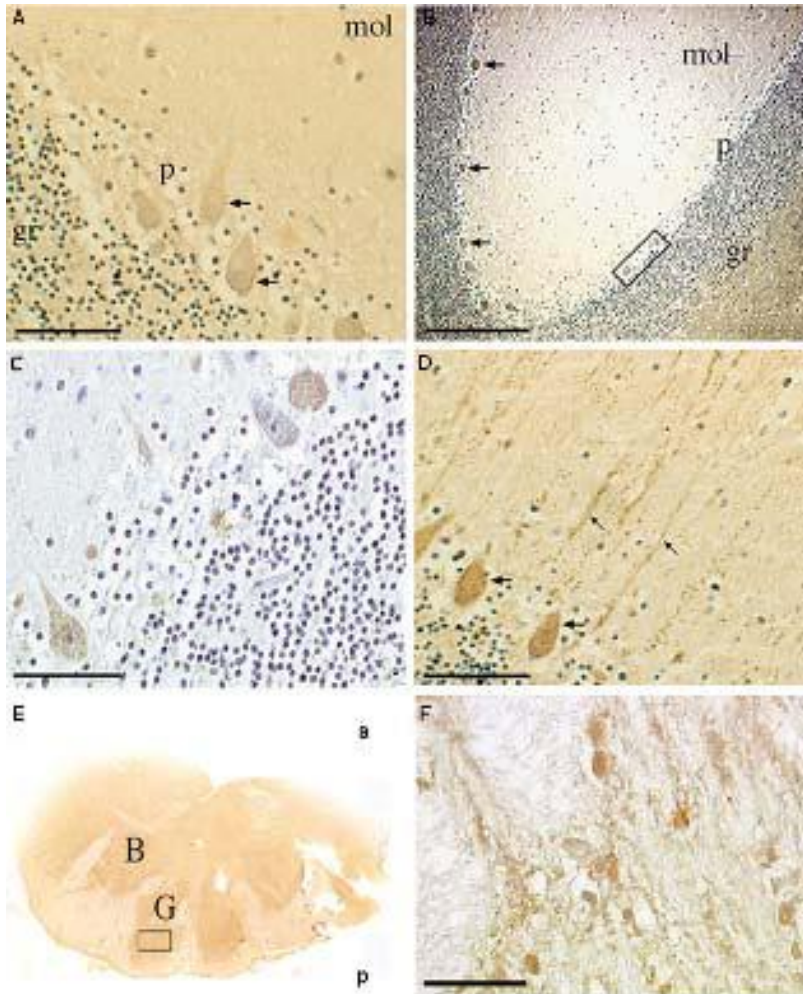


**Figure 4. Aldolase A and aldolase C immunostaining on coronal sections from human anterior cerebellar cortex (A-D) and from spinal cord at the posterior horn (E-F).**

(A) Purkinje cells expressing aldolase A (thick arrows). (B) Stripe-like expression of aldolase C protein in the Purkinje cells (thick arrows indicate aldolase C positive cells). (C) Higher magnification of the box indicated in B: note two positive aldolase C-expressing cells surrounding one negative. (D) Aldolase C protein expression in the cytoplasm and in the dendrites of positive Purkinje cells (thick and thin arrows, respectively). (E) Goll (G) and Burdach (B) nuclei in the spinal cord: aldolase C is strongly expressed in the Goll and Burdach nuclei. (F) Higher magnification of the box indicated in



E: note the stripe-like distribution of aldolase C protein in the neuropil. Scale bars: A, C, D and F: 100  $\mu\text{m}$ ; B: 500  $\mu\text{m}$ . E: the section contains the whole posterior part of the spinal cord: the image is magnified 5 times with respect to the slide. mol, p and gr, molecular, Purkinje cell and granule cell layers, respectively. a, anterior part; p, posterior part.

## 1.6 Aims

The molecular basis of the stripe-like distribution of aldolase C in specific areas of CNS are still unknown. This peculiar expression pattern led us to hypothesize aldolase C exerting moonlight functions besides its glycolytic role. To date, there aren't any published disease-causing mutations in this gene. It is also unclear why the aldolase C gene is acquired during evolution in addition to the other two aldolases and especially in addition to aldolase A that is co-expressed with aldolase C in such areas of CNS.

My PhD thesis project could be split into two main parts:

A) The study of transcriptional regulation of human aldolase C gene as a model useful to understand the complex regulatory mechanisms of genes selectively expressed in CNS through:

- *in vitro* systems, in order to point out promoter region(s) involved in transcriptional activation during neuronal differentiation induced by NGF in PC12 cells;
- *in vivo* systems, in order to identify human aldolase C gene promoter regions responsible for its brain-specific and stripe-like expression in Purkinje cell layer of transgenic mice.

B) The study of the functional role of aldolase C protein in order to improve our knowledge on its hypothetical additional functions:

- *in vitro*, through the production of chimeric aldolases AC and CA in which isozyme specific residues (ISRs) have been switched from aldolase A to C and viceversa. The analysis of kinetic parameters of these recombinant enzymes has been performed in order to explore the role of conformational dynamics in catalytic mechanisms;

*in vivo*, through the production of aldolase C conditional knockout mice as a model to investigate for putative additional functions of aldolase C protein besides its glycolytic role.

## **2. MATERIALS AND METHODS**

### **2.1 Materials**

Reagents were provided by Sigma (St.Louis, USA), Carlo Erba Reagenti (Milano, Italia), Serva (Heidelberg, FRG), Amersham-Pharmacia Biotech. (England), Bio Rad Lab. (CA, USA), Difco (Becton Dickinson , MD, USA).

Kits were provided by Amersham-Pharmacia Biotech (England), Qiagen Inc. (Valencia, USA), Stratagene (La Jolla, USA), Takara Biomedicals Group (Japan), Vector laboratories, (USA), Roche Molecular Biochemicals (Germany), Gibco BRL (Life technologies, Bethesda, USA).

Restriction and modification enzymes were provided by Roche Molecular Biochemicals (Mannheim, Germany), Promega Corporation (Madison, Wisconsin, USA), Invitrogen (Groningen, Netherlands).

Enzymes for RT-PCR, PCR e Real-Time PCR were from Invitrogen (Italy- MI).

Oligonucleotides used as primers for PCR and sequence analysis were provided by Boston University Core Sequencing Facility and by CEINGE (Biotecnologie Avanzate s.c.ar.l., Napoli, Italia).

Vectors used for recombinant constructs preparation were provided by Stratagene (La Jolla, USA), Clontech Lab. Inc. ( Palo Alto, CA, USA).

B6D2F1 and CD1 mice strains were from Charles River (Italy).

C57black6 (C57bl/6) mice strains were from EMBL (European Mouse Biology Laboratory, Monterotondo, Rome).

Tubes and plastic materials were from Falcon (Becton Dickinson, UK).

## 2.2 Generation of reporter constructs and site-directed mutagenesis

Constructs  $\Delta$ 1190-chloramphenicol acetyltransferase (CAT),  $\Delta$ 420-CAT, and  $\Delta$ 164-CAT were made as indicated in Buono et al. 1993 (40), and  $\Delta$ 208-CAT was made as indicated in Buono et al. 1997 (43). The insert of  $\Delta$ 260-CAT construct was obtained by PCR using as template the  $\Delta$ 420-CAT clone, containing 420 bp of the promoter region of human aldolase C gene. The oligonucleotide  $\Delta$ 260 BamHI F 5'-ACTAAGCTGGATCCCCAGCATC-3' (-277/-256) (+1 being the major transcription start site) containing the BamHI restriction site and the oligonucleotide  $\Delta$ 260 PstI R 5'-CAAACAGATGAGGCTGCAGCCCT-3' (+28/+10) containing the PstI site, were used as primers. The reaction was carried out in 50  $\mu$ l buffer containing 0.2 mM dNTPs, 100 ng of primers described above, and 5 units of TaqI polymerase (Invitrogen, Italy). The PCR products were digested by BamHI/PstI, purified from agarose gel, and then cloned in BamHI/PstI sites, upstream the CAT reporter gene in the pEMBL-8-CAT expression vector (59). The construct  $\Delta$ 260\*-CAT was obtained by site-directed mutagenesis with the Quick-Change site-directed mutagenesis kit (Stratagene) using the the construct  $\Delta$ 260-CAT as template. The site-directed mutagenesis was performed according to the manufacturer's instructions and using the oligonucleotides  $\Delta$ 260\* mut (F) 5'-TGGCAGAAATGAACGCTGCAGCAT GGCCAGGCTCCC-3' and its complement as reverse (R) (-216/-181) which carry the restriction site PstI replacing the element D.

The constructs pTK-E1-CAT and pTK-E3-CAT contain one (Con1.USF1 F/R ) and three tandem copies (Con3 USF1 F/R) of the oligonucleotide spanning from -216 to -181 in the promoter of human aldolase C gene, containing the specific element E binding site:

E1- **AAGCTTGTGCCCGGCACGTGGTAAAGGGATTGGGTACC**

E3-AAGCTTGTGCCCGGCACGTGGTAAAGGGATTG-  
GTGCCCGGCACGTGGTAAAGGGATTG-  
GTGCCCGGCACGTGGTAAAGGGATTGGGTACC

These oligonucleotides were designed starting and ending with the restriction sites for HindIII (5') and KpnI (3') restriction enzymes (shown in red) to be used for the cloning in pTK-CAT vector.

### 2.3 Cell cultures

PC12 pheochromocytoma cell line was cultured in Petri plates (Ø 100 mm and 60 mm, Sarstedt, CELL PLUS) . Cells were grown in 10 ml of RPMI culture medium containing 10% horse serum (HS), 5% fetal bovine serum (FBS) and a mixture of 1% penicillin and streptomycin, at 37°C in an atmosphere with 5% CO<sub>2</sub> and 95% air. Cells were subcultured every 2-3 days and induced to neuronal differentiation by adding 100 ng/ml Nerve Growth Factor 7S (NGF 7S) (GIBCO) at different times. SKNBE cells were grown on glass coverslips in RPMI medium containing 15% fetal bovine serum, 1% penicillin and streptomycin at 37° C and with an atmosphere of 5% CO<sub>2</sub>, 95% air, and subcultured 1:3 every 3 days.

### 2.4 Transient transfection and CAT assay

Transfections were performed using the Lipofectamine 2000, according to the manufacturer's instructions (Invitrogen, life technologies).

PC12 cells were seeded at 4 x10<sup>5</sup> cells/60 mm Petri dish and grown overnight. Co-transfections were performed with different aldolase C promoter-CAT constructs, containing serial deletions of the promoter region or site-directed mutation of the NGFI-B transcription factor (Δ-260\*-CAT) binding site, and with pRL-LUC plasmid as internal

standard. pRL-LUC is a plasmid expressing the Renilla luciferase gene used to normalize for differences in the transfection efficiency.

pEMBL8-CAT and CMV-CAT were used as negative and positive controls, respectively.

Cells were co-transfected with 2 µg of each construct containing different deleted regions of human aldolase C gene promoter and 1 µg of pRL-LUC plasmid as internal standard. 6 hours after the transfection, the cells were stimulated with 100 ng/ml NGF for 3 days. Transfections were performed in duplicate and repeated three times.

After NGF treatment, cells were washed with PBS, harvested with TEN (40 mM Tris, 1 mM EDTA, 150 mM NaCl) and centrifuged at 4°C for 5 minutes. Cell pellets were resuspended in 50 µl of 250 mM Tris pH 7.8, subjected to three “freeze and thaw” cycles in order to lyse cell membranes and, finally, centrifuged for 10 minutes at 4°C. The supernatant obtained, containing proteic extracts was aliquoted and kept at -80°C. Proteic extracts were successively used for the CAT assay. CAT assays were performed as described by Gorman et al. (82):

- Cell extracts amounts were added to a mixture containing 55 µl of Tris 0,25 M pH 7.8 and 1µl of <sup>14</sup>C- chloramphenicol and the reaction run at 37°C for 5’;
- 20 µl of acetyl-CoA 4 mM (3,5 mg/7ml in 0,25M di Tris pH 7.8) were added to the mixture and the reaction run at 37°C for 5’;
- Acetylated and non-acetylated forms of chloramphenicol produced during the reaction were extracted with 800 µl of ethyl acetate and centrifuged for 3-5 minutes;
- The supernatant, which contains acetylated and non-acetylated forms of chloramphenicol, was let evaporate in a centrifuge under vacuum (speed-vac) to reduce the volume;
- Pellets were resuspended in 15 µl of ethyl acetate and loaded on a thin-layer chromatographic (TLC) sheet (Polygram SIL-G - 0,25 mm) placed in a chamber with a mixture of chloroform and methanol (39:1) as solvent in the bottom;

- The samples were allowed to migrate up the TLC sheet so that the unacetylated chloramphenicol was separated from its mono- and bis-acetylated derivatives;
- The silica sheet was exposed to a *Phosphoroimager* storage phosphor screen in an appropriate cassette for 3 hours;
- The screen was finally scanned using a Storm-840 instrumentation;
- The intensity of radioactive signals was analysed by using the *ImageQuant* programme.

Luciferase activity in cell extracts was measured essentially according to de Wet et al. (83) using a Berthold Blolumat LB 9501 luminometer. CAT activity in the extracts of transfected cells was normalized to the luciferase activity (RLU, relative luciferase units) determined by the Dual-Luciferase Reporter Assay System (Promega), according to the manufacturer's instructions.

## **2.5 Nuclear extracts and Electro Mobility Shift Assays**

Nuclear extracts from PC12 cells were obtained as described in Dignam et al. (84) with some modifications. Cells were washed in PBS 1X (phosphate buffered saline) (Gibco), centrifuged, resuspended and syringed in the solution I (10 mM Hepes pH 7.9, 10 mM KCl, 1.5 mM MgCl<sub>2</sub>, 0.1 mM EGTA, 0.5 mM PMSF, 0.1 mM DTT). The nuclear extracts pellet was then resuspended in the solution II which contains, differently from solution I, 400 mM NaCl instead of KCl and 5% glycerol. Samples were incubated on ice for 30 minutes and centrifuged at 14.000 rpm for 40 minutes at 4°C. The supernatant was finally aliquoted and kept at -80°C.

EMSA were performed as described in Buono et al. (43), using 4 µg of nuclear extracts from PC12 cells. 3 µg of poly (dI/dC) were added to each sample as non-specific competitor.

The following oligonucleotides were used:

- L1 (-211/-186 bp in the promoter of human aldolase C gene), which contains the specific binding site for NGFI-B (set in bold type) (43):

5'-TGAACGCA**AAGGTC**ATGGCCAGGCTCC-3'

- 21-OHase (-79/-62 bp in the promoter of 21-OHase mouse gene) which binds NGFI-B to the sequence set in bold type (54):

5'-TGAAGCAA**AAGGTC**AGAG-3'

- BRD (-245/-211 bp in the promoter of human aldolase C gene), which contains the consensus sequences for NGFI-B (shown in bold) and for USF1 (shown in bold-italic):

5'GTGCCCGGC**ACGTGG**TAAAGGGATTGTGGCAGAAATGAACGCA**AGGT**  
**CATGG**-3'

- BRD-L1 (-245/194 bp in the promoter of human aldolase C gene), which contains the consensus sequence for USF1 (shown in bold-italic):

5'-GTGCCCGGC**ACGTGG**TAAAGGGATTGTGGCAGAAA-3'

- USF1, which contains the consensus sequence for USF1 (set in bold)

5' -CACCCGGT**CACGTGG**CCTACACC-3'

- NF-I, which contains the consensus sequence for NF-I (set in bold)

5'-TTTT**TGG**ATTGAAGCCAATATGATAA-3'

- Sp1, which contains the consensus sequence for Sp1 (set in bold)

5'-ATTCGATCGGGGCGGGGCGAGC-3'

The probes used for EMSA were labelled as single strand (3 pmol) by using the "Random Primers DNA Labeling System" kit according to the manufacturer's protocol (Invitrogen). The single strand probes were then annealed with their complementary strand as described in Buono et al. 1997. The labelled double strand probes were finally purified by Sephadex-G50 column chromatography (Pharmacia Biotech, Piscataway, NJ, U.S.A.).



The competition analysis was performed using unlabelled oligonucleotides BRD, L1 and USF1 as specific competitors and the oligonucleotides Sp1 and NF1 as non-specific competitors. Supershift analysis was conducted using 2, 4 and 6 µg of anti-USF1 specific polyclonal antibody (Santa Cruz Biotechnology, Inc., California) and 6 µg of non immune IgG as irrelevant polyclonal antibody. Dephosphorylation assay was conducted using 1 and 2,5 units of CIP (Calf Intestinal Phosphatase, Promega Italia) and 2,5 units of inactivated CIP as negative control for 1h at 37°C.

After the incubation of cold probes (self and non-self competitors), binding solution and poly (dI/dC) with nuclear extracts for 20 minutes at 25°C, the hot probes were added (30000 cpm) and the reaction was continued at room temperature for 10 minutes.

The complex DNA-protein was separated from the unbound DNA through electrophoresis in 0.5% Tris-borate EDTA buffer (44 mM Tris-HCl, 44 mM boric acid, 12.5 mM EDTA, pH 7.5) on 4% (w/v) non-denaturing polyacrylamide gel, The gel was subsequently dried and autoradiographed.

## **2.6 Chromatin Immunoprecipitation (X-ChIP)**

SKNBE neuroblastoma cells were grown on glass coverslips (12x10<sup>6</sup> cells/well) as described in the paragraph 2.3. The crosslinking of proteins to DNA was performed by adding formaldehyde to cell culture media at a final concentration of 1%. Fixation proceeded at room temperature for 10 minutes and was stopped by the addition of glycine to a final concentration of 0.125 M. Chromatin immunoprecipitation was performed as described (85):

cells were washed 2 times with 6 ml of PBS 1X and centrifuged at 3.000 rpm for 30 minutes at 4°C. Pellets were resuspended in 1,5 ml of cell lysis buffer (5 mM PIPES pH 8.0, 85 mM KCl, 0,5% NP40, 1mM PMSF, 1/1000 protease inhibitors cocktail). Cell lysate was centrifuged at 5.000 rpm for 5 minutes at 4°C. Pellets were resuspended in 300 µl

nuclei lysis buffer (50 mM Tris HCl pH 8.0, 10 mM EDTA, 0,8% SDS, 1 mM PMSF, 1/1000 protease inhibitors cocktail) and put on ice for 10 minutes. The DNA linked to the proteins was sonicated 6 times for 30 seconds, transferred in 1,5 ml tubes, centrifuged at 14.000 rpm for 10 minutes at 4°C. The supernatant was diluted up to 1 ml with a Dilution Buffer (0,01% SDS, 1% TRITON X-100, 0.5 mM EGTA; 10 mM Tris-HCl pH 8.0, 150 mM NaCl, 1/1000 protease inhibitors cocktail), and kept at a -80°C.

Chromatin aliquots were subdivided into three fractions and 20µl of protein A/G Plus-Agarose (Santa Cruz) were added to each fraction. After an incubation for 2 hours at 4°C (preclearing reaction), samples were centrifuged and the supernatants were incubated O.N. at 4°C with rotation: the first fraction was incubated with 3-5 µg of the specific anti-USF1 antibody, the second and the third fraction were incubated with no antibody (called “No Ab”) and with rabbit IgG, respectively, as negative controls. 20µl of protein A/G Plus-Agarose (Santa Cruz) were added to each sample and let rotate for 3-4 hours at 4°C. Precipitates, beads and supernatant were separated by centrifugation at 13.000 rpm for 1 minute at room temperature. The precipitates were washed 5 times with 1 ml of RIPA Buffer, 1 time with LiCl Buffer (0,25 M LiCl, 0,5% NP-40, 0,5% Na- Deoxycolate, 1 mM Na-EDTA, 10 mM Tris-HCl pH 8.0) and 1 time with TE Buffer (10 mM Tris-HCl pH 8, 1 mM EDTA).

Finally, the precipitates were resuspended in 100 µl of TE. Immunoprecipitated chromatin aliquots were incubated with 1 µg of RNase at 65°C O.N.

To purify immunoprecipitated DNA, samples were added of 0,5% SDS, 500 mg/ml Proteinase K and incubated for 4 hours at 50°C. Successively, samples were centrifuged at 14.000 rpm for 2 minutes at 4°C to remove the resin and treated with an equal volume of phenol-chlorophorm - Tris pH 8.0.

The DNA extraction was repeated by adding an equal volume of Tris-HCl pH 8.0 1 M to the organic phase. The DNA was precipitated with 100µg/ml glycogen as a carrier agent. Finally, both the specific immunoprecipitated DNA and the No Ab fraction were resuspended in 30 µl of water.

Approximately 50 ng of immunoprecipitated DNA were used for PCR reactions producing a final fragment of ~100 bp. Specific oligonucleotides, mapping in the promoter of human aldolase C gene, were designed as described below:

-319 F: 5'- CCACCTACTCAACCTGTTGTT-3'

-201 R: 5'-TGGCTGTTAGGGACTGCCC-3'

PCR reaction were carried out in a final volume of 50µl and performed in a Biorad Thermal Cycler by using the following scheme repeated for 30 cycles:

- Denaturation 94° C x 45''
- Annealing 60°C x 30''
- Polymerization 72°C x 15''

1/10 of the PCR product was analysed by agarose gel electrophoresis to verify the effective amplification.

## **2.7 Western Blot**

Nuclear and cytosolic extracts from PC12 cells wt and treated with NGF were obtained using “Qproteome nuclear protein kit” according to the manufacturer's protocol (Qiagen). The same quantities of protein extracts (40 µg) were separated on a 15% SDS-acrylamide gel (SDS-PAGE), transferred on a nitrocellulose membrane (Amersham Pharmacia Biotech) and checked by Ponceau S staining to determine equal loading. The coloured filter was preincubated with milk 10% in PBS/0.1% Tween-20 for 1 hour, and then incubated with a specific polyclonal anti-USF1 antibody (SantaCruz Biotechnology,

1:1000). After the incubation with a anti-rabbit secondary antibody conjugated with peroxidase (Amersham Pharmacia Biotech), immunoreactive bands were revealed by chemiluminescence (ECL). Polyclonal anti-cyclin A and anti- $\alpha$ -tubulin antibodies were used as control for nuclear and cytosolic extracts respectively.

## **2.8 Immunofluorescence assays**

PC12 cells were grown on chamber-slides polyllysine pre-treated (Nalgene Nunc) (20.000/well, 270  $\mu$ l of fresh RPMI medium) and transfected with recombinant constructs by using Lipofectamine 2000 (Invitrogen), as described in the paragraph 2.8 of Materials and Methods. One day after the transfection some wells were added with NGF 100 ng/ml and the treatment continued for 3 days. Subsequently, cells were fixed with cold 3% paraformaldehyde in PBS, washed with PBS, and permeabilized with 0.2% Triton X- 100 in PBS. Blocking was the next step: cells were incubated with 200  $\mu$ l of a solution containing PBS 1X, BSA (bovine serum albumine) 2%, FBS 10% and Triton 0.1% for 1 hour at room temperature. Cells were then incubated with anti-USF1 antibody 1:100 diluted (Santa Cruz) in the blocking solution for 3 hours at room temperature. The second incubation was conducted in the dark for 1 hour with fluorescent secondary antibody rabbit anti-FITC (fluorescein isothiocyanate) 1:100 diluted. Finally, the last incubation was performed for 5 minutes with DAPI nuclei stain solution 0.05  $\mu$ g/ml (6-Diamidino-2-phenylindole dihydrochloride). Coverslips were then washed in PBS, mounted on a glass microscopic slide (BDH) with fluorescence mounting medium (Dako) and examined using a Zeiss Axiovert 200 microscope equipped with the confocal laser system LSM 510 META. Image processing was performed with Adobe Photoshop software.

## 2.9 Cloning and DNA preparation for microinjection

The transgenic construct pAldC-1580-LacZ was obtained by mutagenesis of the original construct pAldC-2500-LacZ (49). The Quick Change site-directed mutagenesis kit (Stratagene) was used to create an extra SalI restriction site (underlined) in the position – 280 bp.

The sequences of oligonucleotides used for the site-directed mutagenesis are:

Wt-Fw: 5'- GCTTAATCCCCAGCATCCAGCAAGTGCCCGGCACGTGG -3'

Mut-Fw: 5'- GCTTAATCCCCAGCGTCGACCAAGTGCCCGGCACGTGG -3'

Wt-Rev: 5'- CCACGTGCCGGGCACTTGCTGGATGCTGGGGATTAAGC -3'

Mut-Rev: 5'- CCACGTGCCGGGCACTTGGTCGACGCTGGGGATTAAGC-3'

The fragment SalI-SalI (-1200 bp/-280 bp) was removed by digestion and the remaining deleted construct was purified from agarose gel by electroelution, ligated and recircularized by using the T4 Ligase (Invitrogen).

In the same way the construct pAldC-1464-LacZ was obtained by mutagenizing the original construct pAldC-2500-LacZ and creating an extra SalI restriction site (underlined) in the position -164 bp.

The sequences of oligonucleotides used for the site-directed mutagenesis are:

Wt-Fw: 5'-AGGTGGGAGGGCAGTCCCTAACAGCCACGGATGCCTGGG-3'

Mut-Fw:5'AGGTGGGAGGGCAGTTCGACAACAGCCACGGATGCCTGGG-3'

Wt-Rev: 5'-CCCAGGCATCCGTGGCTGTTAGGGACTGCCCTCCCACCT-3'

Mut-Rev: 5'-CCCAGGCATCCGTGGCTGTTGTCGACTGCCCTCCCACCT-3'

The fragment SalI-SalI (-1200 bp/-164 bp) was removed by digestion and the construct was purified from agarose gel by electroelution, ligated and recircularized as described above.

The transgenic construct pAldC-2336-LacZ was obtained by a double mutagenesis of the original construct pAldC-2500-LacZ. The first mutagenesis was performed to create an extra NruI restriction site (underlined) in position -164 bp.

The second mutagenesis created another NruI restriction site just upstream the major transcriptional start site (+1).

The sequences of oligonucleotides used for the first site-directed mutagenesis are:

Wt-Fw: 5'-GTGGGAGGGCAGTCCCTAACAGCCACGGATGC-3'

Mut-Fw: 5'-GTGGGAGGGCAGTTCGCGAACAGCCACGGATGC-3'

Wt-Rev: 5'-GCATCCGTGGCTGTTAGGGACTGCCCTCCCAC-3'

Mut-Rev: 5'-GCATCCGTGGCTGTTTCGCGACTGCCCTCCCAC-3'

The sequences of oligonucleotides used for the second site-directed mutagenesis are:

Wt-Fw: 5'-GCCCCGGAGGAGTCACGTAGCTCTGCGACAT-3'

Mut-Fw: 5'-GCCCCGGAGGAGTTCGCGAAGCTCTGCGACAT-3'

Wt-Rev: 5'-ATGTCGCAGAGCTACGTGACTCCTCCGGGGGC-3'

Mut-Rev: 5'-ATGTCGCAGAGCTTCGCGACTCCTCCGGGGGC-3'

The proximal promoter region (164 bp) was removed by NruI digestion and the remaining deleted construct was purified from agarose gel by electroelution, ligated and recircularized by using the T4 Ligase (Invitrogen).

All oligonucleotides were synthesized by CEINGE, Naples, Italy.

Polymerization reaction were set up in 50 µl final volume containing 20 ng of DNA template, 1 µl of Pfu turbo DNA polymerase (2,5U/ µl), 5 µl of 10x Reaction buffer, 125 ng of Forward and Reverse primers and 1 µl of dNTP mix. PCR reactions were performed as follows:

1 step:

- Denaturation 95°C x 30''

12-18 cycles:

- Denaturation 95°C x 30''
- Annealing 68°C x 1'
- Extension 72°C x 2'

Finally, methylated DNA template and hemimethylated hybrid products (DNA template/target sequence) were digested by adding the DpnI restriction enzyme. E.Coli bacterial cells were transformed with recombinant mutated plasmids, grown and then the plasmids were purified over a Qiagen column maxiprep (49). The sequences were verified by digestion and automated sequencing. After removal of vector sequences by Sal/NotI digestion, the microinjection fragments were purified from agarose gel by electroelution and phenol:chloroform extraction, resuspended in TE buffer at 2 ng/μl and microinjected into 1-cell fertilized eggs.

## **2.10 Generation and identification of transgenic mice**

Single-cell embryos were harvested from the hybrid B6D2F1 mouse strain (Charles River). The purified AldC/LacZ fragments were microinjected into the embryonic male pronuclei and surviving embryos were transferred into the oviducts of pseudopregnant CD-1 foster mothers (Charles River) essentially as described in Hogan et al. (86). Transgenic founders and offspring were identified by Southern blot using a [ $\alpha^{32}$ -P]ATP random-primed LacZ cDNA probe. Three independent stabilized mouse lines were obtained for each construct:

- Construct pAldC-1464-LacZ – lines H5, H62, H69;
- Construct pAldC-1580-LacZ – lines I36, I37, I40;
- Construct pAldC-2336-LacZ – lines N8, N10, N22.

The Animal Experimentation Ethics Committee of the National Institute for Cancer Research of Genoa approved all the animal studies.

## **2.11 $\beta$ -Galactosidase assay**

$\beta$ -Galactosidase ( $\beta$ -gal) activity was assayed in intact and sagittal section of brains and in body parts of adult transgenic mice obtained from the three constructs; sagittal plate sections were identified according to Altman and Bayer (87). Mice were sacrificed by cervical dislocation. Brains were washed in PBS 1X, fixed in 2% paraformaldehyde for 1 h, and then rinsed and incubated overnight at 30 °C in phosphate-buffered saline (PBS) containing 400 mg/ml X-Gal substrate (5-bromo-4-chloro-3-indolyl-b-D-galactoside), 4 mM potassium ferricyanide, 4 mM MgCl<sub>2</sub>, and 0.1% Nonidet P-40 as described in Smeyne et al. (88) and in Oberdick et al. (89). Brains were successively washed in PBS 1X for three times (15'/wash) and then observed under the optic microscope (Zeiss).

## **2.12 Immunohistochemistry**

Formalin-fixed paraffin-embedded nervous tissue blocks were prepared from transgenic mice brains. Serial horizontal and sagittal 7-10  $\mu$ m sections were cut from the formalin-fixed tissue blocks, dewaxed in xylene analogs (Bio-Clear Bio-Optica, Milan, Italy) and rehydrated with graded ethanol concentrations. These sections were incubated for 45 minutes at 97°C in citrate buffer pH 6.0 (DAKO, S2369) in order to reduce immunogenicity. Endogenous peroxidase activity was blocked by immersing slices in 3% hydrogen peroxide methanol for 10 minutes. Aspecific antigen sites were blocked by incubating at room temperature for 30 minutes with background reducing components (DAKO).

Three contiguous brain sections were incubated at room temperature for 1 hour with primary antibodies in the following order: the first slice with anti-calbindin (1:2000 - Abcam) polyclonal antibody, as positive control; the second slice with anti  $\beta$ -gal (1:150 - Chemicon) polyclonal antibody; the third slice with anti-aldolase C (1:500 - PRIMM) polyclonal antibody as positive control. Staining was carried out with LSAB+System-HRP (DAKO); the signal was developed using diaminobenzidine (DAB) chromogen as substrate



(DAKO). The tissue sections were then lightly counterstained with Mayer's hematoxylin and cover-slipped.

Different times were used for developing signal of endogenous aldolase C and calbindin in all transgenic mice (15 and 5 seconds, respectively) and of  $\beta$ -gal in transgenic mice obtained with different constructs: 15–20 sec for pAldC-2500-LacZ (ctrl), 50 s for pAldC-1464-LacZ, 15-20 for pAldC-1580-LacZ, 30 sec for pAldC-2336-LacZ.

Images were acquired by NDP.view software (virtual microscopy by Hamamatsu).

### **2.13 RNA extraction and Reverse Transcription Polymerase Chain Reaction (RT-PCR)**

Total RNA was isolated from cultured PC12 cells using TRIzol® reagent (Invitrogen, life technologies) according to the manufacturer's protocol.

Embryos from pAldC-2500-*LacZ* transgenic mice lines were obtained at developmental stages E13 and E15. pAldC-2500-*LacZ* transgenic mice were sacrificed at different developmental stages: P0 (newborn), P7, P14 and P42 (adult). Finally, pAldC-1580-*LacZ*, pAldC-1464-*LacZ* and pAldC-2336-*LacZ* transgenic mice were sacrificed only at adult stage. Total RNA was obtained from embryos head and from brain, cerebellum, heart, kidney and liver of pAldC-2500-*LacZ* transgenic mice at different developmental stages. Total RNA was also obtained from brain and cerebellum of pAldC-1580-*LacZ*, pAldC-1464-*LacZ* and pAldC-2336-*LacZ* adult transgenic mice. Embryos head and the different organs were resuspended in Tryzol (Invitrogen, life technologies) and homogenized with an electric homogenizer. Successive steps have been performed according to the manufacturer's instructions.

Total RNA was retro-transcribed into cDNA by using the commercial kit SuperScript III Reverse Transcriptase (Invitrogen). 12-18 bp oligo(dT) were used as primers annealing the

mRNA polyA tails. The retrotranscription reaction was performed using the ICycler PCR machine from BioRad and following these steps:

- Denaturation and Annealing            60°C x 5'
- Polymerization                            50°C x 1h
- Inactivation                                70°C x 15'

After DNase I treatment, first-strand cDNA was synthesized from 1 µg total purified RNA from PC12 cells and transgenic mice tissues respectively. Retrotranscription was carried out using 1 µl of 0.5 mg/ml oligo(dT) primers (Invitrogen) and 0.5 µl of 25 mM dNTP for the first step. Then the reaction was stopped and samples were put on ice for 5 minutes to help the stabilization of single strand RNA molecules. Successively, 1 µl of SuperScript III RT (200U/ ml), 4 µl of 5X First-Strand Buffer [250 mM Tris-Hcl pH 8.3, 375 mM KCl, 15 mM MgCl<sub>2</sub>] and 1 µl of 0.1M DTT were added to perform the second and third step. Finally, cDNA samples were kept at 4°C.

## **2.14 Real Time *quantitative*-PCR**

Total RNA was obtained from PC12 cells, embryos and different organs of pAldC-2500-LacZ transgenic mice at different developmental stages and from brain and cerebellum of pAldC-1580-LacZ, pAldC-1464-LacZ and pAldC-2336-LacZ adult transgenic mice as described previously.

Relative cDNA samples obtained by RT-PCR were analysed by Real Time quantitative-PCR (RTqPCR).

To analyze aldolase C messenger expression in PC12 cells untreated and treated with NGF, RTqPCR reactions were set up according to Liss et al. (90) and using: the housekeeping gene ABL, which has a constant copy number during neuronal differentiation, as

normalizer; GAP43 as differentiation marker; the aldolase C mRNA from untreated PC12 cells, as calibrator.

As concern pAldC-2500-LacZ transgenic mice, the aim was to analyse and compare expression pattern of endogenous aldolase C and transgenic LacZ messengers during brain development.

RTqPCR reactions were set up according to Liss (90) and using two standards: the housekeeping gene 18S rRNA, which has a constant copy number in all developmental stages, as normalizer; the aldolase C and LacZ mRNA at developmental stages in which their expression is the lowest in the different tissues, as calibrators.

As concern pAldC-1580-LacZ, pAldC-1464-LacZ and pAldC-2336-LacZ transgenic mice, LacZ messenger expression pattern was analysed and compared with that of pAldC-2500-LacZ transgenic mice only at adult stage.

Even in this case the housekeeping gene 18S rRNA was used as normalization target; instead, LacZ messenger from pAldC-2500-LacZ adult transgenic mice was used as calibrator.

Oligo4 software was used to design oligonucleotides as follows:

**ABL Fw:** 5'-GGTATGAAGGGAGGGTGTACCA-3'

**ABL Rev:** 5'-GTGAACTAACTCAGCCAGAGTGTTGA-3'

**GAP43 Fw:** 5'-CAGGTTGAAAAGAATGATGAGG-3'

**GAP43 Rev:** 5'-GCATCGGTAGTAGCAGAGCC-3'

**Ald C Fw:** 5'-TGCCCTGCGTCGTACTIONGTGC-3'

**Ald C Rev:** 5'-TGCAAGCCCGTTCATCTCTG-3'

**LacZ Fw:** 5'-ATGATTACGGATTCACCTGGCCGTC-3'

**LacZ Rev:** 5'-TCGGCATAACCACCACGCTCATC-3'

**18S rRNA Fw:** 5'-CATGGTGACCACGGGTGAC-3'

**18S rRNA Rev:** 5'-TTCCTTGGATGTGGTAGCCG-3'

The efficacy and specificity of these primers were tested by dilution experiments and melting curves.

Real-time quantitative PCR was performed using an iQ5-iCycler Optical System (Bio-Rad). IQ SYBR [100 mM KCL, 40 mM Tris-HCl pH8.4, 0.4 mM dNTPs, iTaq DNA polymerase 50U/ml, 6 mM MgCl<sub>2</sub>, SYBR Green I, 20 nM fluorescein, stabilizer] (Bio-Rad) was used according to the manufacturer's instructions. Reactions were incubated for 10' at 95°C, followed by 40 cycles of 15'' at 95°C and 1' at 60°C. Finally, a temperature gradient was applied starting at 55°C and increasing the temperature of 0,5°C every 10'' up to 95°C. Fluorescence signals were measured during the elongation step. All reactions were performed in triplicate.

The “ $2^{-\Delta\Delta Ct}$ ” method of relative quantification was used as reported elsewhere (91).

### 2.15 Site-directed Mutagenesis by PCR

The mutant genes coding for chimeric AC and CA aldolases were generated via multiple site-directed mutagenesis using overlapping oligodeoxyribonucleotides that complement the high copy ATG vector pPB14 (92) expressing rabbit aldolase A and human C used as template, respectively.

Primers used to amplify AC chimeric aldolase gene are:

**F1 (gene U):** 5'-ACGACCGAGCGCAGCGAGTCAGTGAG-3'

**R1-AC:** 5'-CTTCGCcATGCTCCCGGTCGACTCATCTG-3'

**F2-AC:** 5'-GAGTCGACCGGGAGCATgGCGAAGAGGCTGCAAcaGATCG  
GTAC-3'

**R2-AC:** 5'-GGAAGAGGATGACGCCCCCGATGCActtGTTACGCGGTCA-3'

**F3-AC:** 5'-GACCGCGTGAACaagTGCATCGGGGGCGT-3'

**R3-AC:** 5'-GCCCACAACAatGCCCTTGGACTTGATAACTTGCGGGAAGGG  
AacCCCATCGTCC-3'

**F4-AC:** 5'-TATCAAGTCCAAGGGC**at**TGTTGTGGGCATCAAG-3'

**R4-AC:** 5'-GAGGGGGT**Gc**GTTCCCAATCTTCAG-3'

**F5-AC:** 5'-GCTGAAGATTGGGGA**Cg**CACCCCCTCAGC-3'

**R5-AC:** 5'-CCTTCTTCCC**ACg**CCAGGC**g**TT**CAGAGCCGA**-3'

**F6-AC:**5'-GCAGGCCTCGGCTCTG**AAc**GCCTGG**c**GTGGGAAGAAGGAG-3'

**R6-AC:**5'-GTTGGC**Ctc**GGCCCGCTT**CACGa**ACTCCTC**c**GTGGCAGCCTT-3'

**F7-AC:** 5'-GCC**ac**GGAGGAG**Tt**CGTGAAGCGGGCC**ga**GGCCAACAGCCT-3'

**R7-AC:** 5'-AGGCGTGGTT**AGc**GATGAAGAGGG**ACTg**GgcGGCCG**Gc**CCC  
CGGCCT-3'

**F8-AC:** 5'-CCCTCTTCATC**g**CTAACCACGCCTACTA-3'

**R8 (Gene L):** 5'-GCTACTGCCGCCAGGCAA**ACTGTTTTATCAG**-3'

Primers used to amplify CA chimeric aldolase gene are:

**F1 (gene U):** 5'-ACGACCGAGCGCAGCGAGTCAGTGAG-3'

**R1-CA:** 5'-CAGCCGCTTGGC**g**ATGCTGCCTACA-3'

**F2-CA:** 5'-CTGTAGGCAGC**ATc**GCCAAGCGGCTGAGC**tc**AATTGGGG  
TGG-3'

**R2-CA:** 5'-GACGCCTCCAATGC**ACgg**TTTCACACGGTCA-3'

**F3-CA:** 5'-GCTGATGACCGTGTGAAA**cc**GTGCATTGGAG-3'

**R3-CA:** 5'-GCCACGAC**Gcc**GCCCTTATCCTGGATGGTTCGGACGAA  
GGG**Acg**ACCATTATCA-3'

**F4-CA:** 5'-CCAGGATAAGGGC**gg**CGTCGTGGGCATC-3'

**R4-CA:** 5'-GCAGAGGGTGT**At**GCTCACTGATTTTCA-3'

**F5-CA:** 5'-GCTGAAAATCAGTGAG**Ca**TACACCCTC-3'

**R5-CA:** 5'-CCCGTTGCC**TCc**CCAGGC**t**TTGAGTGCAGAGGCT-3'

**F6-CA:** 5'-CTGCACTC**AAa**GCCTGG**g**AGGGCAACGGGACAATGCTGG  
GGCTGCC**caa**GAGGAG**Ta**CATCAAGCGGGCT**ct**GGTGAATGGGC-3'

**R6-CA:** 5'-CAGCCAAGCTTCAGTAGGCATGGTTGGaAATGTAGAGTGA

CTcactTGCTGCTgCACCATCTTCT-3'

Red nucleotides refer to the codon that has been changed from that of the wild-type aldolases A and C. Mutated nucleotides are shown in lower case. The resulting missense mutations and their consequent amino acid substitutions are shown in Table 1.

The production of the two chimeric genes involved three steps (see schematic representation in Fig. 5 A and B):

- 1) 8 and 6 different overlapping fragments were amplified for generating AC and CA chimera genes, respectively;
- 2) the amplified fragments 1, 2 and 3 were fused together by PCR using F1 and R3 primers for AC and CA genes; the fragments 4 and 5 were fused by using F4 and R5 for AC and CA genes; the fragments 6, 7 and 8 were fused by using F6 and R8 (only for chimeric gene AC);
- 3) the fusion products 1-2-3, 4-5 and 6-7-8 were further fused together by using only F1-AC and R8-AC primers for amplifying the whole AC chimera gene; the fusion products 1-2-3, 4-5 and 6 were fused together by using only F1-CA and R6-CA primers for amplifying the whole CA chimera gene.

The amplification of each single fragment (first step) was performed using the recombinant DNA polymerase taq (Roche) by incubating samples at 95 °C for 1 minute followed by 35 cycles of denaturation at 95 °C for 30 seconds, annealing at 50 °C for 30 seconds, and elongation at 72 °C for 1 minute. A final step was performed at 72°C for 10 minutes. The fusion fragments (second step) were amplified using the same protocol of single fragments except for the annealing temperature which ranged between 50°C and 60°C for the different fragments and for the elongation step of 2 minutes instead of 1. The final fragments (third step) were amplified by incubating samples at 95°C for 2 minutes, followed by 28 cycles of denaturation at 95 °C for 1 minute, annealing at 50-54 °C for 30

seconds, and elongation at 72 °C for 2 minutes. A final step was performed at 72°C for 10 minutes.

25 ng of pPBI vectors expressing wt rabbit A and human C aldolases were used as template for generating single fragments. For the second and third steps, 100fmol of single and fused fragments were used as template.

The final mutant genes were screened by DNA sequence analysis at CEINGE (Biotecnologie Avanzate s.c.ar.l., Napoli, Italia).

Enzyme	Primers	Codon substitutions	Residue number	Aminoacid substitution
AC chimera	R1, F2	ATC__ATg	39	Ile_Met
AC chimera	F2	TCG__caG	45	Ser_Gln
AC chimera	R2, F3	CCC__aag	71	Pro_Lys
AC chimera	R3	CGT__gtT	91	Arg_Val
AC chimera	R3, F4	GGT__atT	102	Gly_Ile
AC chimera	R4, F5	CAC__CgC	156	His_Arg
AC chimera	R5, F6	AAG__AAc	311	Lys_Asn
AC chimera	R5, F6	GGT__cGT	314	Gly_Arg
AC chimera	R6, F7	CAG__acG	324	Gln_Thr
AC chimera	R6, F7	TAC__TtC	327	Tyr_Phe
AC chimera	R6, F7	CTG__gaG	332	Leu_Glu
AC chimera	R7	GCC__GgC	350	Ala_Gly
AC chimera	R7	AGC__gcC	353	Ser_Ala
AC chimera	R7	GAG__cAG	354	Glu_Gln
AC chimera	R7, F8	TCT__gCT	359	Ser_Ala
CA chimera	R1, F2	ATG__ATc	39	Met_Ile
CA chimera	F2	CAA__tcA	45	Gln_Ser
CA chimera	R2, F3	AAG__ccG	71	Lys_Pro
CA chimera	R3	GTT__cgT	91	Val_Arg
CA chimera	R3, F4	ATC__ggC	102	Ile_Gly
CA chimera	R4, F5	CGT__CaT	156	Arg_His
CA chimera	R5, F6	AAT__AAa	311	Asn_Lys
CA chimera	R5, F6	CGA__gGA	314	Arg_Gly
CA chimera	F6	ACT__caa	324	Thr_Gln
CA chimera	F6	TTC__TaC	327	Phe_Tyr
CA chimera	F6	GAG__ctG	332	Glu_Leu
CA chimera	R6	GGA__GcA	350	Gly_Ala
CA chimera	R6	GCA__agt	353	Ala_Ser
CA chimera	R6	CAG__gAG	354	Gln_Glu
CA chimera	R6	GCC__tCC	359	Ala_Ser

**Table 1. Site directed mutagenesis.** Primers, codon and aminoacid substitutions with relative residue number are indicated both for chimeric aldolase AC and CA.



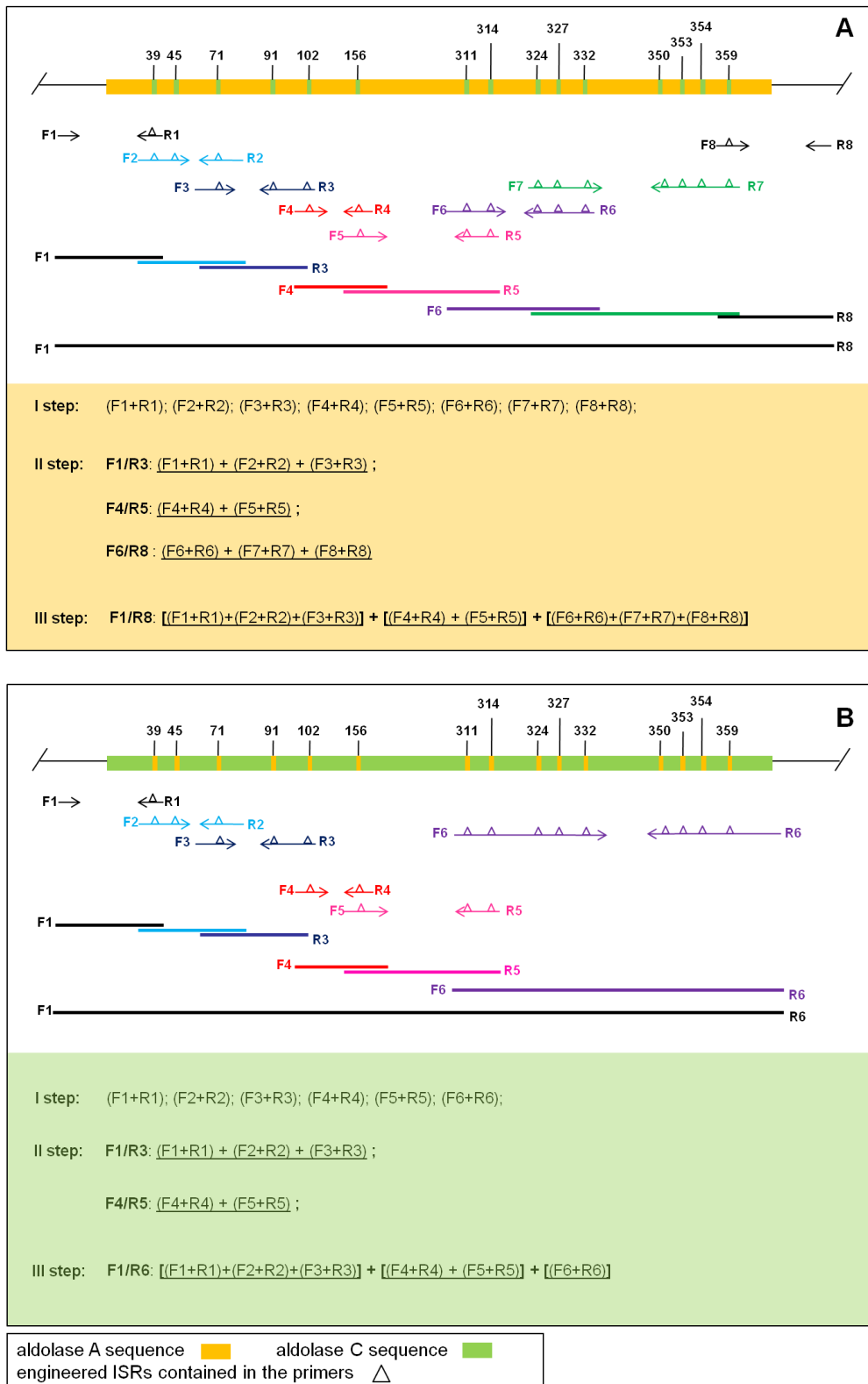


**Figure 5. Schematic representation of three steps of PCR-assisted multiple site-directed mutagenesis performed to amplify AC (A) and CA (B) aldolase chimeric genes.** Engineered ISRs, primers location and relative overlapping regions are shown both regarding AC and CA chimera genes. The three steps of PCR are also shown with a schematic overview.

## 2.16 Cloning and expression of chimeric aldolase A/C and C/A genes

The final PCR fusion products coding for chimeric AC and CA aldolase genes were purified from agarose gel (Qiaquick gel extraction kit, Qiagen) and cloned in TOPO-TA cloning vector (Invitrogen). Further mutagenesis were performed in order to insert restriction enzymes sites for NdeI at 3' end of AC and CA gene and for XhoI at 5' end of CA gene, using relative AC- and CA-TOPO-TA constructs as template. The primers used for the mutagenesis are:

Fw mut NdeI AC: 5'-TCACACAGGAAACAGCATATGCCTCACTCCCATCCAGCG-3'

Rv mut NdeI AC: 5'-CGCTGGATGGGAGTGAGGCATATGCTGTTTCCTGTGTGA-3'

Fw mut NdeI CA: 5'-CACACAGGAAATAGCATATGTCACCTCACTCGTACCCAGCC-3'

Rv mut NdeI CA: 5'-GGGCTGGGTACGAGTGAGGTGACATATGCTATTTTCCTGTGTG-3'

Fw mut XhoI AC: 5'-CGCCCCCTCAACACTCGAGGCTCCAGCACCGG-3'

Rv mut XhoI AC: 5'-CCGGTGCTGGAGCCTCGAGTGTTGAGGGGGCG-3'

These mutagenized genes were digested, purified (Qiaquick gel extraction kit, Qiagen) and cloned in the expression vector PET16b by using restriction enzymes NdeI (3') and XhoI (5') for AC aldolase gene and NdeI (3') and BamHI (5') for CA aldolase gene. PET16b expression vector carries the IPTG (indolyl- $\beta$ -D-galactopyranoside) inducible T7 promoter at the 5' of the multiple cloning sites, and an His-Tag coding sequence (6 histidine residues) at the 3' end. Each step of cloning and mutagenesis was followed by sequencing (CEINGE Biotecnologie Avanzate s.c.ar.l., Napoli, Italia). The resulting N-terminal HIS-tagged chimeric aldolase proteins were expressed in BL21 competent cells which express the T7 RNA polymerase.

## 2.17 Affinity chromatography and recombinant aldolases purification

The HIS-tagged chimeric aldolases were purified through affinity chromatography using a Nickel resin (Ni-NTA Superflow, Qiagen) binding the HIS-tag of wt and chimeric proteins. Buffers containing 300 mM NaCl, 50 mM NaH<sub>2</sub>PO<sub>4</sub> pH 8.0, 20% glycerol and increasing concentration of Imidazole were used to lysate the cells (20 mM Imidazole), wash the columns (50 mM Imidazole) and elute the samples (250 mM Imidazole competing with the proteins HIS-tag for the Nickel resin binding).

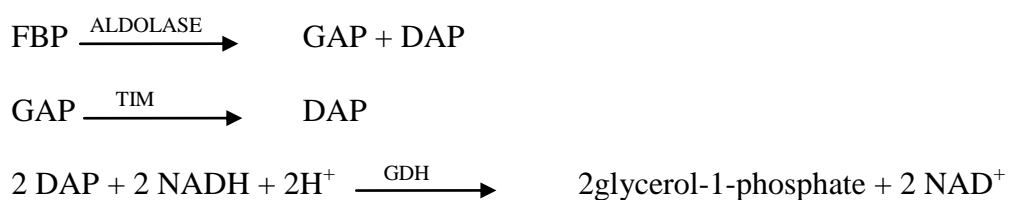
The preparation and purification of chimeric proteins was performed as follows:

- 25 µl from stabs of BL21 bacterial cells transformed with PET16b constructs containing wt and chimeric genes (PET16b-AldoAwt; PET16b-AldoCwt; PET16b-AldoAC; PET16b-AldoCA) were inoculated in 5 ml LB (Luria Bertani) medium plus ampicillin and let grow O.N at 37°C;
- Inocules were diluted 1:100 in 500 ml of LB medium plus ampicillin and let grow at 37°C until they reach an inducible 0,4-0,6 optical density (O.D.) measured at 600 nm with the spectrophotometer (Cary 50 Bio, Varian);
- BL21 cell cultures were induced by adding IPTG to a final concentration of 1 mM;
- After 3 hours, cell cultures growth was stopped and the O.D. units were measured with the spectrophotometer (1,5-2 O.D.);
- BL21 cell cultures were centrifuged at 3.000 rpm for 30 minutes;
- Pellets were put on ice, resuspended in 20 mM Imidazole Buffer, sonicated 30'' for 6 times and syringed 2 times;
- Samples were centrifuged at 9.000 rpm for 45 minutes at + 4°C;
- Supernatants were incubated with 450 µl of Nickel resin (Promega) for 1 hour on a rotating platform at + 4°C;
- Samples were loaded on columns;

- Columns were washed 2 times with 4 ml of 50 mM Imidazole buffer;
- 10 fractions were eluted with 225  $\mu$ l of 250 mM Imidazole Buffer;
- The concentration of each proteic fraction was determined with the spectrophotometer (Cary 50 Bio, Varian) by performing a Biorad assay and 5  $\mu$ l of each fraction was also loaded on a 10% acrylamide gel (SDS-PAGE) and checked through coomassie staining ;
- The more concentrated fractions, generally the first 7 fractions, were pulled together and dialysed against TRIS 20 mM and Glycerol 50% O.N. at 4°C;
- Concentration of dialysed proteins was quantified by spectrophotometer readings;
- Purified proteins were aliquoted and kept at -20°C.

### 2.18 Steady-state Kinetics

Aldolase activity toward fructose-1,6-bisphosphate (FBP) was measured as described previously (93, 94). Briefly, a decrease in absorbance at 340 nm was measured from an assay coupled to  $\beta$ -NADH oxidation by glycerol-3-phosphate dehydrogenase. The reaction was as follows:



Loss of NADH is proportional to conversion of DHAP to G3P, and the creation of DHAP is proportional to FBP cleavage (aldolase activity).

Enzymes were diluted in 50 mM TRIS-HCl (pH 7.4), 10 mM EDTA, 20  $\mu$ g/ml glycerol-3-phosphate dehydrogenase, 20  $\mu$ g/ml triosephosphate isomerase (Sigma), and 0.2 mM  $\beta$ -

NADH (Sigma). Assays were performed at 20°C and 30 °C in triplicate using a Cary 1E UV-vis spectrophotometer (Varian) in a final volume of 1 ml. Reactions were monitored every second for 5 minutes. For the AC chimera, the FBP concentration ranged from 10 mM to 50  $\mu$ M with 3  $\mu$ g/ml enzyme. For the CA chimera the FBP concentration ranged from 3 mM to 10  $\mu$ M with 3  $\mu$ g/ml enzyme. For the wt A and C aldolases, the FBP concentration ranged from 2 mM to 10  $\mu$ M with 3  $\mu$ g/ml enzyme. Results were analysed by the Kaleidagraph programme.

### **2.19 Preparation of construct for aldolase C - conditional knockout**

The EMBL (European Molecular Biology Laboratory) of Monterotondo (Rome) provided us the construct to produce a conditional knockout mouse for aldolase C gene.

The construct is 11.555 bp long. It shows, from the origin (5') to the end (3'), the ampicillin resistance cassette, the aldolase C gene from the 3' end to the 5' end, interrupted between the VII and the VI exon where the neomycin (neo) cassette is inserted. The neo cassette is flanked by FRT sequences (target of the FLP recombinase) and two loxP sequences (target of CRE recombinase) are present, one between the VII exon and the first FRT sequence and the other between the third and second exon of aldolase C gene.

The strategy includes a first recombination event mediated by the FLP recombinase, in order to excise the neo cassette, and a second recombination mediated by CRE recombinase excising the central part of the gene, from exon II to VI.

### **2.20 From electroporation of ES cells to microinjection into mouse blastocysts: chimera mouse**

The steps going from the electroporation of ES cells to the final production of chimeric mice were provided from EMBL as well as the production of the construct.

BRUCE 4 cells deriving from C57black/6 mice were electroporated, 500 clones were picked and the first 200 were screened by Southern Blot. 8 clones were found to be positive (4% recombination). Positive clones were expanded and reconfirmed by Southern Blot. Three of these positive clones were microinjected into the blastocysts of C57bl/6 wt sacrificed pregnant mice and the blastocysts were reimplanted into the uterus of C57bl/6 wt pseudopregnant mice. A total of 4 chimeric mice (1 female and 3 males) were finally provided us from EMBL.

### **2.21 Screening of F1 generation by PCR**

4 chimeric mice provided us from EMBL were crossed at CEINGE animal house with wt mice. About 375 pups were obtained (F1 generation) and screened for germline transmission by PCR.

DNA was extracted from the tail of the pups using the following protocol:

- 750  $\mu$ l of lysis buffer ( Tris HCl pH 8.5 100 mM, EDTA 5 mM, NaCl 200 mM and SDS 0,2 %) and 40  $\mu$ l of Proteinase K (stock 10mg/ml) were added to the tails and incubated O.N. at 55°C on a platform shaker;
- The day after, samples were vortexed 5 minutes, added with 250  $\mu$ l of 6 M NaCl and vortexed again for 10 minutes;
- Samples were centrifuged at 14.000 rpm, 10 minutes at 4°C;
- 500  $\mu$ l of isopropanol were added to the supernatant and samples were vortexed for 2 minutes;
- Samples were centrifuged at 14.000 rpm, 5 minutes at 4°C;
- Pellets were resuspended in 1 ml of 70% cold ethanol and centrifuged at 14.000 rpm for 3 minutes at 4°C;
- Supernatants were taken off and samples were centrifuged again 20 seconds;

- Supernatant residues were gently removed and pellets were dried at room temperature for 15 minutes;
- 100-200  $\mu$ l of TE were added to the pellets and mixed at 4°C until the DNA was completely dissolved.

50 ng of DNA from F1 mice were amplified by PCR using the following primers and protocol:

Fw: 5'-GGTTAGGAGAGGAAGTAGAAGG-3'

Rev: 5'-CCCAATGCACTTTTTTCACAC-3'

1 step:

- Denaturation 94°C x 2'
- 35 cycles of:
- Denaturation 94° C x 30''
  - Annealing 55°C x 30''
  - Polymerization 72°C x 30''

A final step of

- Extension 72°C x 2'.

Forward and reverse primers were located at the 5' and 3' of the first loxP sequence, in the second intron. The amplified product from F1 mice positive to germline transmission is a DNA doublet (386 and 424 bp) relative to the wt and the floxed allele. In case of negative germline transmission, the primers would map only on the wt gene and the amplified product would be a 386 bp DNA singlet. DNA from chimeric mice was used as positive control.

### **3. RESULTS**

#### **3.1 Transcriptional regulation of human aldolase C gene during NGF-induced neuronal differentiation in PC12 cells**

##### **3.1.1 Analysis of aldolase C messenger expression during NGF-induced neuronal differentiation**

We previously demonstrated that human aldolase C mRNA expression is positively regulated by 8 Br-cAMP treatment in PC12 cells (44). Here, we analysed aldolase C mRNA expression in PC12 cells induced to neuronal differentiation with NGF.

Aldolase C mRNA expression was measured in PC12 cells untreated and treated with 100 ng/ml NGF for different times (30 min, 4 h, 1, 3, 7 and 14 days) by Real Time quantitative PCR, as described in the paragraph 2.12 of Materials and Methods. At the same time, we evaluated the effect of neuronal differentiation mediated by cell-growth inhibition in PC12 cells on aldolase C mRNA expression.

We used GAP43 mRNA as marker for neuronal differentiation which expression is known to be positively modulated during neuronal differentiation induced by NGF treatment.

In fact, GAP43 mRNA expression is barely detectable in undifferentiated PC12 cells (ctrl); significant increase mRNA expression is evident from 30 minutes NGF treatment with a 40-fold maximal expression found after 14 days of treatment (Fig. 6A, 30 min, 4h, 1, 3, 7 and 14 days, blue bars).

In untreated cells, GAP43 mRNA expression was significantly up-regulated from 7 days after plating, when cells reached confluence, and no additional increase was evidenced after 14 days of culture compared with 7 days (Fig. 6A, 7 days vs 14 days, green bars).

This observation supports the hypothesis that GAP43 mRNA is specifically up-regulated



by NGF, and that cell growth arrest had minimal role in the modulation of GAP43 expression (maximum 8-fold to respect ctrl, Fig. 6A, green bars).

Similarly to GAP43, a slight positive modulation of aldolase C mRNA expression is detectable 7 days after plating (about 3-fold increase compared to ctrl); further increase is present after 14 days, about 8-fold (Fig. 6B, green bars). This increase parallels GAP43 mRNA increase (Fig.6 A-B, compare green bars) suggesting that neuronal differentiation induced by cell-growth inhibition is also able to induce a weak up-regulation of aldolase C mRNA expression (Fig. 6A green bars).

In NGF treated cells, an early increase (about 2-fold) of aldolase C mRNA expression is already evident after 30 minutes of treatment, compared to ctrl; further significant increases are evident after 4 hours and until 7 days of treatment; maximal increase, about 10-fold, is evident after 14 days of treatment (Fig. 6B, blue bars).

Aldolase C mRNA expression parallels GAP43 mRNA expression starting from 30 minutes of treatment and reaching maximal expression levels after 14 days of treatment, even if aldolase C levels are lower than those of GAP43 (Fig. 6B, blue bars).

These results support the hypothesis that aldolase C mRNA expression is specifically up-regulated during neuronal differentiation mediated by NGF. Moreover our results indicated that aldolase C mRNA up-regulation is mediated by NGF treatment during the first 3 days, and from 7 to 14 days of treatment an additive effect, due to cell-growth inhibition, positively modulates aldolase C mRNA expression.

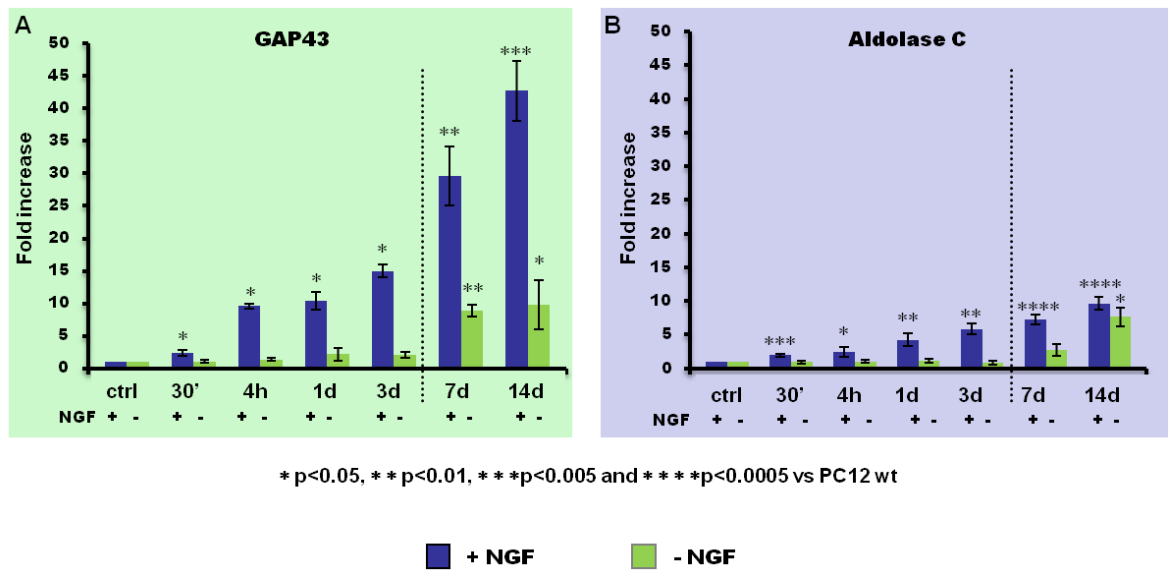


**Figure 6.**

**Real Time *quantitative* PCR of GAP43 and aldolase C.**

Relative abundance of GAP43 (A) and aldolase C (B) mRNA were determined by RT-qPCR, using c-ABL mRNA as internal standard. PC12 cells were treated for 30 min, 4 h, 1, 3, 7 and 14 days with 100 ng/ml of NGF. Arbitrary expression value 1 was assigned to untreated PC12 cells (ctrl). Relative aldolase C mRNA increase was calculated as  $2^{\Delta\Delta CT}$ . Data shown represent the mean +/- SD of three independent experiments that gave same results.

### 3.1.2 Identification of human aldolase C gene promoter region responsive to NGF

Two regions in the promoter of human aldolase C gene have been identified and characterized so far. These regions are involved in the complete and correct transcription of the gene in human cell lines and in the adult mouse brain, Fig. 1A (40). In the distal promoter region of the human aldolase C gene we identified the element D (-203/-196 bp, Fig. 1A) that binds the transcriptional activator NGFI-B and mediates cAMP up-regulation of the aldolase C mRNA in PC12 cells. In order to assess whether increased expression of the messenger, detectable after 3 days of NGF treatment, was due to a transcriptional event, and to identify *cis*-element(s) responsive to NGF in the promoter of the gene, we performed transient transfection experiments in PC12 cells treated with NGF. Six CAT-reporter plasmids containing the complete promoter region (from -1190 to +20bp),  $\Delta$ -1190-CAT, or deleted regions of the promoter:  $\Delta$ -420-CAT,  $\Delta$ -260-CAT,  $\Delta$ -260\*-CAT,  $\Delta$ -208-CAT and  $\Delta$ -164-CAT, have been used.  $\Delta$ -164-CAT construct, containing the proximal promoter region (-164/+20 bp) shows minimal transcriptional activity, about 4% (Fig. 7, green bar) and no significant variation in CAT-activity was observed after NGF treatment (100 ng/ml) for 3 days (Fig. 7, blue bar). This demonstrates that, similarly to that previously observed in SKNBE and in PC12 cells treated with cAMP, the proximal promoter region (-164 to +20 bp) of the human aldolase C gene is required only for minimal transcriptional activity (40). The region from -208 to -260 bp is required for transcriptional activation of the gene, as evidenced by significant increase, about 3-fold of CAT activity of  $\Delta$ -208-CAT, and about 4-fold of CAT activity of the  $\Delta$ -260- and  $\Delta$ -260\*-CAT constructs with respect to  $\Delta$ -164-CAT construct (Fig. 7, green bars). Treatment with NGF for 3 days produced a further increase, about 5-fold, in the CAT activity of  $\Delta$ -208-CAT compared to  $\Delta$ -164-CAT construct (Fig. 7, blue bar) and of about 8-fold in  $\Delta$ -260- and  $\Delta$ -260\*-CAT constructs with respect to  $\Delta$ -164-CAT (Fig. 7, blue bars). This result

supports the hypothesis that increase in aldolase C mRNA expression found after 3 days of NGF treatment was due to a transcriptional activation mechanism and indicates the region from -208 to -260 bp in the distal promoter as responsive. Furthermore, since the binding site for element D in the  $\Delta$ -260\*-CAT construct was destroyed, this indicates that further cis-elements different from element D, mediate the up-regulation of human aldolase C gene transcription during NGF treatment. Our results also evidenced in the distal region of the human aldolase C gene two additional segments involved in the transcriptional regulation: the segment from -260 to -420 bp and the segment from -420 to -1190 bp. CAT activity of  $\Delta$ -420- and  $\Delta$ -1190-CAT constructs were similar to  $\Delta$ -164-CAT construct activity and was reduced with respect to  $\Delta$ -260-CAT construct (Fig. 7, green bars). This suggests that transcriptional repressor(s) bind the region from -260- to -1190 bp. Interestingly, NGF treatment produces about 2-fold increase in the  $\Delta$ -420-CAT and  $\Delta$ -1190-CAT constructs activity (Fig. 7, blue bars), suggesting that NGF mediates removal of negative transcriptional regulators from distal region of aldolase C promoter region.

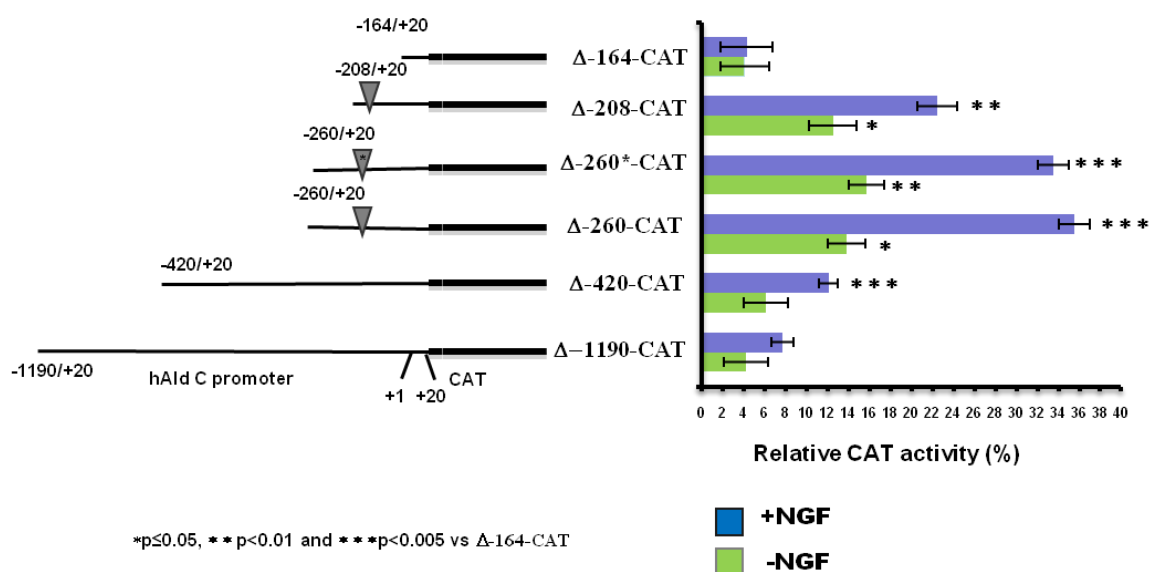


**Figure 7.**

**Scheme of CAT-constructs and relative CAT activity.**

PC12 cells were transiently co-transfected with pRL-LUC plasmid as internal standard and with different aldolase C promoter-CAT constructs, containing serial deletions of the promoter region or site-directed mutation of the NGFI-B transcription factor ( $\Delta-260^*$ -CAT) binding site. Aldolase C-CAT constructs are shown on the left. pEMBL-CAT and CMV-CAT are used as negative and positive controls, respectively. Cells were untreated (green bars) and treated with 100 ng/ml NGF for 3 days (blue bars). The data represent the mean  $\pm$  SD from three independent experiments performed in duplicate. Relative CAT activity is reported as the percentage to respect to CMV-CAT activity (taken as 100%).

### **3.1.3 Identification of a transcriptional factor binding in the distal promoter region of human aldolase C gene responsive to NGF**

In order to identify binding site(s) for transcriptional activators in the distal promoter fragment (-164/-260 bp) of human aldolase C gene, responsive to NGF treatment, we performed electrophoretic mobility shift assays using nuclear extracts from PC12 cells untreated and 3 days-treated with NGF and BRDL1 oligonucleotide (-245/-194 bp, Fig. 8A) as probe. In untreated cells 4 shifted complexes are detectable: C1, C2, X and C3 (Fig. 8B, lane 2). These complexes are specifically competed by a 100 X molar excess of the same cold oligonucleotide BRDL1 (Fig. 8B, lane 3). When a 100 X molar excess of Sp1 specific oligonucleotide (Fig. 8A) is used, the binding of the 4 complexes does not disappear, thus confirming the specificity of this binding (Fig. 8B, lane 6). C1, C2 and C3 complexes are specifically competed when a 100 X molar excess of L1 oligonucleotide (-211/-186 bp, Fig. 8A), containing the element D, and of 21-OH oligonucleotide (Fig. 8A), containing the binding site for NGF-IB in the 21-OH murine gene promoter, are used (Fig. 8B, lanes 4, 5, 9, 10). These results suggest that complexes C1, C2 and C3 are represented by NGF-IB and evidenced another specific complex that we called complex X, not due to NGF-IB binding. Furthermore the intensity of the complex X increased after the NGF treatment and two additional complexes appeared, C4 and C5 (Fig. 8B, lane 7). A 100 X molar excess of L1 and 21-OH oligonucleotides specifically competed the binding of C4 and C5 complexes suggesting that this could be due to two different NGF-IB isoforms.

In order to look for the identity of the complex X we used the TRANSFAC® database and the bioinformatic program EMBOSS TFSCAN. Two putative binding sites were found in the region spanning from -245 to -194 bp: the first was the target of the “Upstream stimulatory factor I” (USF1) transcriptional factor and the second was the target of the “Nuclear factor -I” (NF-I). A 35 bp oligonucleotide (BRD) spanning from -245 to -211 bp in the human aldolase C gene promoter (Fig. 8A) was used as probe in EMSA experiments

conducted with nuclear extracts from PC12 cells untreated and 3 days-treated with NGF. A retarded complex X is evidenced using nuclear extracts from untreated and 3 days NGF-treated PC12 cells and oligonucleotide BRD as probe (Fig. 8C, lanes 2 and 7). The complex X disappeared when a 100 X molar excess of the same (BRD) unlabelled oligonucleotide (Fig. 8C, lanes 3 and 8) or 100 X molar excess of oligonucleotide Cons USF1, which contains the consensus sequence for USF1 (Fig. 8A), were added to the mixture (Fig. 8C, lanes 4 and 9). Retarded complex X didn't disappear when a 100 X molar excess of oligonucleotide Cons NF-I, which contains the consensus sequence for NF-I (Fig. 8A), or 100 X oligonucleotide L1, which contains the promoter sequence of human aldolase C gene spanning from -211 to -186bp (Fig. 8A), were added as aspecific competitors (Fig. 8C, lanes 6 and 11). Furthermore, a slight increase in retarded complex X, is evident after PC12 cells treatment with NGF for 3 days (Fig. 8C, lanes 7-11), that is in line with the CAT-activity increase of  $\Delta$ -260CAT plasmid after 3 days of NGF treatment (Fig. 7).

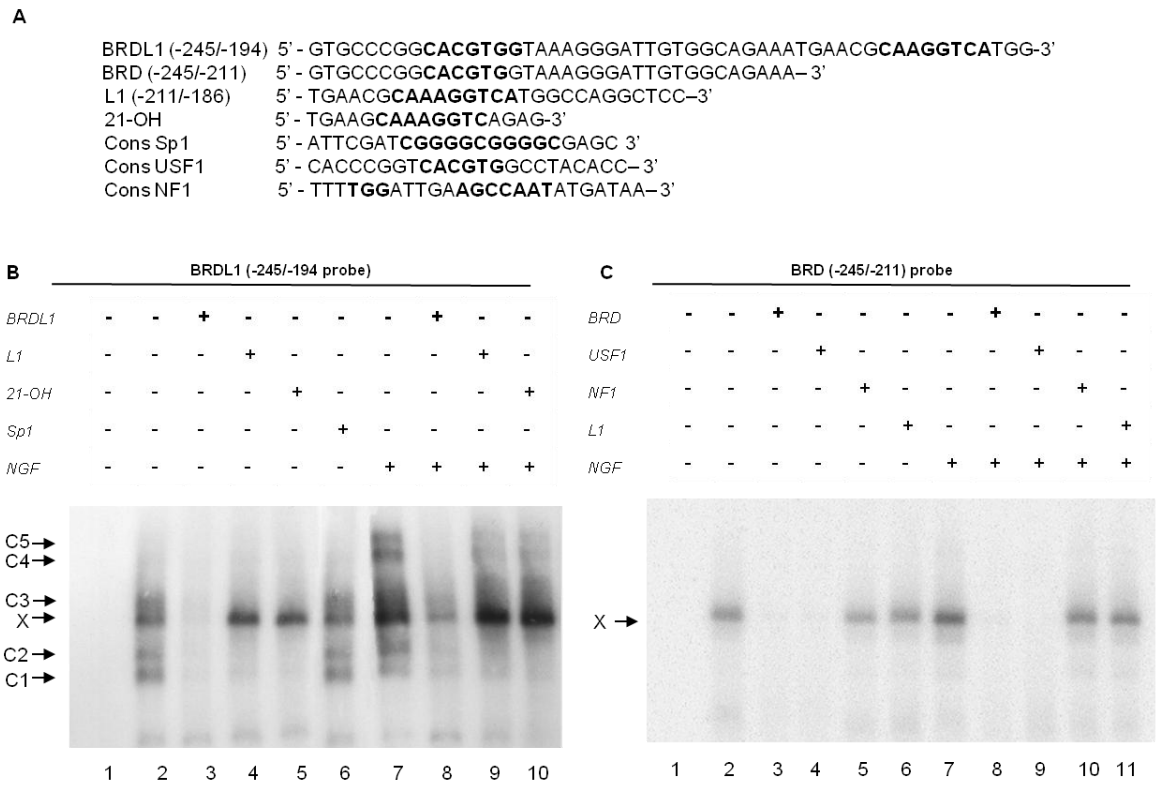


**Figure 8. (A) Oligonucleotide sequences of probes and competitors. (B) EMSA of -245/-194 *BRDL1* fragment in the promoter of human aldolase C gene.** The <sup>32</sup>P-labelled *BRDL1* probe was incubated in the absence (lane 1) or presence of 4 µg nuclear extracts from untreated PC12 cells (lanes 2-6) and 3-days NGF-treated cells (lanes 7-10). For competition experiments, a 100-fold molar excess of the unlabelled *BRDL1* (lanes 3 and 8), *L1* (lanes 4 and 9), *21-OH* (lanes 5 and 10) and *Cons Sp1* (lanes 6) oligonucleotides were added to the binding reaction. **(C) EMSA of -245/-211 *BRD* fragment in the promoter of human aldolase C gene.** The <sup>32</sup>P-labelled *BRD* probe was incubated in the absence (lane 1) or presence of 4 µg nuclear extracts from untreated PC12 cells (lanes 2-6) and 3-days NGF-treated cells (lanes 7-11). For competition experiments a 100-fold molar excess of the unlabelled *BRD* (lanes 3 and 8), *Cons USF1* (lanes 4 and 9), *Cons NF1* (lanes 5 and 10) and *L1* (lanes 6 and 11) oligonucleotides were added to the binding reaction.



### **3.1.4 Identification of USF1 as transcriptional factor binding to the distal region of human aldolase C gene promoter responsive to NGF treatment by chromatin immunoprecipitation (CHIP) assay**

To confirm the specificity of USF1 transcriptional factor binding to the element E (-245/-211 bp) in the aldolase C gene promoter, a supershift experiment was conducted using specific anti-USF1 antibodies. Nuclear extracts from PC12 cells untreated (Fig. 9A, lanes 2-9) and NGF 100 ng/ml treated for 3-days (Fig. 9A, lanes 10-15) were challenged with BRD oligonucleotide as probe. The specific complex X (Fig. 9A, lane 2) disappeared in presence of increasing amounts of anti-USF1 antibody both in untreated (Fig. 9A, lanes 6-8) and in cells treated with NGF (Fig. 9A, lanes 12-14). Complex X remains evident when an aspecific antibody “Ab-asp ” was added to the binding mix (Fig. 9A, lanes 9 and 15).

To validate the results obtained *in vitro* by EMSA, we tested whether USF1 binds the element E (-245/-211 bp) in the distal promoter region of human aldolase C gene, *in vivo*, by ChIP assay. The chromatin was cross-linked, sheared and immunoprecipitated with anti-USF1 antibody or using an aspecific antibody. The immunoprecipitated DNA fragments were PCR-amplified with primers called -319F and -201R (as described in Materials and Methods, Fig. 9B). A 100 bp amplicon, containing the -238/-233 E-box (Fig. 9B), was detected from the “input DNA” and from DNA fraction that was immunoprecipitated with anti-USF1 antibody (Fig. 9C, lanes 1 and 4); no amplicon was detected from DNA fraction immunoprecipitated with aspecific antibody (Fig. 9C, lane 3) or when no-antibody was added to the mixture (Fig. 9C, lane 2) . These results indicate that endogenous USF1 in PC12 cells binds the -238/-233 E-box in the distal promoter region of human aldolase C gene *in vivo*.

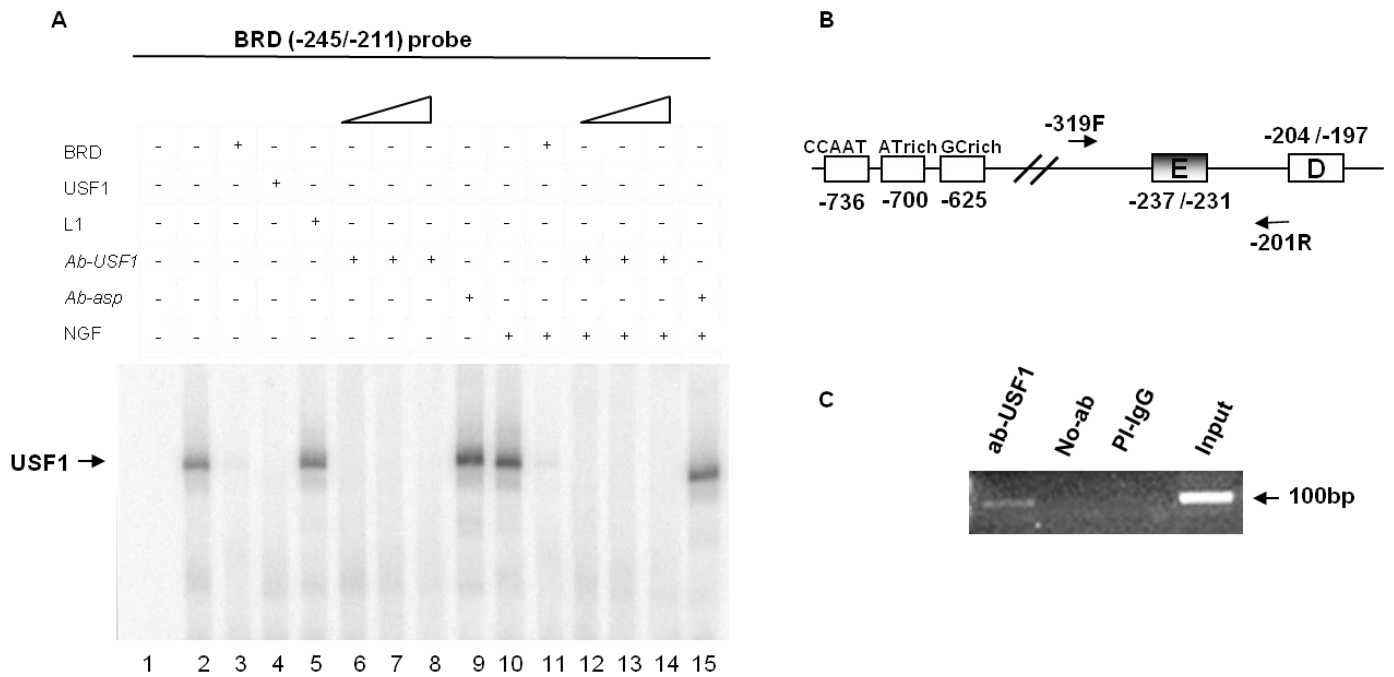


**Figure 9.**

**(A) EMSA of -245/-211 BRD fragment in the promoter of human aldolase C gene.**

4  $\mu$ g of nuclear extracts from untreated (Fig. 4A, lanes 2-9) and 3-days NGF-treated (Fig. 4A, lanes 10-15) PC12 cells were incubated with increased amounts of polyclonal anti-USF1 antibody (Fig. 4A, lanes 6-8, 12-14) using the  $^{32}$ P-labelled BRD probe described above. A 100-fold molar excess of the unlabelled probe was added to lanes 3 and 11. L1 oligonucleotide was added as non-specific competitor to lane 5 and a non-specific antibody (Ab-asp) was added to lanes 9 and 15. **(B) Schematic representation of a fragment of human aldolase C gene promoter.** The location of primers -319F and -201R (arrows) used to amplify the Input DNA containing the E-box are shown. **(C) Chromatin immunoprecipitation analysis of USF1 binding to the aldolase C promoter *in vivo*.**

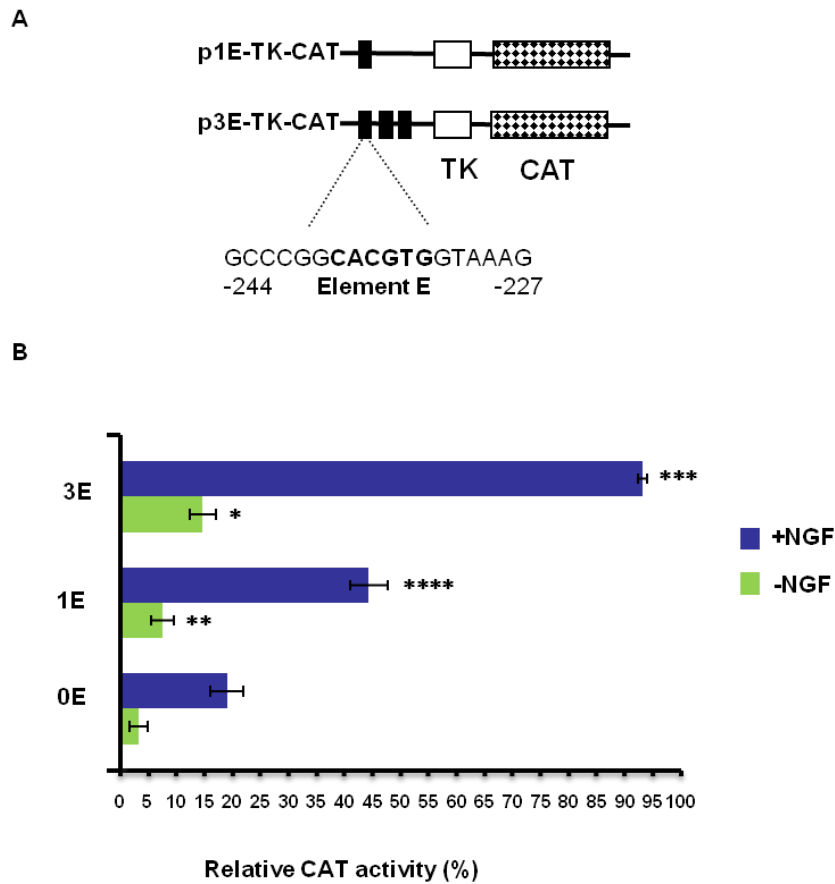
Soluble chromatin from SKNBE cells was immunoprecipitated using the USF1 antibody (ab-USF1) or incubated with normal rabbit serum (PI-IgG) or no antibody (No-ab) as negative control. The total extracted DNA (Input) prior to immunoprecipitation and the immunoprecipitated samples (anti-USF1, PI-IgG, no antibody) were PCR-amplified using primers specific to the -319/-201 fragment.

### **3.1.5 Functional analysis of USF1 binding to element E in distal region of human aldolase C gene promoter**

To confirm that USF1 acts as a transcriptional activator of human aldolase C gene we prepared two constructs, p1E-TK-CAT and p3E-TK-CAT, containing one and three concatenated elements E, respectively, inserted upstream TK promoter and CAT reporter gene in the pTK-CAT plasmid (Fig. 10A). We used these constructs to perform transient transfection experiments in PC12 cells. Relative CAT activity was measured and compared to the activity of the empty pTK-CAT plasmid.

One element E inserted before TK promoter in the p1E-TK-CAT plasmid accounted for about 5% of relative CAT activity compared with empty vector (p0E-TK-CAT) in untreated PC12 cells after 3 days from plating (Fig. 10B, green bars); this activity was 3-fold increased when p3E-TK-CAT plasmid was used (Fig. 10B, green bar), suggesting that endogenous USF1 acts as a transcriptional activator in PC12 cells. p1E-TK-CAT plasmid activity was increased of 2,5-fold after 3 days of NGF treatment with respect to p0E-TK-CAT activity in treated cells (Fig. 10B, blue bars). As could be expected p3E-TK-CAT plasmid activity was increased of about 5-fold after NGF treatment compared to p0E-TK-CAT activity in treated cells (Fig. 10B, blue bars).

These results strongly validate results obtained *in vitro* from transient transfection experiments in PC12 cells. Particularly, we suggest that the 2,5-fold increase in transcriptional activation of the construct  $\Delta$ -260-CAT after NGF treatment (Fig. 7) is closely related to USF1 binding to element E in the promoter region of human aldolase C gene.



\*  $p < 0.05$ , \*\*  $p < 0.01$ , \*\*\*  $p < 0.001$  and \*\*\*\*  $p < 0.0005$  vs 0E

**Figure 10. (A) Scheme of p1E-TK-CAT and p3E-TK-CAT constructs.** A schematic representation of the two constructs used for transient transfections of PC12 cells is shown. The sequence of element E is also reported. **(B) Relative CAT activity of p1E-TK-CAT and p3E-TK-CAT constructs.** PC12 cells were transfected with the p1E-TK-CAT or the p3E-TK-CAT reporter plasmid, containing one and three tandem copies of Element E, respectively, located upstream TK promoter and CAT reporter gene. pTK-CAT plasmid, not containing the Element E, was used as negative control. Cells were untreated (green bars) and treated (blue bars) with 100 ng/ml NGF for 3 days. pRL-LUC plasmid was co-transfected as internal standard to normalize for differences in the transfection efficiency. The data represent the mean  $\pm$  SD from three independent experiments performed in duplicate. Relative CAT activity is reported as the percentage to respect CMV-CAT activity (taken as 100%).

### **3.1.6 Subcellular localization of USF1 in PC12 cells treated with NGF**

In order to assess if NGF treatment induces nuclear translocation of USF1 inducing its binding to element E in the promoter region of human aldolase C gene, we performed immunofluorescence experiments on PC12 cells untreated and treated for 3 days with NGF. We used anti-USF1 as primary antibody and the anti-Rabbit, FITC Conjugate, as secondary antibody. Cells were treated with DAPI solution for the nucleus staining.

Results obtained pointed out that USF1 in untreated cells was localized in the cytosol (Fig. 11, panel a) and after 3 days of NGF treatment it almost completely translocated into the nucleus (Fig. 11, panel b).

Western blot analysis confirmed decreased levels of USF1 in cytosolic extracts from PC12 cells after NGF treatment for 3 days (Fig. 12A, lane 2) compared with untreated cells (Fig. 12A, lane 1). Moreover, after 3 days of NGF treatment, more abundant levels of USF1 and its phosphorylated forms are present in nuclear extracts of PC12 cells (Fig. 12A, lane 4) with respect to untreated cells (Fig. 12A, lane 3) and compared with cytosolic extracts (Fig. 12A, lanes 1, 2).

Further EMSA experiments were performed in order to verify if USF1 phosphorylation mediates its binding to element E in the human aldolase C gene promoter. BRD labelled probe was incubated with nuclear (Fig. 12B, lanes 2-8, 16-18) and cytosolic (Fig. 12B, lanes 9-15) extracts from PC12 cells untreated (Fig. 12B, lanes 2, 9) and treated with NGF for 30 min, 4h, 1 day (Fig. 12B, lanes 3-5, 10-12) and 3 days (Fig. 12B, lanes 6-8, 13-18). 100 X molar excess of the BRD (Fig. 12B lanes 8, 15) and L1 unlabelled oligonucleotides (Fig. 12B, lanes 7, 14) were used as self and non self competitors, respectively. 1 and 2,5 units of CIP (Fig. 12B lanes 16, 17) and 2,5 units of CIP(in) (Fig. 12B, lane 18) were incubated with nuclear extracts from PC12 treated with NGF for 3 days.

Results obtained support the hypothesis that in cytosolic extracts USF1 is unphosphorylated (see Fig. 12A, lanes 1, 2) and hence unable to bind DNA (Fig. 12B, lanes 9-15). Treatment with NGF induced USF1 phosphorylation and nuclear translocation thus determining an increased binding to element E (Fig. 12A, lane 4). Finally, the treatment with increasing amounts of phosphatase added to the mixture, induced a decrease of USF1 binding (Fig. 12B, lanes 16, 17), which was restored by inactivating the phosphatase (Fig. 12B, lane 18).

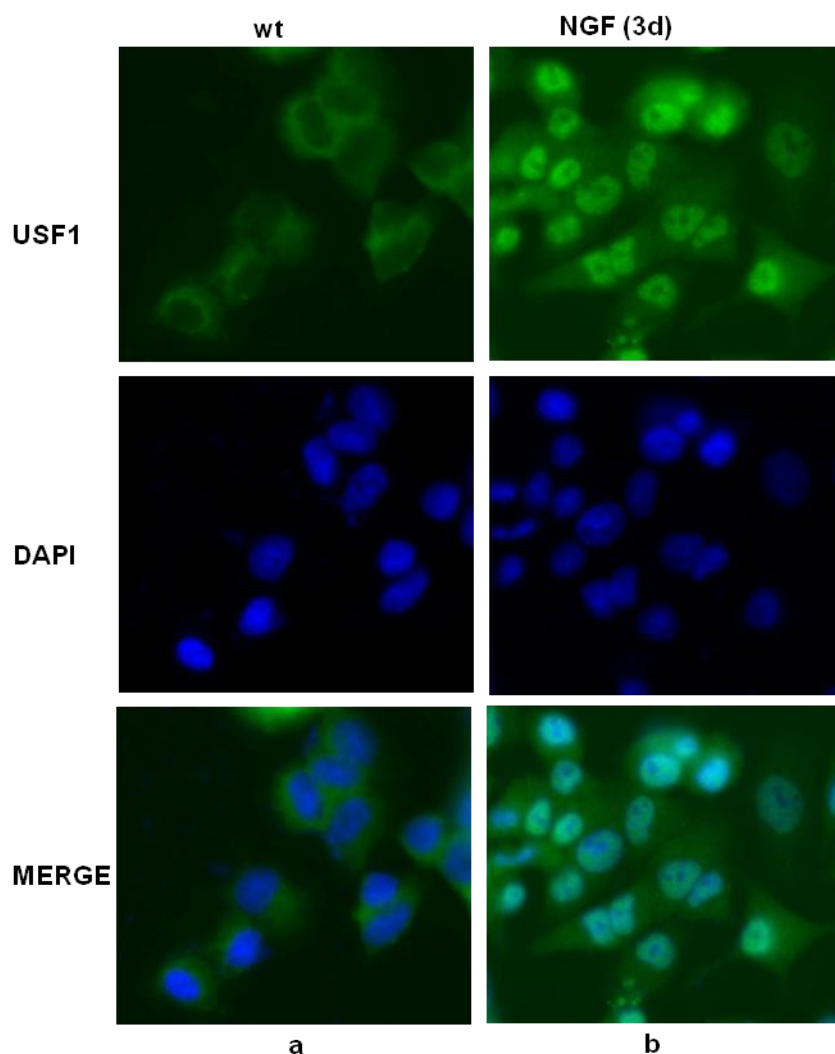


**Figure 11. Immunofluorescence analysis of PC12 cells and USF1 subcellular compartmentalization.** PC12 cells untreated (a) and 100 ng/ml NGF treated for 3 days (b) were analyzed by immunofluorescence experiments. Protein expression was detected using a primary anti-USF1 specific polyclonal antibody and revealed using a secondary fluoresceinated antibody (anti-FITC) (USF1 a and b). Nuclei were stained with DAPI (Dapi a and b). Green and blue images were merged ( Merge a and b).

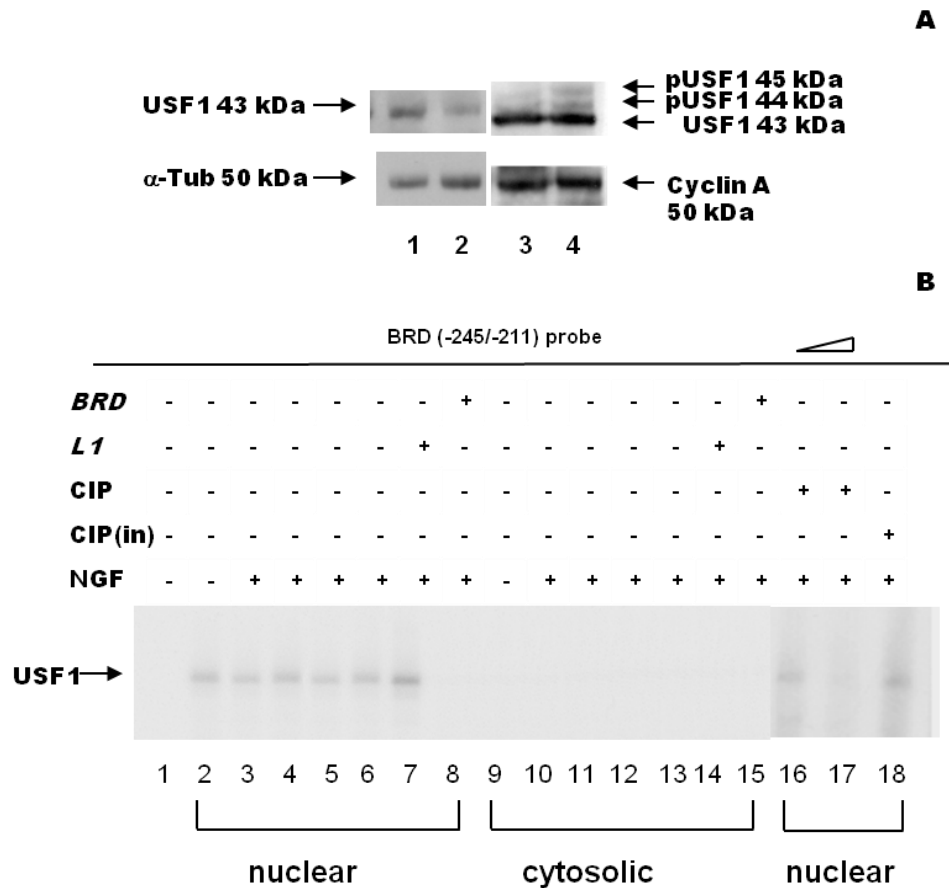


**Figure 12. (A) Western blot.** Cytosolic (lanes 1-2) and nuclear (lanes 3-4) protein extracts (50  $\mu$ g) obtained from PC12 cells untreated (lane 1 and 3) and 100 ng/ml NGF treated for 3 days (lanes 2 and 4) were analysed by SDS-PAGE. Polyclonal anti-USF1 antibody was used to reveal USF1 and phosphorylated USF1 forms (pUSF1). As control, the anti- $\alpha$ -tubulin ( $\alpha$ -Tub) and the anti-cyclin A (Cyclin A) antibodies were used for cytosolic and nuclear extracts respectively. **(B) EMSA of -245/-211 BRD fragment in the promoter of human aldolase C gene.** The  $^{32}$ P-labelled BRD probe was incubated in the absence (lane 1) or presence of nuclear extracts from untreated PC12 cells (lane 2) and treated with NGF for 30', 4h, 1 day (lanes 3-5) and for 3 days (lanes 6-8). BRD probe was also incubated with cytosolic extracts from untreated PC12 cells (lane 9) and treated with NGF for 30', 4h, 1 day (lanes 10-12) and for 3-days (lanes 13-15). For competition experiments 100-fold molar excess of the unlabelled probe (lane 8, 15) or non-specific competitor (L1, lanes 7, 14) were added to the binding reaction. 1 and 2,5 units of CIP (lanes 16, 17) and 2,5 units of CIP(in) (lane 18) were incubated with nuclear extracts from PC12 treated with NGF for 3 days.



## **3.2 Transcriptional regulation of human aldolase C gene during development in transgenic mice**

### **3.2.1 Expression analysis of endogenous aldolase C and LacZ transgene messengers in pAldC-2500-LacZ transgenic mice during development**

As described in the introduction, we previously demonstrated that the construct pAldC-2500-LacZ, containing the complete promoter region so far described (1200 bp) of human aldolase C gene up to the methionine in the second exon (1300 bp) fused to the reporter gene LacZ, directs brain-specific expression of the transgene in adult mice, with a stripe-like distribution in the Purkinje cell layer of the cerebellum.

During my PhD I contributed to the analysis of endogenous and hybrid aldolase C mRNAs expression in the brain and other organs of pAldC-2500-LacZ transgenic mice at different developmental stages in order to understand if this construct was able to drive brain-specific LacZ expression also during development.

Embryos from pAldC-2500-LacZ transgenic mice line were obtained at developmental stages E13 and E15. Mice from pAldC-2500-LacZ transgenic mice line were sacrificed at different developmental stages: P0 (newborn), P7, P14 and P42 (adult). We obtained total RNA from embryos body, head and liver at developmental stages E13 and E15; total RNA was also obtained from brain, cerebellum, heart, kidney and liver of transgenic mice at developmental stages P0 (newborn), P7, P14 and P42 (adult). Total RNA was reverse transcribed into cDNA to then perform RT-qPCR experiments as described in Materials and Methods.

In liver, kidney and heart, both aldolase C endogenous and AldC/LacZ hybrid messengers are barely detectable in the earlier developmental stages and absent in adult stages (Fig. 13).

Endogenous aldolase C mRNA starts to be detectable at E15 stage, then, in the brain, is abundant at birth (P0) and reaches maximal expression levels in the adult stage (P42) (Fig. 14, blue bars); the AldC-LacZ hybrid messenger appears with a slight delay to respect to the endogenous messenger (P0 instead of E15) and is expressed at lower extent to respect to the endogenous mRNA in developmental brain (from P0 to P14) (Fig. 14, yellow bars). However, its expression pattern follows the endogenous aldolase C mRNA expression pattern and the difference between endogenous and hybrid mRNAs levels becomes even lower in the adult stage (Fig. 14, green bars, P42).

In the cerebellum, the hybrid messenger expression pattern (Fig. 15, yellow bars) is similar to that of the endogenous (Fig. 15, blue bars) even if it is postponed in time.

These results suggest that the human aldolase C promoter, present in the construct pAldC-2500-LacZ, contains all the elements necessary to direct brain-specific expression of the LacZ reporter gene in the adult mice brain. Lower levels of hybrid messenger in the developing brain also suggest that pAldC-2500-LacZ construct lacks some enhancer elements. Further experiments are in progress to verify these data and to obtain a larger construct containing the putative enhancer elements up to the 2500 bp fragment of human aldolase C promoter.

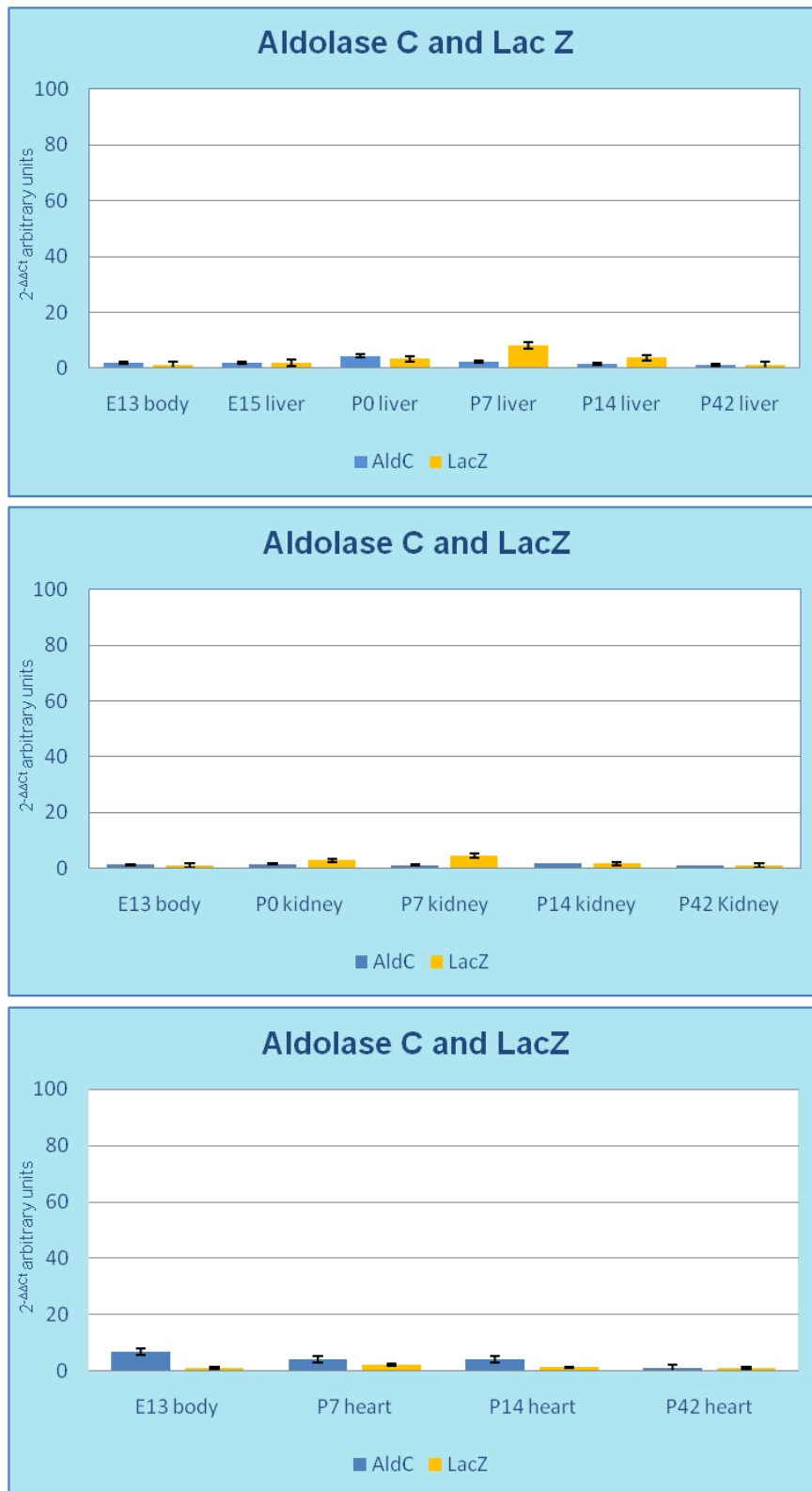


**Figure 13. RT-qPCR on cDNA from heart, kidney and liver of pAldC-2500-LacZ transgenic mice during development.** Endogenous aldolase C (blu bars) and LacZ (yellow bars) mRNA expression levels are shown. Data are presented as the means  $\pm$  standard deviation of three separate experiments.

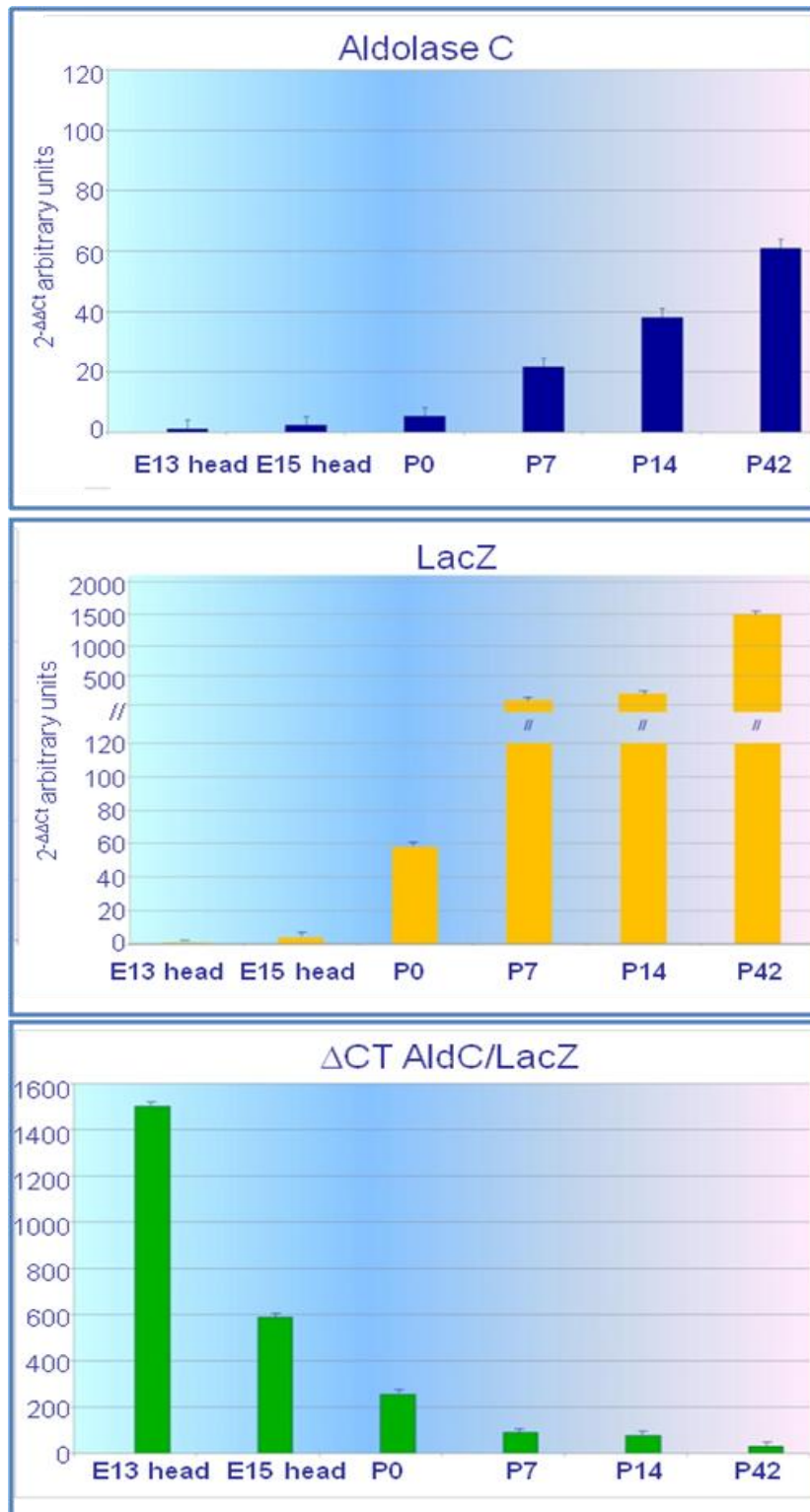


**Figure 14. RT-qPCR on cDNA from brain of pAldC-2500-LacZ transgenic mice during development.** Endogenous aldolase C (blue bars) and LacZ (yellow bars) mRNA expression levels are shown. Green bars represent the ratio between AldC and LacZ  $\Delta C_t$  values. Data are presented as the means  $\pm$  standard deviation of three separate experiments.

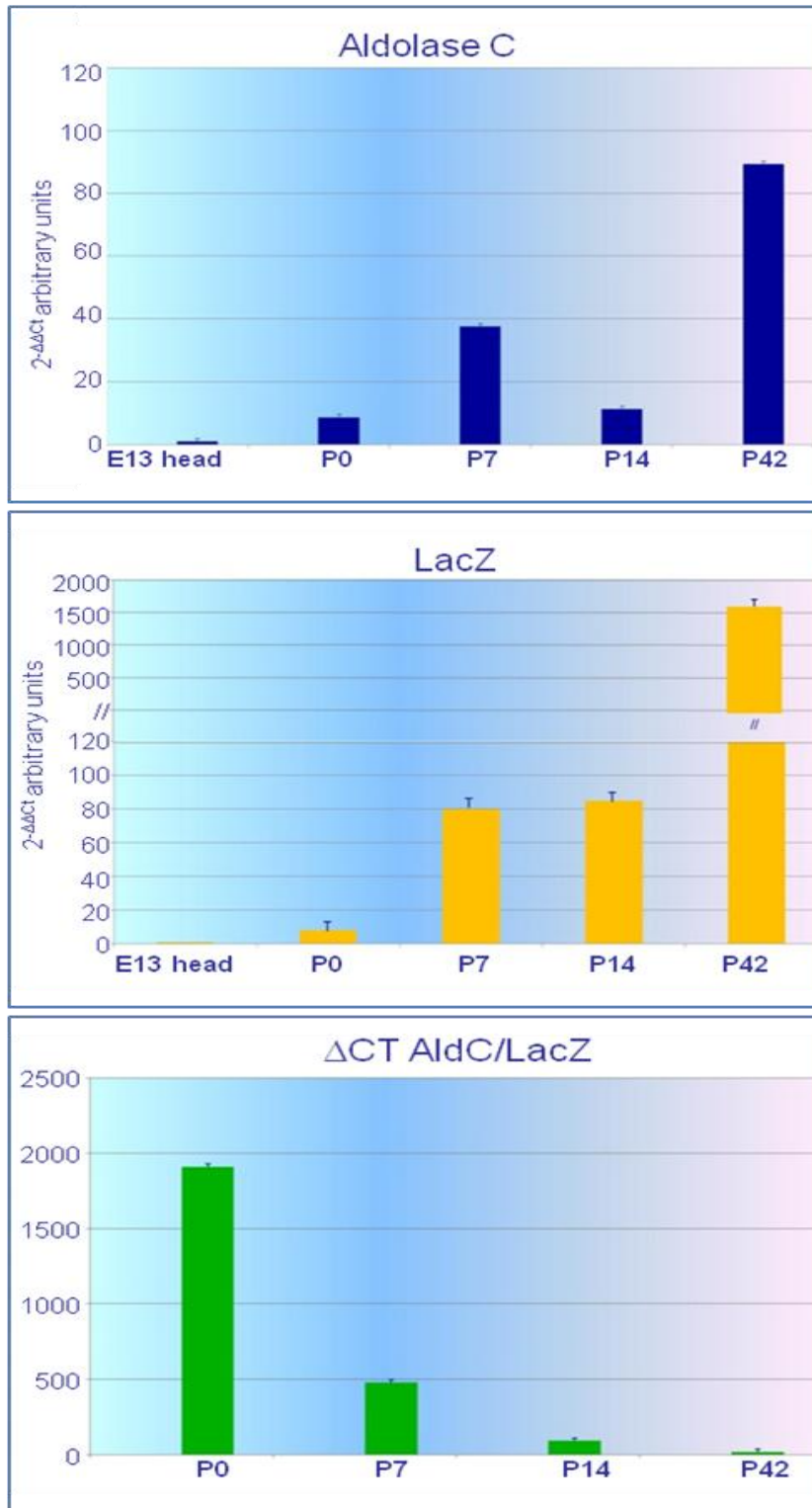


**Figure 15. RT-qPCR on cDNA from cerebellum of pAldC-2500-LacZ transgenic mice during development.** Endogenous aldolase C (blu bars) and LacZ (yellow bars) mRNA expression levels are shown. Green bars represent the ratio between AldC and LacZ  $\Delta C_t$  values. Data are presented as the means  $\pm$  standard deviation of three separate experiments.

### **3.2.2 Identification of human aldolase C gene promoter region(s) regulating $\beta$ -galactosidase activity in restricted areas of adult transgenic mice CNS**

To further investigate the promoter regions of the human aldolase C gene involved in its brain-specific and compartment-limited expression, we produced new transgenic mice lines using three different constructs (Fig. 16):

- construct pAldC-1464-LacZ, which contains only the proximal promoter region (164 bp);
- construct pAldC-1580-LacZ, which contains the proximal region plus part of the distal region including the element E (280 bp);
- construct pAldC-2336-LacZ, which contains only the distal region (1036 bp) without the proximal promoter region.

The deleted regions (164 bp, 280 bp, 1036 bp) of human aldolase C promoter in all three constructs were cloned up to a 1300 bp fragment containing the first exon and the first intron up to the methionine in the second exon fused in frame with the reporter gene LacZ (Fig. 16):

At least three different transgenic mice lines for each construct were stabilized and analysed by  $\beta$ -galactosidase ( $\beta$ -gal) assay:

- construct pAldC-1464-LacZ, lines H5, H62, H69;
- construct pAldC-1580-LacZ, lines I36, I37, I40;
- construct pAldC-2336-LacZ, lines N8, N10, N22

Transgenic mice bodies were dissected from the brains and both were analysed by  $\beta$ -gal assays: no  $\beta$ -gal activity was found in the bodies of all transgenic mice lines (data not shown). Brains from transgenic mice lines obtained with the same construct showed similar  $\beta$ -galactosidase expression patterns. As expected, among the three different lines,

$\beta$ -gal activity was found in different brain areas and with different expression levels (Fig. 17, 18, 19).

$\beta$ -gal assays were performed on whole mount brain from transgenic mice lines H, I and N, and in some cases on brain sagittal sections.

$\beta$ -gal activity was found to be very low in the brain of line H transgenic mice, specifically, in the hippocampus (h), amygdala (amg) and olfactory bulbs areas (ob) (Fig. 17, panels A, B, C). No  $\beta$ -gal activity was revealed in the cerebellum.

Transgenic mice from line I showed very strong  $\beta$ -gal activity in different areas of the brain like olfactory bulbs (ob), hippocampus (h), amygdala (amg), medulla (m) and cerebellum (cb) (Fig. 18A). Panels B and C of figure 18 show higher magnifications of cerebellum, with a clearly detectable striped-distribution of  $\beta$ -gal, and hippocampus with the dentate gyrus (DG), CA1 and CA3 neurons strongly expressing  $\beta$ -gal.

Finally, transgenic mice from line N showed a scattered  $\beta$ -gal expression in cerebral cortex (cc), olfactory bulbs (ob), hippocampus (h) and midbrain (mb) with a highest staining in the Purkinje cell layer of the cerebellum (cb) (Fig. 19, panels A and B).

$\beta$ -gal expression was successively analysed through immunohistochemistry in order to validate these results also at a single-cell level.

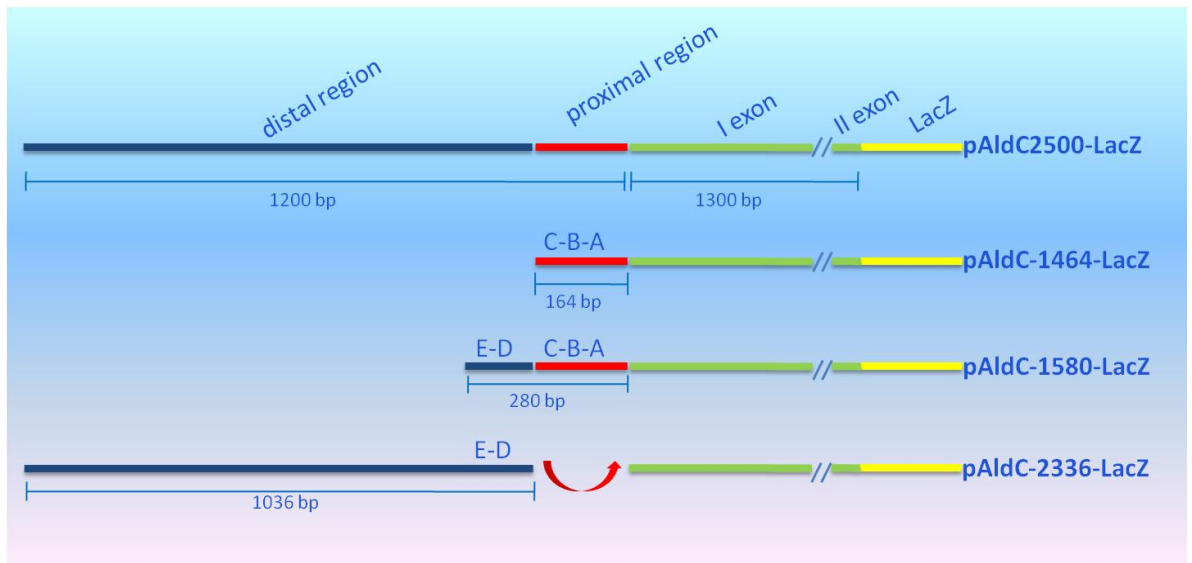


**Figure 16.**

**Schematic representation of constructs pAldC-1464-LacZ, pAldC-1580-LacZ and pAldC-2336-LacZ compared to pAldC-2500-LacZ.**

Each construct contains different deleted regions of human aldolase C gene promoter (blue bars represent the distal region and red bars the proximal region) plus a 1300 bp fragment containing the first exon, the first intron and the second exon up to the methionine (green bars) fused in frame with LacZ reporter gene (yellow bars). pAldC-2336-LacZ does not contain the proximal region and the distal region is directly fused to the first non-coding exon.



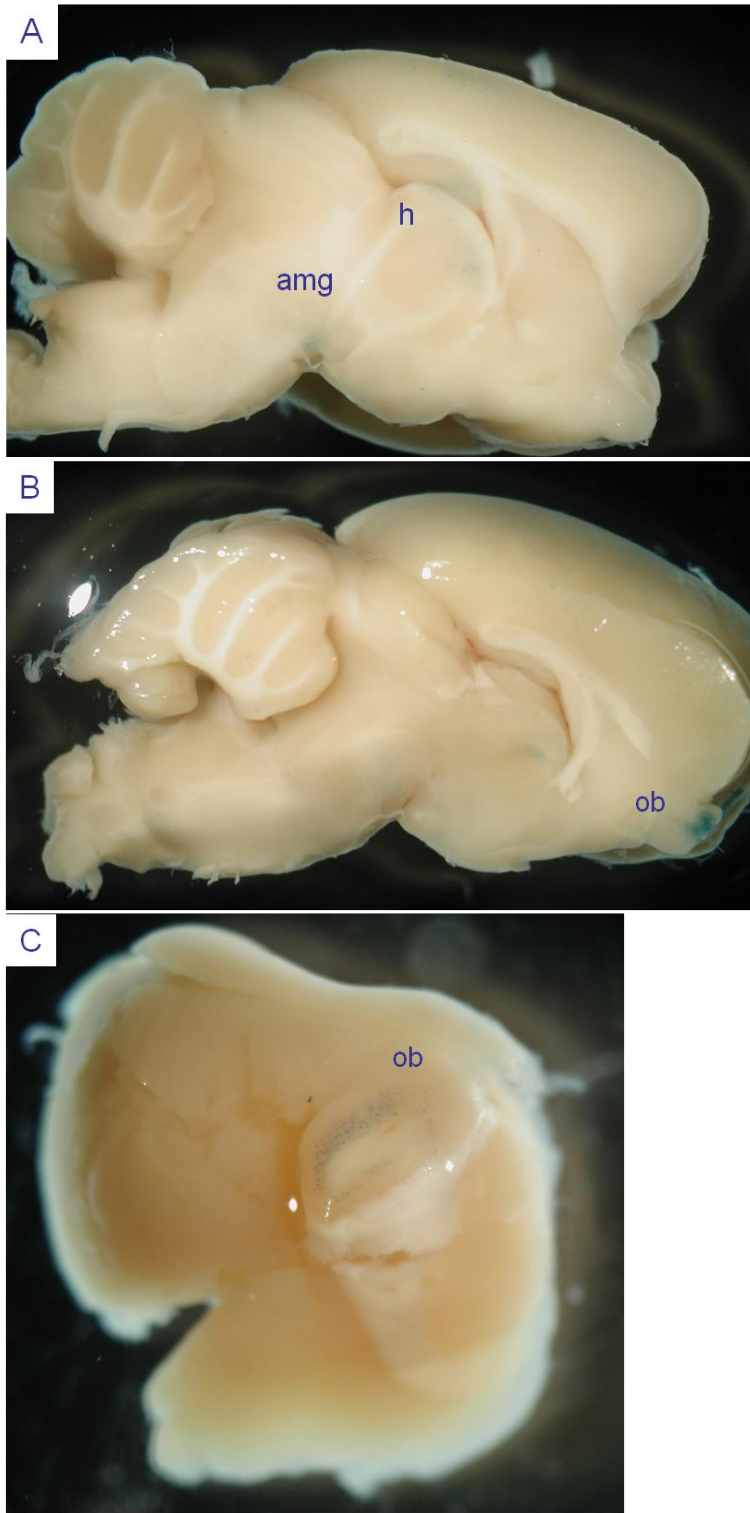


**Figure 17.  $\beta$ -galactosidase assay – line H.**  $\beta$ -gal immunostaining of whole-mount (**A, C**) and sagittal section (**B**) of brain from H5 transgenic mice line. (amg: amygdala; h: hippocampus; ob: olfactory bulbs).

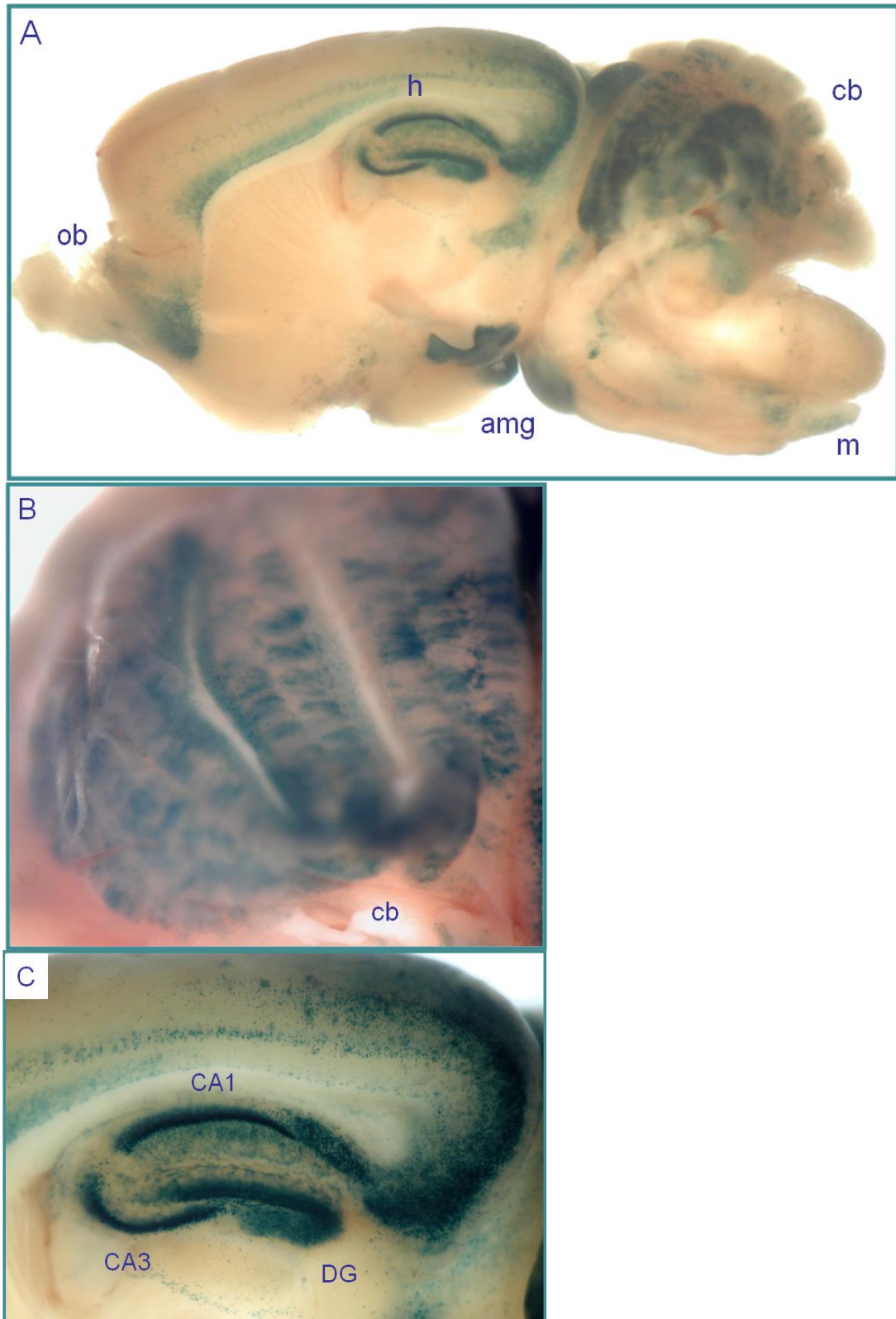


**Figure 18.  $\beta$ -galactosidase assay – line I.**  $\beta$ -gal immunostaining of a sagittal section (A) from transgenic mice brain of line I36. Panels B and C show cerebellum and hippocampus at a higher magnification (m: medulla, cb: cerebellum, amg: amygdala; h: hippocampus; ob: olfactory bulbs; CA1 and CA3 hippocampal neurons; DG: dentate gyrus).

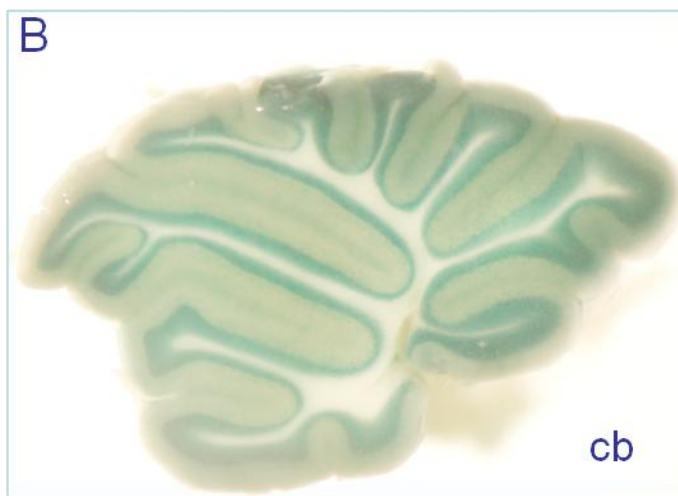
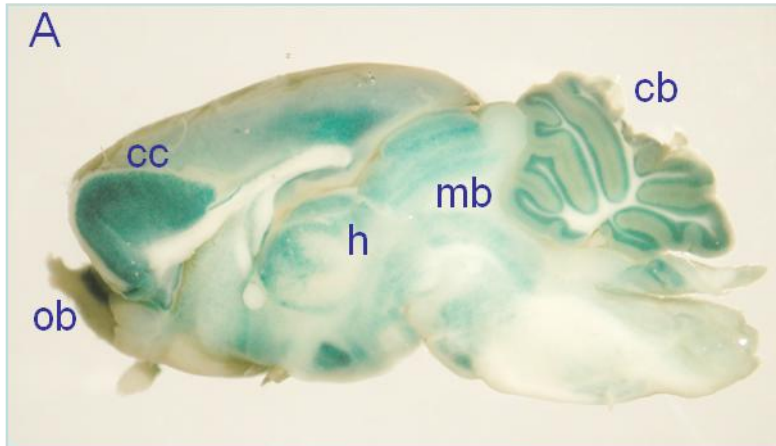


**Figure 19.  $\beta$ -galactosidase assay – line N.**  $\beta$ -gal immunostaining of whole mount brain and cerebellar sagittal section (**A**) from transgenic mice of line N22. Panels **B** show a higher magnification of the cerebellar sagittal section. (cb: cerebellum, mb: midbrain, h: hippocampus; cc: cerebral cortex; ob: olfactory bulbs).

### **3.2.3 Expression analysis of endogenous aldolase C and recombinant $\beta$ -galactosidase proteins in brain and cerebellar sections of transgenic mice**

Serial sagittal and horizontal sections of brains from lines H, I and N have been cut and immunostained with anti-calbindin and anti aldolase C polyclonal antibodies as positive controls. Calbindin is a calcium-binding protein expressed in all Purkinje cells. As already described in the Introduction, the endogenous aldolase C is expressed in groups of Purkinje cells alternating with non-expressing cells, thus giving rise to the peculiar stripe-like pattern, clearly detectable especially when brain slices are cut transversally (Fig. 3) (76).

We analysed both sagittal (data not shown) and horizontal (Fig. 20, 21, 22) cerebellar sections of transgenic mice lines H, I and N by immunohistochemistry, using a polyclonal anti- $\beta$ -galactosidase antibody, in order to understand if the different deleted regions of aldolase C promoter contained in the three LacZ-constructs, were able to drive a stripe-like expression of LacZ transgene and hence a peculiar distribution of the hybrid  $\beta$ -galactosidase protein in the Purkinje cell layer, similar to that of the endogenous aldolase C protein.

Purkinje cells of mice carrying the pAldC-1464-LacZ construct (line H), which contains the smallest fragment of human aldolase C gene promoter (164 bp), were found to be immunopositive to  $\beta$ -gal, even if its levels were very low and a longer exposure time was required for this line, to develop the specific signal (paragraph 2.12) (Fig. 20, panels E-H).

This result is in agreement with the reduced  $\beta$ -gal activity found in the brain of transgenic mice from the same line (line H, Fig. 17). The apparent discrepancy between undetectable  $\beta$ -gal activity in the cerebellum of pAldC-1464-LacZ and the presence of  $\beta$ -gal protein in the cerebellum of mice carrying the same construct can be ascribed to the greater sensitivity of the immunohistochemistry method versus the  $\beta$ -gal assays procedure.

On the contrary,  $\beta$ -gal immunoreactivity was very intense in the Purkinje cell layer of mice carrying the pAldC-1580-LacZ construct (line I), which contains the proximal promoter

region plus the element E of the distal region (Fig. 21, panels E-H). We believe that the presence of the element E in this construct makes the difference in terms of immunoreactivity levels. USF1 transcription factor binding to this element has been previously shown *in vitro* to be a transcriptional activator (chapter 3.1).

Similar results were obtained with cerebellar sections from the transgenic mice carrying the pAldC-2336-LacZ construct, which contains only the distal region (element E included) directly fused to the first non-coding exon of the gene. A mild  $\beta$ -gal immunoreactivity signal was present in the Purkinje cells of also transgenic mice of line N (Fig. 22, panels E-H).

In all three transgenic mice lines,  $\beta$ -gal expression was localized in the cytoplasm of groups of stained Purkinje cells (see higher magnification in Figs. 20, 21, 22, panels H, thick red arrows) alternating to groups of Purkinje cells don't expressing  $\beta$ -gal protein (Figs. 20, 21, 22, panels H, thin red arrows).

Finally, we found that all the three lines show a stripe-like distribution of  $\beta$ -galactosidase protein in the Purkinje cell layer of the cerebellum, even if, at different extent. These results demonstrate that even only the first 164 bp of the human aldolase C gene promoter are able to direct striped expression of  $\beta$ -gal in the Purkinje cell layer of transgenic mice. Probably, the peculiar stripe-like expression of the endogenous aldolase C and of the transgene could be also driven by sequence containing the first exon, the first intron and the second exon up to the methionine that are present in all three LacZ-constructs. Finally, we cannot exclude that also non-transcriptional event may be involved in stripe-like expression of aldolase C in the brain and cerebellum (see Discussion).

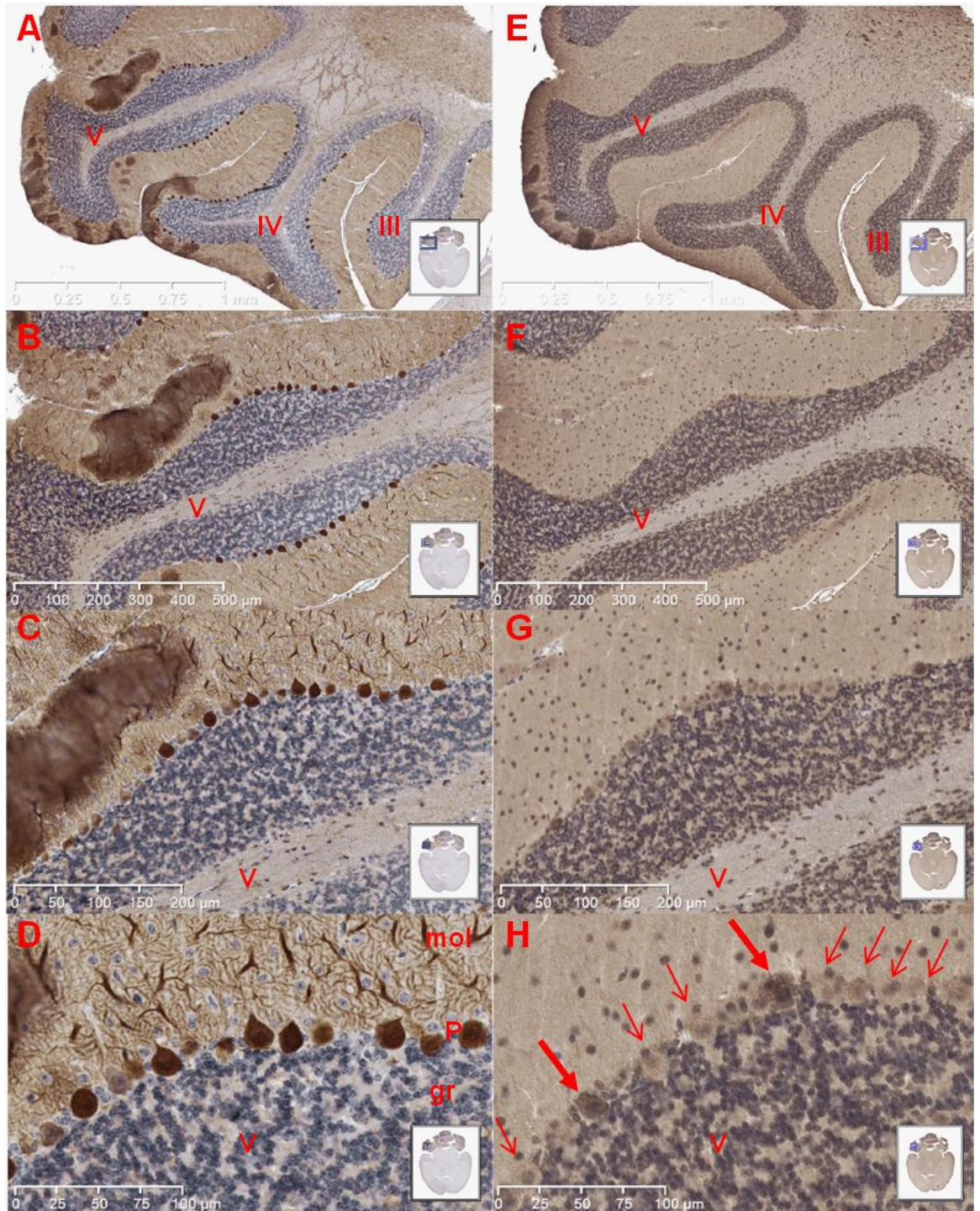


**Figure 20. Calbindin and  $\beta$ -galactosidase immunostaining on horizontal cerebellar sections of adult transgenic mice from line H.** Anti-calbindin (panels A-D) and anti- $\beta$ -gal (panels E-H) immunostaining are shown with increasing magnification of the selected cerebellar lobule V (from top to down) from transgenic mice of line H5.  $\beta$ -gal immunopositive and immuno-negative cells are indicated with red thick and thin arrows, respectively. (gr: granular layer; mol: molecular layer; P: Purkinje cell layer).

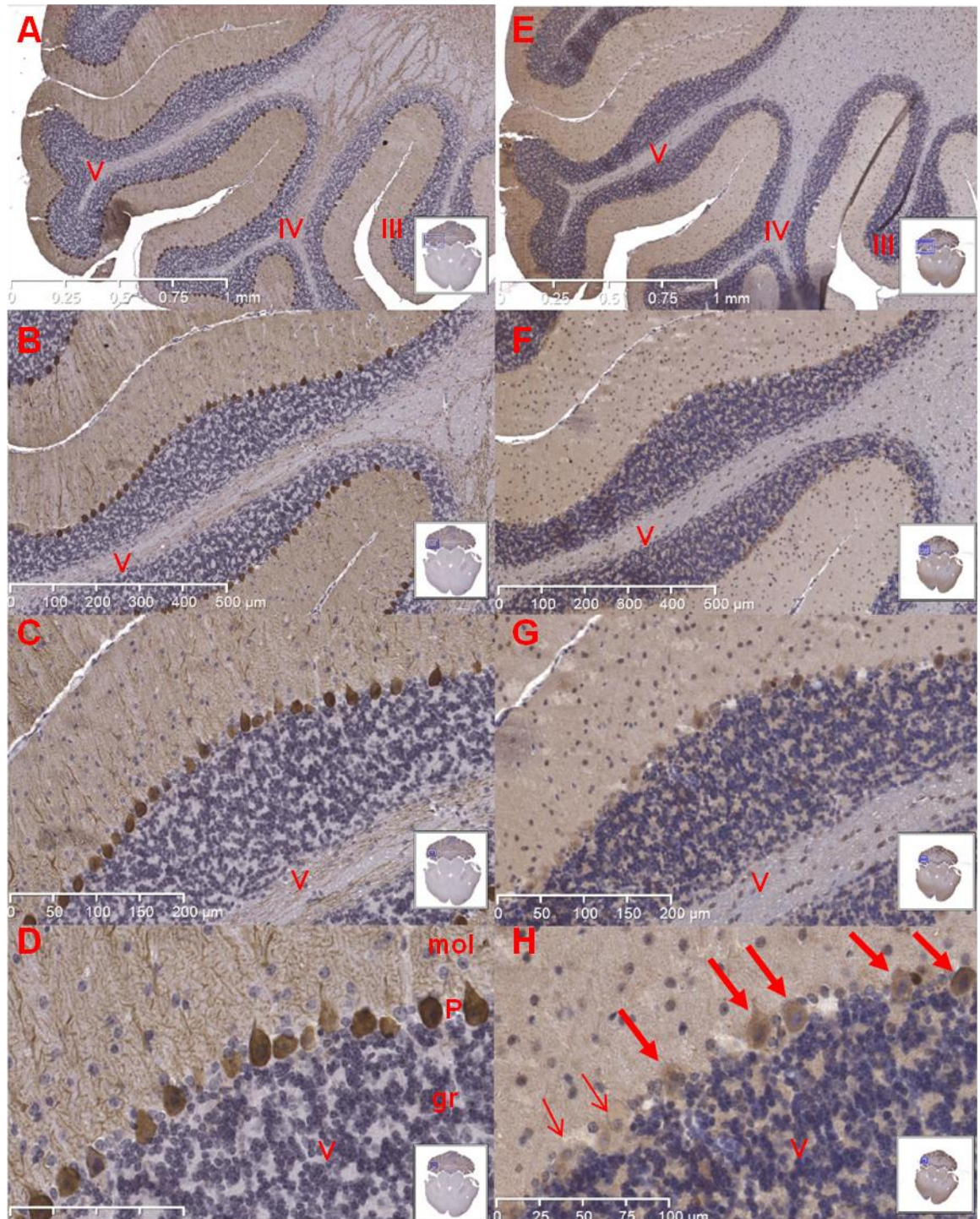


**Figure 21. Calbindin and  $\beta$ -galactosidase immunostaining on horizontal cerebellar sections of adult transgenic mice from line I.** Anti-calbindin (panels A-D) and anti- $\beta$ -gal (panels E-H) immunostaining are shown with increasing magnification of the selected cerebellar lobule V (from top to down) from transgenic mice of line I36.  $\beta$ -gal immunopositive and immuno-negative cells are indicated with red thick and thin arrows, respectively. (gr: granular layer; mol: molecular layer; P: Purkinje cell layer).

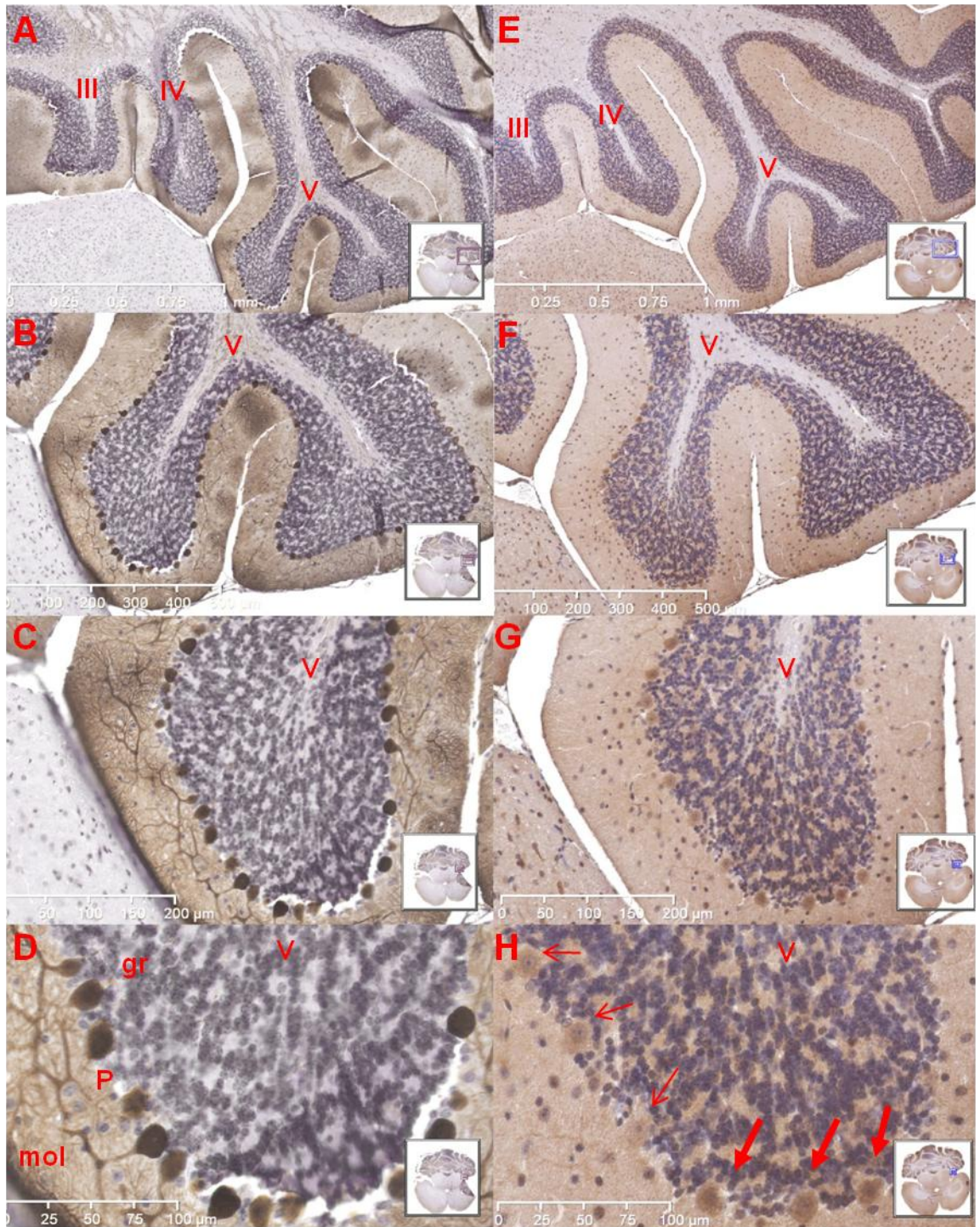


**Figure 22. Calbindin and  $\beta$ -galactosidase immunostaining on horizontal cerebellar sections of adult transgenic mice from line N.** Anti-calbindin (panels A-D) and anti- $\beta$ -gal (panels E-H) immunostaining are shown with increasing magnification of the selected cerebellar lobule V (from top to down) from transgenic mice of line N22.  $\beta$ -gal immunopositive and immuno-negative cells are indicated with red thick and thin arrows, respectively. (gr: granular layer; mol: molecular layer; P: Purkinje cell layer).



### **3.2.4 Expression analysis of LacZ transgene messenger in adult pAldC-1580-LacZ, pAldC-1464-LacZ and pAldC-2336-LacZ transgenic mice**

We analysed LacZ expression levels of at least three different stabilized transgenic mice lines for each construct: lines H5, H62, H69, for construct pAldC-1464-LacZ; lines I36, I37, I40 for construct pAldC-1580-LacZ; lines N8, N10, N22 for construct pAldC-2336-LacZ.

Among the different lines H, I and N LacZ mRNA levels were expressed at different extent.

Line H (Fig. 23, red bars) showed barely LacZ expression levels in brain and cerebellum compared with line B18 (pAldC-2500-LacZ construct) (Fig. 23, blue bars).

Line I (Fig. 23, violet bars) showed, both in brain and in cerebellum, LacZ expression levels 2-fold higher than in B18 line (Fig. 23, blue bars).

Finally, line N (Fig. 23, green bars) showed LacZ mRNA levels very low in the brain, and 3.5 fold higher than B18 line in the cerebellum, suggesting that transcriptional regulation of LacZ reporter gene in a construct lacking the proximal region is dysregulated.

As expected, line H obtained with construct pAldC-1464-LacZ containing only 164 bp of aldolase C promoter, showed the lowest LacZ expression level. We suggest that this proximal promoter region is not responsible of transcription activation but is important for a correct transcriptional regulation which results impaired when this region is lacking (see line N).

Line I showed the highest LacZ levels even if the relative pAldC-1580-LacZ construct contains only 120 bp more than pAldC-1464-LacZ construct. We believe that this transcriptional activation event is due to the presence of Element E binding the transcription activator USF1 as we previously demonstrated.

These *in vivo* results are in agreement with those obtained from  $\beta$ gal assays and immunohistochemistry and strongly validate results obtained from *in vitro* experiments we described in the chapter 3.1.

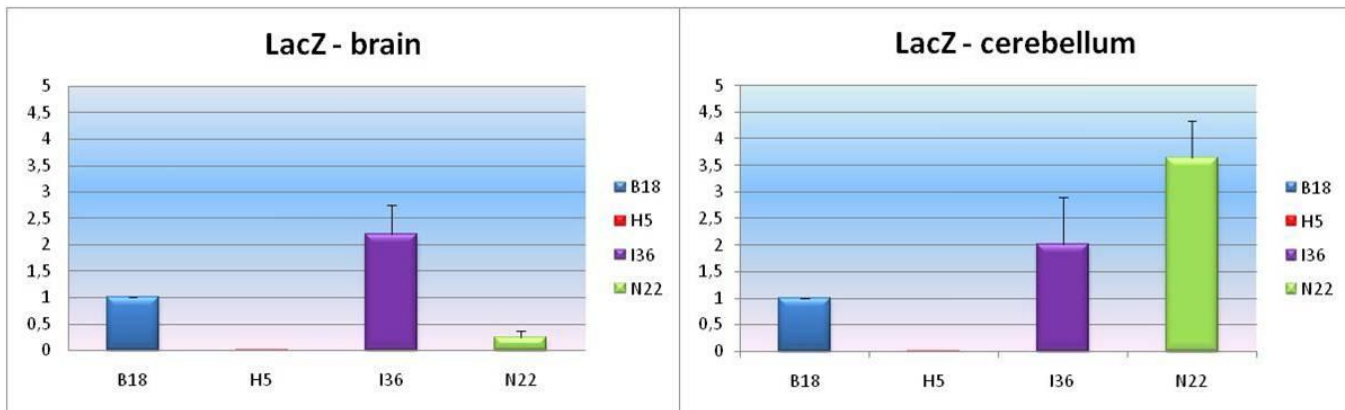


**Figure 23. RT-qPCR on cDNA from brain and cerebellum of adult transgenic mice from line B, H, I and N.** LacZ mRNA expression levels are shown and compared to those of B18 line adult mice (blue bars). Red, violet and green bars represent LacZ mRNA levels of lines H5, I36 and N22, respectively. Data are presented as the means  $\pm$  standard deviation of three separate experiments.

### 3.3 Functional role of recombinant aldolases

#### 3.3.1 Production of aldolase chimeras

The amino acid sequences of 21 vertebrate aldolase isozymes were previously analyzed to identify individual residues specific to each aldolase isozyme (22). Multiple sequence alignment revealed a total of 11 aldolase A and 4 aldolase C ISRs (Fig. 24). The conservation of ISRs among orthologs implies that they play a role in conferring the specific kinetic properties of each isozyme. In the last years, many papers have been published by Tolan et al. in which partial and total AB recombinant aldolases have been produced. They showed that  $K_m$  and  $k_{cat}$  values of wt aldolase A modified appropriately in AB chimera to closely mimic the kinetic parameters of wt aldolase B, thus demonstrating that the set of ISRs swapped between the two aldolases, is “necessary and sufficient” for determining isozyme-specific kinetic properties (22, 95). Although the location of almost all these ISRs on the tertiary and quaternary structures of aldolase was found largely on the surface and outside of hydrogen bonding distance to any active site residue, one model is that these residues influence kinetic properties at a distance from the active site (22). Long distance effects have been documented in other enzymes, such as trypsin (96) and lactate dehydrogenase (97).

In order to test this model and verify the importance of these ISRs in conferring kinetic properties to the different isozymes we engineered two mutant enzymes (chimeric aldolases) from aldolase A to C (AC aldolase) and from aldolase C to A (CA aldolase). To create the AC chimera, the complete set of ISRs from aldolase C isozyme was incorporated into the primary sequence of the aldolase A and, at the same time, the ISRs of the aldolase A were removed and substituted with the analogous residues in aldolase C. Viceversa, to create the CA chimera, we swapped ISRs from aldolase A into C, whereas at the same time exchanging the aldolase C ISRs with the analogous residues from aldolase A (Table 1).

To accomplish this, PCR-assisted multiple site-directed mutagenesis was used to engineer 22 nucleotide substitutions in the expression plasmid for wt rabbit aldolase A and 24 nucleotide substitutions in the expression plasmid for wt human aldolase C. In both the cases 15 amino acid substitutions were performed (Table 1). Finally, recombinant aldolases were expressed and purified as described in Materials and Methods (paragraphs 2.16 and 2.17) and subjected to steady-state kinetics.

### *Isozyme-specific Residue Clusters in Aldolase*

Residue	38	40	58	71	102	156	262	311	320	327	350	354	359													
	39	45	60	91	113	182	296	314	324	332	353	358	361													
Human A	S	I	A	S	Y	Q	P	R	G	V	H	I	P	A	K	G	L	Q	Y	L	A	S	E	V	S	H
Mouse A	S	I	A	S	Y	Q	P	R	G	V	H	I	P	A	K	G	L	Q	Y	L	A	S	E	I	S	H
Rabbit A	S	I	A	S	Y	Q	P	R	G	V	H	I	P	A	K	G	L	Q	Y	L	A	S	E	I	S	H
Rat A	S	I	A	S	Y	Q	P	R	G	V	H	I	P	A	K	G	L	Q	Y	L	A	S	E	I	S	H
Chicken A	S	I	A	S	Y	Q	P	R	G	V	H	I	P	A	K	S	T	Q	Y	L	A	S	E	I	S	H
Xenopus A	S	I	A	S	Y	Q	P	R	G	V	H	I	P	P	K	G	T	Q	Y	L	A	S	E	I	S	H
Human B	T	M	G	R	F	E	Q	K	I	A	Q	L	A	K	A	G	K	Q	F	M	A	T	Q	T	A	Y
Mouse B	T	M	G	R	F	E	Q	N	I	A	Q	L	A	K	A	G	K	Q	F	M	A	T	Q	T	A	Y
Rabbit B	T	M	G	R	F	E	Q	K	I	A	Q	L	A	K	A	G	K	Q	F	V	A	T	Q	T	A	Y
Rat B	T	M	G	R	F	E	Q	K	I	A	Q	L	A	K	A	G	K	Q	F	V	A	T	Q	T	A	Y
Chicken B	T	M	G	R	F	E	K	K	M	A	T	L	A	K	A	L	K	Q	F	Q	T	T	Q	T	A	Y
Sheep B	T	M	G	R	F	E	Q	K	I	A	Q	L	A	K	A	G	K	Q	F	L	S	T	Q	T	A	Y
Sbream B	T	M	G	N	F	D	N	K	I	A	G	L	A	K	A	Q	K	Q	F	K	Q	Q	Q	T	A	Y
Salmon B	T	M	G	K	F	D	N	V	I	A	A	L	A	K	A	K	K	Q	F	K	Q	M	Q	T	A	Y
Human C	S	M	A	Q	Y	Q	K	V	I	V	R	I	P	A	N	R	A	T	F	E	G	A	Q	I	A	H
Mouse C	S	M	A	Q	Y	Q	K	V	I	V	R	I	P	A	N	R	A	T	F	E	G	A	Q	I	A	H
Rat C	S	M	A	Q	Y	Q	K	V	I	V	R	I	P	A	S	R	A	T	F	E	G	A	Q	V	A	H
Chicken C	S	M	A	Q	Y	Q	K	T	I	V	N	I	P	A	S	R	A	T	F	E	G	G	Q	V	A	H
Xenopus C	S	M	D	G	Y	Q	E	T	I	V	T	I	P	A	N	R	E	T	F	E	G	G	Q	V	A	H
Goldfish C	S	M	A	P	Y	Q	K	T	I	V	T	I	P	A	S	R	E	T	F	E	G	G	Q	V	A	H
Pufferfish C	S	M	A	P	Y	Q	S	V	I	V	T	I	P	A	N	K	E	T	F	E	G	A	Q	V	E	H

**Figure 24. Isozyme-specific residues (ISRs) in vertebrate aldolases.**

Aminoacidic sequences of aldolase A isozymes from various sources were aligned and compared with aldolase B and C ISRs. Shaded and open boxes indicate the presence of non-conservative and conservative differences paralogous isozyme groups. This figure was taken from Pezza J.A. et al. (22).

### 3.3.2 Evaluation of kinetic parameters of chimeric aldolases A/C and C/A

After expression and purification of AC and CA chimeric aldolases, the steady-state kinetics toward the substrate FBP were determined using an enzyme-coupled assay (see Materials and Methods, paragraph 2.18).

By comparing data obtained from AC and CA chimeric aldolases with data obtained from wt aldolases A and C (Table 2) we expected that AC chimera should have had a decrease in both  $K_m$  and  $k_{cat}$  values. Both at RT and at 30°C we got a decrease in  $k_{cat}$  but not in  $K_m$ , which, on the contrary, showed a significant increase. We concluded that this chimera shows an activity severely impaired. As regards CA chimera, we expected it would have shown an increase in both  $K_m$  and  $k_{cat}$  values. Instead, it showed an increase in  $K_m$  but not in  $k_{cat}$  (Table 2), so we should conclude that this second chimera seems to work but not mimicking aldolase A, as it should be. Relative Lineweaver-Burk plots are shown in Figures 25 and 26 where we compared data from AC chimera to those of wt C and data from CA chimera to those of wt A aldolase.

These results show that ISRs we swapped between wt aldolases A and C unfortunately seem to be not involved in determining isozyme-specific kinetic properties, or, perhaps other, less highly conserved, residues are important. Nevertheless, these are very preliminary results of experiments that need to be repeated with some modifications at protocols and reagents components in order to get higher  $k_{cat}/K_m$  values not only for chimeras but also for wt aldolases. In fact, wt aldolases used as control, showed  $K_m$  values similar to those recently published in scientific literature, but  $k_{cat}$  values were too low, thus meaning that the efficiency of our catalytic reactions has still to be improved. Furthermore, since kinetic properties of wt A and C aldolases are not as different as for A and B isozymes, the analysis and the interpretation of data from kinetics of AC and CA recombinant aldolases is not so immediate. For this reason we thought it will be very useful to look at the activity of chimeric AC and CA aldolases also toward F1P substrate.

Steady-State Kinetics of aldolases performed at RT toward FBP			
	$K_m$ ( $\times 10^{-6}M$ )	$k_{cat}$ ( $sec^{-1}$ )	$k_{cat} / K_m$
A wt	43±0,8	3,7±0,2	0,086
C wt	32±0,6	3,6±0,2	0,112
AC	1335±90	1,66±0,05	0,0012
CA	135±1,2	1,93±0,04	0,0142

Steady-State Kinetics performed at 30°C toward FBP			
	$K_m$ ( $\times 10^{-6}M$ )	$k_{cat}$ ( $sec^{-1}$ )	$k_{cat} / K_m$
A wt	95,9±2,2	7,55±0,2	0,078
C wt	74±1,0	7,12±0,1	0,096
AC	6738±300	6,2±0,2	0,0009
CA	112,5±0,5	3,2±0,1	0,028

**Table 2.**  $K_m$  and  $k_{cat}$  values of wt and recombinant aldolases, measured at Room Temperature and at 30°C. Data represent media±SD of three separate experiments.



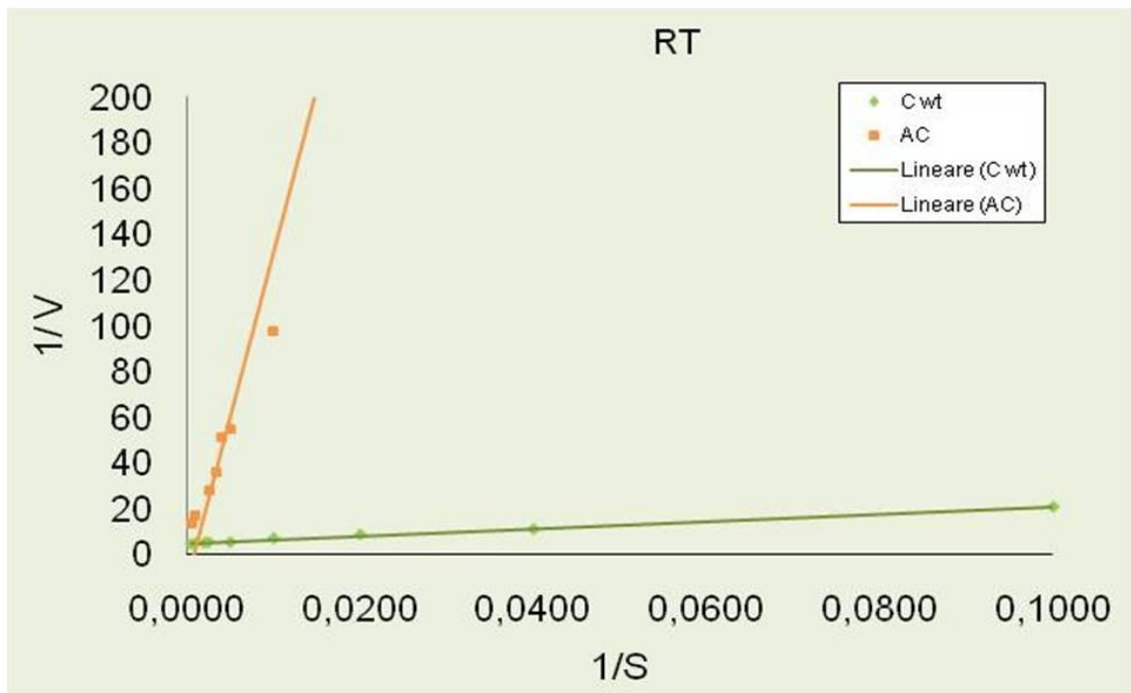
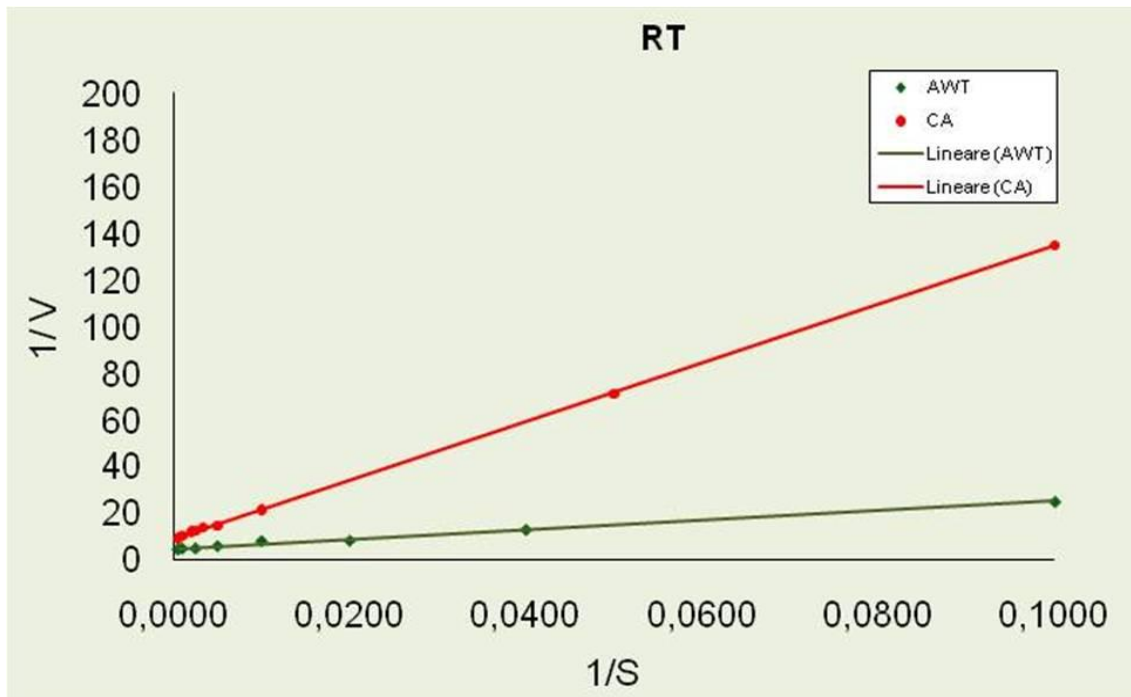


**Figure 25. Lineweaver Burk plot of kinetics from wt and recombinant aldolases glycolytic reactions toward FBP substrate.** These data were obtained at RT using FBP concentration ranging from 2 mM to 10  $\mu$ M for aldolase A wt; from 10 mM to 10  $\mu$ M for aldolase C wt; from 10 mM to 50  $\mu$ M for AC chimera; from 3 mM to 10  $\mu$ M for CA chimera. 3  $\mu$ g/ml of all enzymes were used.

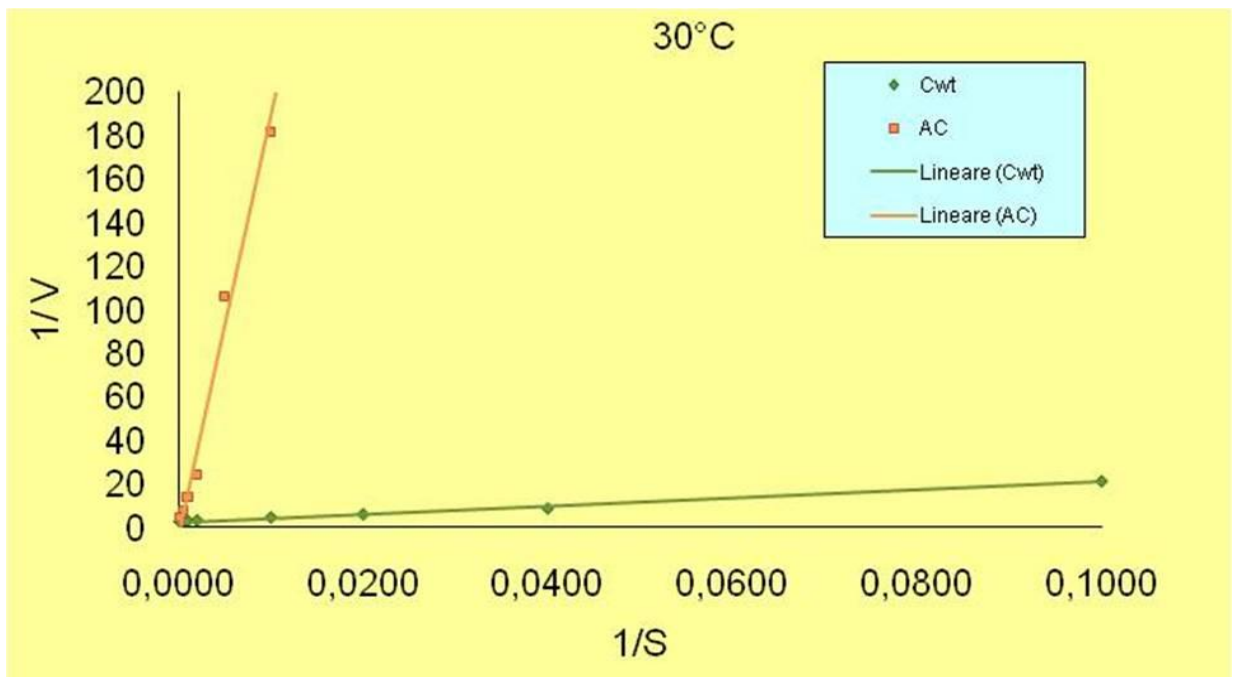
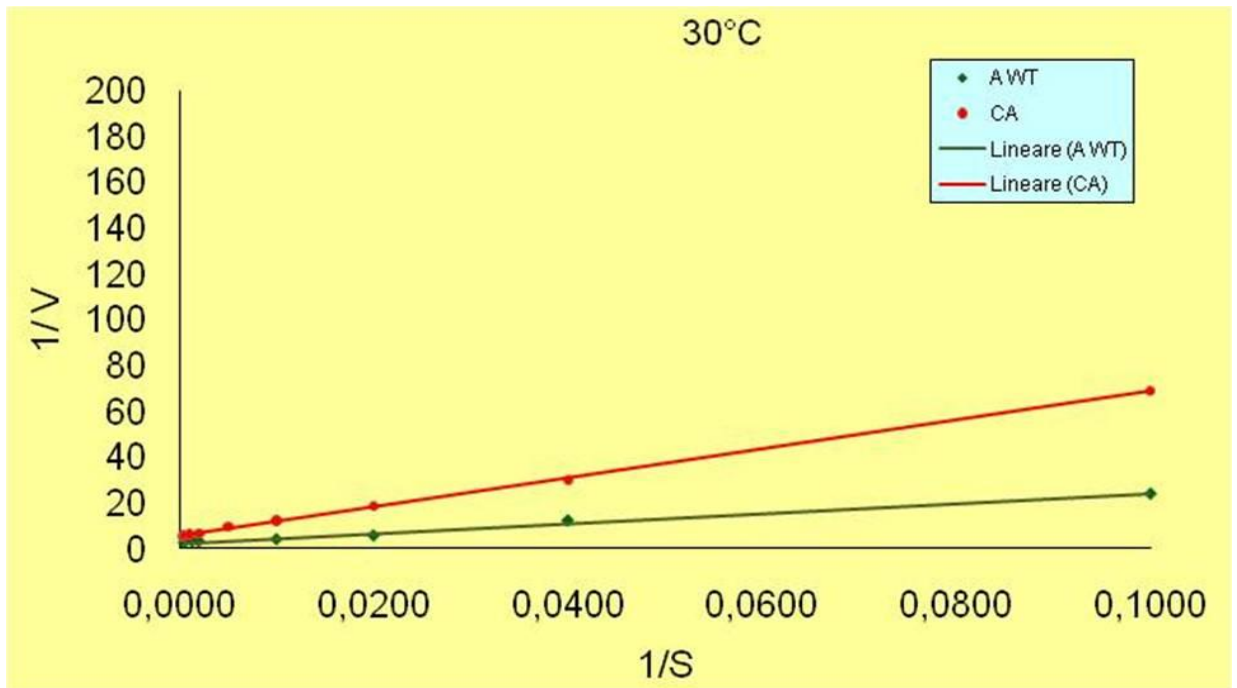


**Figure 26. Lineweaver Burk plot of kinetics from wt and recombinant aldolases glycolytic reactions toward FBP substrate.** These data were obtained at 30°C using FBP concentration ranging from 2 mM to 10  $\mu$ M for aldolase A wt; from 10 mM to 10  $\mu$ M for aldolase C wt; from 10 mM to 50  $\mu$ M for AC chimera; from 3 mM to 10  $\mu$ M for CA chimera. 3  $\mu$ g/ml of all enzymes were used.

### **3.4 Aldolase C Knockout mice**

#### **3.4.1 Screening of chimeric mice**

As previously described in Materials and Methods, all the steps from ES cells electroporation of the aldolase C knock-out construct (Fig. 27) to the production of chimeric mice were provided by EMBL from Monterotondo (Rome).

Once we got chimeric mice, we proceeded by crossing them with wt mice and we screened F1 generation for germline transmission by PCR (Fig. 28).

Primers used for the screening were designed as to amplify two fragments of different size in case of positive germline transmission (from wt and floxed alleles of heterozygous F1 mice) and one only fragment in the opposite case (from the allele of wt F1 generation). DNA from chimeric mice (previous step) was used as positive control (Fig. 28, lane 10).

Unfortunately, none of 375 pups screened, was found to be heterozygous for the floxed allele.

Recently, a new hybrid ES cell line (129 x C57bl/6), which has been shown to be very effective in generating highly chimeric animals (frequently fully ES cell-derived), has been electroporated with the same construct in order to have a higher probability to generate chimeric animals capable of germ line transmission.

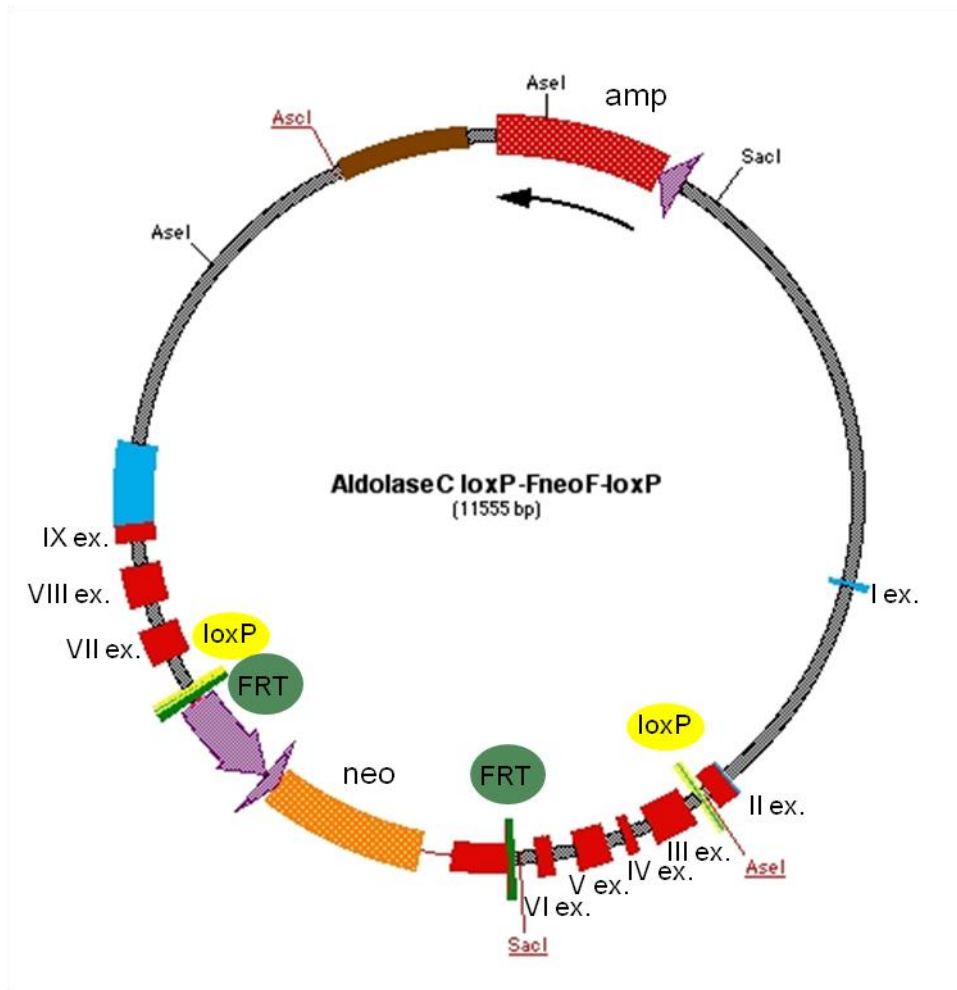


**Figure 27. Aldolase C construct for conditional knockout.**

Neo cassette is located, from 5' to 3' end, between VII and VI exons. It is flanked by FRT sequences (green bars), target of FLP recombinase. Two loxP sequences (yellow bars) are located in the II and VI introns, respectively.

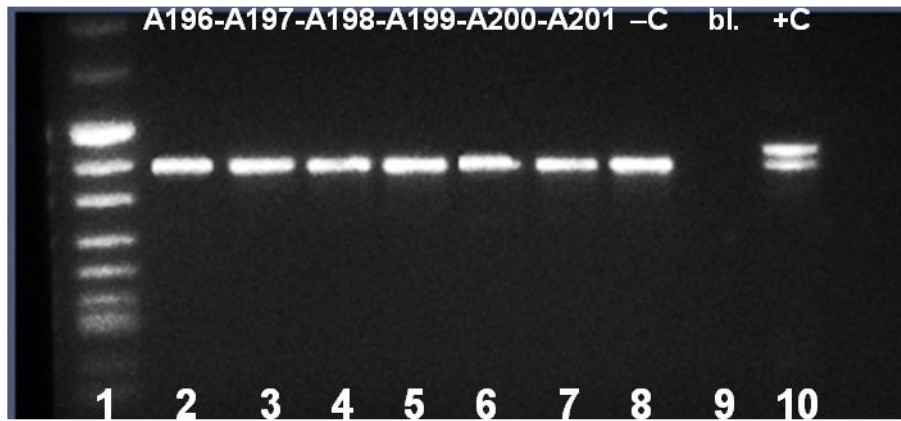


**Figure 28. Screening of F1 generation for germline transmission by PCR.**

Amplification products of genomic DNA random samples from F1 mice (lanes 2-8). All DNA singlet represent samples negative to germline transmission (lanes 2-7). The DNA doublet is the positive control (lane 10) which has been obtained by amplifying genomic DNA from chimeric mice. Size marker, negative control and blank have been loaded in lanes 1, 8 and 9, respectively.

#### 4. DISCUSSION

In the first part of my thesis, we show that human aldolase C gene transcription is positively modulated by NGF during PC12 cells neuronal differentiation. Moreover, we evidenced a new cis-acting element, element E, in the distal promoter region, which binds the transcription factor USF1 both *in vitro* and *in vivo*. Interestingly, we found that NGF regulation of human aldolase C gene is mainly mediated by USF1 binding to the distal promoter region and that phosphorylation events contribute to the activation of USF1 thus inducing its binding to DNA.

USF1 is an ubiquitous transcription factor, member of the upstream stimulatory factor (USF) family of transcription factors (98). The protein is characterized by highly conserved elements in the C terminal region like the basic region, helix-loop-helix (HLH) motif, and, in the case of the human proteins, the C-terminal leucine repeat (LR) (99-101). Amino acids 143-197 have been shown to regulate DNA-binding activity in a phosphorylation-dependent manner (100).

The promoters of many neuronal genes have been found to contain the E-box binding USF transcription factors. Among these genes we may list:

the neuron-specific K-Cl cotransporter (KCC2), which has been found to be regulated by USF1 in neuroblastoma cell lines and in cortical neurons (102);

the Machado-Joseph disease gene (MJD), involved in a neurodegenerative disorder caused by the expansion of CAG triplet repeats (103);

the GABABR1a and GABABR1b subunit gene, whose expression is also regulated by cAMP in hippocampal neurons (104);

the calcitonin/calcitonin gene-related neuropeptide gene (CGRP) (105), which has been shown to be regulated by USF1 through  $Ca^{2+}$  influx after neuronal depolarization and by NGF stimulation;

the brain-derived neurotrophic factor (BDNF), the nicotinic acetylcholine receptor 7 subunit (nAChR7), the cyclooxygenase-2 (COX-2) activity-dependent genes, whose transcriptional regulation by USF1 has been demonstrated *in vivo*, suggesting a new function for the USFs in the regulation of activity-dependent transcription in neurons of CNS (106);

the rat preprotachykinin A gene (rtPPTA), that has been shown to be responsive to NGF in dorsal root ganglion (DRG) neurons (107).

Finally, in neurons, USF proteins, together with cAMP response element binding (CREB) proteins and/or calcium-responsive transcription factors (CaRF) has been shown to activate transcription in response to Ca<sup>2+</sup>-activated signaling pathways (104, 108). Particularly, USF1/USF2 heterodimer is phosphorylated by Ca<sup>2+</sup> signaling pathways, such as extracellular signal-regulated kinase/mitogen-activated protein kinase, CaM (calmodulin) kinase IV and adenylyl cyclase/cAMP-dependent protein kinase, and involved in the transcriptional activation through mediation of cAMP-responsive element-binding protein-binding protein (CBP) (108). These findings are well correlated with what we previously evidenced regarding human aldolase C gene transcriptional regulation (44).

To complement and validate data obtained *in vitro* from the study of transcriptional regulation of human aldolase C gene, we then focused on the analysis of transgenic mice as *in vivo* model to point out the promoter regions responsible for the peculiar brain-specific and stripe-like expression of the gene.

Recently, aldolase C became the most extensively studied marker for antigenic cerebellar compartmentation (65, 66). Messenger and protein are expressed by a subset of Purkinje cells forming parasagittal stripes in cerebellar transversal AZ and PZ that are highly reproducible between individuals and across species (64, 65, 70, 71). An apparent correlation among the molecular, morphological and physiological compartments of Purkinje cells has been suggested by many authors, for example: aldolase C

immunopositive and immunonegative Purkinje cell stripes are shown to correspond to afferent and efferent projection patterns, to somatotopic maps revealed by tactile or electrical face stimulation, and to molecular layer inhibition evoked by parallel fiber stimulation (67, 109-117). The organization of parasagittal Purkinje cell stripes is thought to be an intrinsic, cell-autonomous property that is conferred when, or shortly after, these cells arise in the subventricular zone of the fourth ventricle (77, 118, 119). Correspondingly, particular subsets of parasagittally clustered Purkinje cells were shown to have the same birth date (120).

Possible involvement of cell signaling molecules, including the cell–cell recognition molecules cadherin (121) and Eph-ephrin (122) and the reelin receptors Apoer2 and Vldlr (123), in the formation of Purkinje cell clusters has been shown.

Several transcription factors have also been implicated in differential transcriptional regulation between Purkinje cell stripes (124, 125).

Particularly, Sillitoe et al. showed that Engrailed transcription factors (En1 and En2) encode positional information that is required for proper organization of the molecular properties of the cerebellum (ML molecular coding) in addition to specific anatomical divisions of the cerebellum (lobules), and that the two are patterned independently. Engrailed homeobox genes thus determine the organization of Purkinje cell sagittal stripe gene expression in the adult cerebellum (124).

Moreover, Chung et al. found the early B-cell factor 2 (EBF2) transcription factor as one of the major responsible of the aldolase C stripe-like expression pattern (125). They produced EBF2 null mice and found that aldolase C is uniformly expressed in the cerebellar PZ, while it is expressed in stripes in the heterozygote. Several P<sup>+</sup> stripe markers in the EBF2 null cerebellum show the same ectopic expression pattern as that of aldolase C. In contrast, P<sup>-</sup> stripe markers are expressed relatively normally in the PZ and AZ. They concluded that EBF2 acts not only by repressing the aldolase C-positive Purkinje cell



phenotype but also regulating the expression of all genes associated with aldolase C+ Purkinje cell phenotype. The aldolase C negative Purkinje cell subtype seems to be specified independently (125). Unfortunately, this does not explain the persistent stripe-like expression of aldolase C gene in the AZ of EBF2 null mice.

However, notwithstanding numerous studies, the complex molecular mechanism underlying Purkinje cell stripe formation remains unclear as well as the human gene promoter region governing brain- and cell-specific aldolase C expression.

We have long looked for the key of this peculiar compartment-limited, stripe-like expression pattern in the transcriptional regulation of aldolase C gene. This is the reason why we produced stabilized transgenic mice lines by using constructs containing different deleted regions of human aldolase C gene promoter fused with the transgene LacZ.

We found that the proximal promoter region (164 bp) of human aldolase C gene is responsible for low-levels, brain-specific expression of AldC/LacZ in brain and cerebellum of transgenic mice and, for the first time, we evidenced that it is also the minimal promoter region sufficient to drive the peculiar stripe-like pattern of the transgene in the Purkinje cells. The distal region, including the *cis*-element E, is responsible for high-levels of AldC/LacZ in specific areas of CNS with a stripe-like distribution in the Purkinje cells. Since the first intron and the first non-coding exon sequences of the human gene are present in the three constructs carried by all transgenic mice lines, it is also likely that these regions are involved in the regulation of the peculiar stripe-like expression pattern of aldolase C.

Moreover, we found consensus sequences specific for EBF2 transcription factor in the promoter of human aldolase C gene and of genes that have an identical expression pattern to that of aldolase C such as the sphingosine kinase (SPHK) 1a isoform (126), the GABA B receptor 2 (GABABR2) (127, 128) and phospholipase C (PLC) b3 (129). We confirmed the binding of EBF2 to the promoter of human aldolase C gene by performing Shift and

Supershift Assays (data not shown). Except for EBF specific consensus sequence, no other sequence identity was found between the promoter of aldolase C and all the genes that show the same stripe-like distribution in the cerebellum . Of course, there should be some mechanisms up to the binding of EBF2 to the promoter of aldolase C gene that support EBF2 role. We believe that one possible mechanism could be the Notch signaling pathway, a clear example of juxtacrine signalling in which two adjacent cells must make physical contact in order to communicate (130). Notch could be one of the cell-cell recognition molecules leading the formation of Purkinje cell positive and negative clusters, as has already been shown for other molecules (cadherins, eph-ephrins and reelin receptors) (121-123). Notch has a crucial role in cerebellar development and functioning. It has been found to interact directly with EBF proteins by inhibiting them, thus diminishing the capacity of EBF to bind DNA and down-regulating EBF-regulated promoters (130).

We hypothesize that the Notch-EBF2-aldolase C pathway could be implicated in the induction of the stripe-like expression not only of aldolase C, but also of all the other genes showing both an identical and complementary expression pattern, thus contributing to the compartmentalization of the cerebellum. Further studies will be conducted to investigate or validate the hypothesis we suggested.

We strongly believe that the cerebellum compartmentalization has a functional significance. For this reason we have long intended aldolase C exerting moonlight functions besides its glycolytic role. Since it is present in olives and spinal cord in the human brain we suggested it could evidence an extrapyramidal sensorial transmission pathway; it may also have a role in establishing subsets of neurons during cerebellar development (64) or during differentiation of progenitor cells in the subventricular zones of the developing brain (131).

Moreover, only recently, the association of aldolase C with a neuronal mRNA was uncovered for the first time by Canete-Soler et al. (132). Aldolase C has shown, *in vivo*, to

be the major neurofilament light (NF-L) mRNA binding protein that regulate the stability of the transcript by competing with polyA-binding protein (PABP) (133). Particularly, aldolase C dimer is a zinc-activated ribonuclease that cleaves the NF-L transcript at sites closed to the end-terminal structures and takes part to an important ribonucleoproteic complex. PABP shields the NF-L transcript from aldolase C degradation. Definitively, aldolase C and PABP act in conjunction to modulate the levels of NF-L expression *in vivo*. These findings might have important consequences for understanding causal mechanisms underlying neurodegenerative diseases such as amyotrophic lateral sclerosis (ALS) which hallmark is the NF accumulation in degenerated motor neurons (133). It is still unknown whether the aldolase C uses the same active center for both glycolysis and ribonucleolysis. The identification of the active center for the ribonucleolytic activity of aldolase C awaits further studies.

Finally, Funari et al. suggested an additive metabolic role for aldolase C in specific areas of brain and cerebellum: since certain neuronal cells perform fructose oxidation and aldolase B has never been reported to be expressed in the brain, they suggested aldolase C performing fructose metabolism, at least much better than aldolase A according to kinetic parameters (134, 135). Related to another potential role for aldolase C, Welsh et al. suggested a protective function in combination with the excitatory amino acid transporter, EAAT4, that prevents subsets of Purkinje cells from death following global brain ischemia (136). This would be consistent with an important endogenous role for fructose metabolism in cells expressing aldolase C and is consistent with the documented protective effect of dietary fructose in myocardial ischemia/reperfusion injury (136-138). Nevertheless, the presence of aldolase C in specific brain cells where it is not supported by the presence of related enzymes required for fructose metabolism (GLUT transporters, ketoexokinase, triokinase) could mean once again that aldolase C may play additional non-catalytic roles in that cells (135). Based on the peculiar expression pattern of aldolase C

and according to Staugaitis et al.(64, 131), Funari et al. also suggested aldolase C exerting a role in organizing neuronal circuits (135).

Why the human body expresses three different forms of aldolase, two of which, aldolase A and C, co-localized in some areas of CNS and with very similar glycolytic activities, is not yet understood. One of the possibilities is that evolution has allowed redundancy in favor of specificity (139, 140) and cells that express one isoform or the other, or isoform combinations, may produce complexes that bind and act differently in different cells, at different developmental or maturation stages, or in response to different intra/extracellular environmental or physiopathological stimuli (141 – 147).

To improve our knowledge on kinetic parameters of aldolase C versus aldolase A, which co-localize in some brain areas and show similar glycolytic activities and to learn more about these enzymes from a biochemical point of view, we thought to produce recombinant aldolases by swapping ISRs from aldolase A to C and viceversa. Kinetic studies with these kind of mutant enzymes, previously conducted by Tolan et al. (22, 95) regarding aldolases A and B (AB partial and total chimeras), allowed to understand which are ISRs really involved in conformational dynamics of catalytic mechanisms and hence responsible of kinetic parameters of aldolases. Our results from kinetic studies of AC and CA chimeras are still preliminary and don't allow us to draw here significative conclusions. Of course, we expected that both the chimers would act relatively to their parent enzyme. As regards AC aldolase, we found that this chimera did not work at all, being characterized by a strong decrease in affinity toward FBP substrate. Instead, CA chimera showed a good  $K_m$  value but  $k_{cat}$  was lower than we expected. Since  $k_{cat}$  values of wt aldolases, used as control, were also lower than those published in scientific literature, we need to repeat protein preparations and kinetic studies with some protocols modification in order to get better  $K_m / k_{cat}$  values and hence, more efficient catalytic reactions.

Finally, the best way to discover the hypothetical additive functions of aldolase C was, of course, the production of a knockout mouse model. The probability to get embryonic lethality led us to plan to obtain a conditional rather than conventional knockout mouse.

Based on aldolase C expression pattern in the brain, we expect to get a mouse model characterized by an impaired motor control or an ataxic gait. Moreover, according to Canete-Soler et al. (147) the absence of ribonucleolytic activity could lead to the accumulation of non-degraded NF-L transcripts and to the development of ALS.

To shed light on the redundant or different functions of co-localized aldolase A and C in the brain we also think to produce, in the near future, a knock-in mouse model in which to replace aldolase A with C gene.

## 5. REFERENCES

1. Horecker B.L., Tsolas O., Lay C.Y. (1972). Aldolases. In: *The Enzymes*. Edited by Boyer PD. 3<sup>rd</sup> Edition. Academic Press, New York. Vol. 7: pp213-258.
2. Salvatore F., Izzo P., Paoletta G. (1986). Aldolase gene and protein families: structure, expression and pathophysiology. In: *Human Genes and Diseases. Horizons in Biochemistry and Biophys.* Edited by Blasi F. John Wiley & Sons, Ltd, New York. Vol. 8: pp 611-665.
3. Izzo P., Costanzo P., Lupo A., Rippa E., Paoletta G., Salvatore F. (1988). Human aldolase A gene. Structural organization and tissue-specific expression by multiple promoters and alternate mRNA processing. *Eur. J. Biochem.* 174:569-578.
4. Tolan D.R. and Penhoet E.E. (1986). Characterization of the human aldolase B gene. *Mol. Biol. Med.* 3:245-264.
5. Cox T.M. (1994). Aldolase B and fructose intolerance. *Faseb J.* 8, 62-71
6. Rocchi M., Vitale E., Covone A., Romeo G., Santamaria R., Buono P., Paoletta G., Salvatore F. (1989). Assignment of human aldolase C gene to chromosome 17, region cen----q21.1. *Hum Genet.* 82:279-82.
7. Tolan D.R., Niclas J., Bruce B.D., Lebo R.V. (1987). Evolutionary implications of the human aldolase A, B, C and pseudogene chromosome locations. *Am. J. Hum. Genet.* 41:907-924.
8. Paoletta G., Buono P., Mancini F.P., Izzo P., Salvatore F. (1986). Structure and expression of mouse aldolase genes. *Eur. J. Biochem.* 156: 229-235.
9. Kukita A., Mukai T., Miyata T., Hori K. (1988). The structure of brain-specific rat aldolase C mRNA and the evolution of aldolase isozyme genes. *Eur. J. Biochem.* 171:471-478.
10. Penhoet E.E. and Rutter W. (1971). Catalytic and immunochemical properties of homomeric combination of aldolase subunits. *J. Biol. Chem.* 246:318-323.

11. Yao DC, Tolan DR, Murray MF, Harris DJ, Darras BT, Geva A, Neufeld EJ. (2004). Hemolytic anemia and severe rhabdomyolysis caused by compound heterozygous mutations of the gene for erythrocyte/muscle isozyme of aldolase, ALDOA (Arg303X/Cys338Tyr). *Blood*, 103 (6), 2401.
12. Esposito G, Vitagliano L, Cevenini A, Amelio T, Zagari A, Salvatore F. (2005). Unraveling the structural and functional features of an aldolase A mutant involved in the hemolytic anemia and severe rhabdomyolysis reported in a child. Unraveling the structural and functional features of an aldolase A mutant involved in the hemolytic anemia and severe rhabdomyolysis reported in a child. *Blood*. Jan 15;105(2):905.
13. Santamaria R, Esposito G, Vitagliano L, Race V, Paglionico I, Zancan L, Zagari A, Salvatore F. (2000). Functional and molecular modelling studies of two hereditary fructose intolerance-causing mutations at arginine 303 in human liver aldolase. *Biochem J.*, 350, 823.
14. Esposito G, Vitagliano L, Santamaria R, Viola A, Zagari A, Salvatore F. (2002). Structural and functional analysis of aldolase B mutants related to hereditary fructose intolerance. *FEBS Lett.*, 531, 152.
15. Esposito G, Santamaria R, Vitagliano L, Ieno L, Viola A, Fiori L, Parenti G, Zancan L, Zagari A, Salvatore F. (2004). Six novel alleles identified in Italian hereditary fructose intolerance patients enlarge the mutation spectrum of the aldolase B gene. *Hum. Mutat.*, 24, 534.
16. Willson VJ, Thompson RJ. (1980). Human brain aldolase C4 isoenzyme: purification, radioimmunoassay, and distribution in human tissues. *Ann. Clin. Biochem.*, 17, 114.
17. Skala H., Vibert M., Lamas E., Maire P., Schweighoffer F., Kahn A. (1987). Molecular cloning and expression of rat aldolase C messenger RNA during development and hepatocarcinogenesis. *Eur. J. Biochem.* 163: 513-518.

18. Izzo P., Costanzo P., Lupo A., Ripa E., Borghese A.M., Paoletta G., Salvatore F. (1987). A new human species of aldolase A mRNA from fibroblasts. *European Journal of Biochemistry*.164:9-13.
19. Rottmann, W. H., Deselms, K. R., Niclas, J., Camerato, T., Holman, P. S., Green, C. J., and Tolan, D. R. (1987). The complete amino acid sequence of the human aldolase C isozyme derived from genomic clones. *Biochimie (Paris)* 69, 137–145.
20. Rottmann, W. H., Tolan, D. R., and Penhoet, E. E. (1984). Complete amino acid sequence for human aldolase B derived from cDNA and genomic clones. *Proc. Natl. Acad. Sci. U. S. A.* 81, 2734–2742.
21. Kusakabe, T., Motoki, K., and Hori, K. (1994). Human aldolase C: characterization of the recombinant enzyme expressed in *Escherichia coli*. *J. Biochem. (Tokyo)* 115, 1172–1177.
22. Pezza, J. A., Choi, K. H., Berardini, T. Z., Beernink, P. T., Allen, K. N., and Tolan, D. R. (2003) Spatial clustering of isozyme specific residues reveals unlikely determinants of isozyme specificity in fructose 1,6-bisphosphate aldolase, *J. Biol. Chem.* 278, 17307-17313.
23. Buono P., Paoletta G., Mancini F.P., Izzo P., Salvatore F. (1988). The complete nucleotide sequence of the gene coding for the human aldolase C. *Nucleic Acids Res.* 16:4733.
24. Buono P., Mancini F.P., Izzo P., Salvatore, F. (1990). Characterization of the transcription-initiation site and of the promoter region within the 5' flanking region of the human aldolase C gene. *Eur. J.Biochem.* 192 : 805-811.
25. Atsuchi Y., Yamana K., Yatsuki H., Hori K., Ueda S., Shiokawa K. (1994). Cloning of a brain-type aldolase cDNA and changes in its mRNA level during oogenesis and early embryogenesis in *Xenopus laevis*. *Biochimica et Biophysica Acta.* 1218:153-157.



26. Kajita E., Motoaki W., Miura K., Mizumoto K., Oka T., Komuro I., Miyata T., Yatsuki H., Hori H., Shiokawa K. (2000). Isolation and characterization of *Xenopus laevis* aldolase B cDNA and expression patterns of aldolase A, B and C genes in adult tissues, oocytes and embryos of *Xenopus laevis*. *BBA*. 1493:101-118.
27. Shiocawa K., Kajita E., Hara H., Yatsuki H., Hori K. (2002). A developmental biological study of aldolase gene expression in *Xenopus laevis*. *Cell Reserch*. 12:85-96.
28. Zhang R., Yatsuki H., Kusakabe T., Iwabe N., Miyata T., Imai T., Yoshida M., Hori K. (1995). Structures of cDNAs Encoding the Muscle-Type and Non-Muscle-Type Isozymes of Lamprey Fructose Bisposphate Aldolase and the evolution of Aldolase Genes. *J. Bioch.* 117:545-553.
29. Lannoo M.J., Hawkes R. (1997). A search for primitive Purkinje cells: zebrin II expression in sea lampreys (*Petromyzon marinus*). *Neuroscience Letters*. 237:53-55.
30. Berardini T.Z., Drygas-Williams M., Callard G.V., Tolan D.R. (1997). Identification of neuronal isozyme specific residues by comparison of Goldfish aldolase C to other aldolases. *Comp. Biochem. Physiol.* 117A: 471-476.
31. Kai T., Sugimoto Y., Kusakabe T., Zhang R., Koga K., Hori, K. (1992). Gene structure and multiple mRNA species of *Drosophila melanogaster* aldolase generating three isozyme with different enzymatic properties. *J. Biochem.* 112:677-688.
32. Zhang R., Kai T., Sugimoto Y., Kusakabe T., Takasaki Y., Koga K., Hori K. (1995). *Drosophila megalonaster* aldolase: characterization of the isozymes generated from a single gene. *J. Biochem.* 118:183-188.
33. Brenner, S. (1974) The genetics of *C. elegans*. *Genetics* 77: 71-94
34. Wood, W. B. (1988) The Nematode *Caenorhabditis elegans*, Cold Spring Harbor Laboratory, New York.

35. The Nematode *Caenorhabditis elegans* II (edited by Don Riddle, Tom Blumenthal, Barbara Meyer and Jim Priess), Cold Spring Harbor Laboratory (Jan 1997).
36. [www.wormbase.org](http://www.wormbase.org)
37. Inoue T., Yatsuki H., Kusakabe T., Joh K., Takasaki Y., Nikoh N., Miyata T., Hori K. (1997). *Caenorhabditis elegans* has two isozymic forms, CE-1 and CE-2, of fructose- 1,6-bisphosphate aldolase which are encoded by different genes. Archives of Biochemistry and Biophysics. 339:226-234.
38. [www.ebi.ac.uk](http://www.ebi.ac.uk)
39. Vibert M., Henry J., Kahn A., Skala H. (1989). The brain-specific gene for rat aldolase C possesses an unusual housekeeping-type promoter. Eur. J. Biochem. 181:33-39.
40. Buono P., de Conciliis L., Olivetta E., Izzo P., Salvatore, F. (1993). Cis-acting elements in the promoter region of the human aldolase C gene. FEBS Lett. 328:243-249.
41. Thomas M., Makeh I., Briand P., Kahn A., Skala H. (1993). Determinants of the brain-specific expression of the rat aldolase C gene: ex vivo and *in vivo* analysis. Eur. J. Biochem. 218:143-151.
42. Cibelli G., Schoch S., Pajunk H., Brand I.A., Thiel G. (1996). A (G+C)-rich motif in the aldolase C promoter functions as a constitutive transcriptional enhancer element. Eur. J. Biochem. 237:311-317.
43. Buono P., de Conciliis L., Izzo P., Salvatore F. (1997). The transcription of the human aldolase fructose-bisphosphate aldolase gene is activated by nerve-growth-factor-induced B factor in human neuroblastoma. Biochem. J. 323:245-250.
44. Buono P., Cassano S., Alfieri A., Mancini A., Salvatore F. (2002). Human aldolase C gene expression is regulated by adenosine 3',5'-cyclic monophosphate (cAMP) in PC12 cells. Gene. 291:115-121.

45. Thomas M., Skala H., Khan A., Tuy F. (1995). Functional dissection of the brain-specific rat aldolase C gene promoter in transgenic mice. *J.Biol.Chem.* 270:20316-20321.
46. Phan Dinh Tuy F., Porteu A., Kahn A., Skala H. (2001). Bidirectional activity and orientation-dependent specificity of the rat aldolase C promoter in transgenic mice. *FEBS.* 499:143-146.
47. Makeh I., Thomas M., Hardelin J.P., Briand P., Khan A., Skala, H. (1994). Analysis of a brain-specific isozyme. *J.Biol.Chem.* 269:4194-4220.
48. Skala H., Porteu A., Thomas M., Szajnert M.F., Okazawa H., Khan A., Tuy, F. (1998). Upstream elements involved *in vivo* in activation of the brain-specific rat aldolase C gene. *J.Biol.Chem.* 273:31806-31814.
49. Buono, P., Barbieri, O., Alfieri, A., Rosica, A., Astigiano, S., Mancini, A. Fattoruso, O., Salvatore, F. Diverse human aldolase C promoter regions are required to direct *LacZ* expression in hippocampus and Purkinje cells of transgenic mice. *FEBS Letters* 578 (2004) 337-334.
50. Buono P., Alfieri A. and Salvatore F. The human aldolase C gene: Transcriptional regulation and expression in the mammalian central nervous system. (2008). *Recent Res. Devel. Biochem.*, 8: ISBN: 978-81-308-0215-2.
51. Skala-Rubinson H., Vinh J., Labas V., Kahn A. and Tuy F.P.D. (2002). Novel target sequences for Pax-6 in the brain-specific activating regions of the rat aldolase C gene. *J. Biol. Chem.*, 277, 47190-47196.
52. Maruyama K., Tsukada T., Ohkura N., Bandoh S., Hosono T., Yamaguchi K. (1998). The NGFI-B subfamily of the nuclear receptor superfamily (review). *International journal of Oncology.* 12:1237-1243.
53. Watson M.A., Milbrandt J. (1990). Expression of the nerve growth factor-regulated NGFI-A and NGFI-B genes in the developing rat. *Development* 110:173-183.

54. Wilson T.E., Mouw A.R., Weaver C.A., Milbrandt J., Parker K.L. (1993). The orphan nuclear receptor NGFI-B regulates expression of the gene encoding steroid 21-hydroxylase. *Mol.Cell.Biol.* 13:816-868.
55. Chin LS, Li L, Greengard P. (1994). Neuron-specific expression of the synapsin II gene is directed by a specific core promoter and upstream regulatory elements. *J Biol Chem.*, 269, 18507.
56. Minowa MT, Minowa T, Mouradian MM. (1993). Activator region analysis of the human D1A dopamine receptor gene. *J Biol Chem.*, 268, 23544.
57. Brown AM, Lemke G. (1997). Multiple regulatory elements control transcription of the peripheral myelin protein zero gene. *J Biol Chem.*, 272, 28939.
58. Lawson MA, Whyte DB, Mellon PL. (1996). GATA factors are essential for activity of the neuron-specific enhancer of the gonadotropin-releasing hormone gene. *Mol Cell Biol.*, 16, 3596.
59. Arai Y., Kajihara S., Masuda J., Ohishi S., Zen K., Ogata J., Mukai T. (1994). Position-independent, high-level, and correct regional expression of the rat aldolase C gene in the central nervous system of transgenic mice. *Eur. J. Biochem.* 221:253-260.
60. Walther E.U., Dichgans M., Maricich S.M., Romito R.R., Yang F., Dziennis S., Zackson S., Hawkes R., Herrup K. (1998). Genomic sequences of aldolase C (Zebrin II) direct lacZ expression exclusively in non-neuronal cells of transgenic mice. *Proc. Natl. Acad. Sci. USA.* 95:2615-2620.
61. Romito-Di Giacomo RR, Walther EU, Williams EA, Herrup K. (2005). Purkinje cell expression of the mouse aldolase C gene in transgenic mice is directed by an upstream regulatory element. *Mol Brain Res.*, 133, 47.
62. Popovici T., Berwald-Netter Y., Vibert M., Kahn A., Skala H. (1990). Localization of aldolase C mRNA in brain cells. *FEBS Letters.* 268:189-193.

63. Mukai T., Yatsuki H., Masuko S., Arai Y., Joh K., Hori, K. (1991). The structure of the brain-specific rat aldolase C gene and its regional expression. *Biochemical and Biophysical Research Communications* 174: 1035-1042.
64. Anh A.H., Dziennis S., Hawkes R., Herrup K. (1994). The cloning of zebrin II reveals its identity with aldolase C. *Development* 120:2081-2090.
65. Brochu G, Maler L, Hawkes R. (1990). Zebrin II: a polypeptide antigen expressed selectively by Purkinje cells reveals compartments in rat and fish cerebellum. *J Comp Neurol* 291:538–552.
66. Hawkes R, Brochu G, Doré L, Gravel C, Leclerc N. (1992). Zebrins: molecular markers of compartmentation in the cerebellum. In: *The cerebellum revisited* (Llinás R, Sotelo C, eds), pp 22–55. New York: Springer-Verlag.
67. Hawkes R. (1997). An anatomical model of cerebellar modules. *Prog Brain Res* 114:39–52.
68. Hawkes R, Eisenman LM. (1997). Stripes and zones: the origins of regionalization of the adult cerebellum. *Perspect Dev Neurobiol* 5:95–104.
69. Herrup K, Kuemerle B. (1997). The compartmentalization of the cerebellum. *Annu Rev Neurosci* 20:61–90.
70. Oberdick J, Baader SL, Schilling K. (1998). From zebra stripes to postal zones: deciphering patterns of gene expression in the cerebellum. *Trends Neurosci* 21:383–390.
71. Armstrong C, Hawkes R. (2000). Pattern formation in the cerebellar cortex. *Biochem Cell Biol* 78:551–562.
72. Akintunde A, Eisenman LM. (1994). External cuneocerebellar projections and Purkinje cell zebrin II bands: a direct comparison of parasagittal banding in the mouse cerebellum. *J Chem Neuroanat* 7:75–86.

73. Ji Z, Hawkes R. (1994). Topography of Purkinje cell compartments and mossy fiber terminal fields in lobules II and III of the rat cerebellar cortex: spinocerebellar and cuneocerebellar projections. *Neuroscience* 61:935–954.
74. Ozol K, Hayden JM, Oberdick J, Hawkes R. (1999). Horizontal zones in the vermis of the mouse cerebellum. *J Comp Neurol* 412: 95–111.
75. Sillitoe RV, Hawkes R. (2002). Whole-mount immunohistochemistry: a high-throughput screen for patterning defects in the mouse cerebellum. *J Histochem Cytochem* 50: 235–244.
76. Apps R., Hawkes R. (2009). Cerebellar cortical organization: a one-map hypothesis. *Nature Reviews Neuroscience* 10: 670-681.
77. Leclerc N., Gravel C., Hawkes R. (1988). Development of parasagittal zonation in the rat cerebellar cortex: MabQ113 antigenic bands are created postnatally by the suppression of antigen expression in a subset of the Purkinje cells. *J. Comp. Neurol.* 273:399-420.
78. Tano D, Napieralski JA, Eisenman LM, Messer A, Plummer J, Hawkes R. (1992). Novel developmental boundary in the cerebellum revealed by zebrin expression in the *lurcher* (*Lc/\_*) mutant mouse. *J Comp Neurol* 323:128–136.
79. Sillitoe RV., Gopal N., Joyner AL. (2009). Embryonic origins of ZebrinII parasagittal stripes and establishment of topographic Purkinje cell projections. *Neuroscience*. 162 (3): 574-88.
80. Hawkes R., Herrup K. (1995). Aldolase C/zebrin II and the regionalization of the cerebellum. *Journal of Molecular Neuroscience*. 6: 147-158.
81. Buono P., D'Armiento F.P., Terzi G., Alfieri A., Salvatore F. (2002). Differential distribution of aldolase A and C in the human central nervous system. *J. Neurocytology*, 30, 957-965.

82. Gorman, C.M., Moffat, L., F. and Howard B.H. (1982). Recombinant genomes which express chloramphenicol acetyltransferase in mammalian cells. *Mol. Cell. Biol.* 2, 1044-1051.
83. De Wet. J.R., Wood, K.V. De Luca, M., Helinski. D.R and Subramani. S. (1987). Firefly luciferase gene: structure and expression in mammalian cells. *MolCell.* Vol. 7, 725-737.
84. Dignam, J.D., Lebowitz, R.M. and Roeder, R.G. (1983). Accurate transcription initiation by RNA polymerase II in a soluble extract from isolated mammalian nuclei. *Nucl. Acids Res.* 11, 1475-1489.
85. Weinmann, A.S. and P.J. Farnham. (2002). Identification of unknown target genes of human transcription factors using chromatin immunoprecipitation. *Methods* 26: 37-47.
86. Hogan, B., Beddington, R., Costantini, F. and Lacy, E. (1994). *Manipulating the Mouse Embryo: A Laboratory Manual*, Cold Spring Harbor Laboratory Press, Cold Spring Harbor, New York.
87. Altman, J. and Bayer, S.A. (1994). *Atlas of Prenatal Rat Brain Development*, CRC Press, USA, pp. 1-736.
88. Smeyne, R.J., Oberdick, J., Schilling, K., Berrebi, A.S., Mugnaini, E. and Morgan, J.I. (1991). Dynamic organization of developing Purkinje cells revealed by transgene expression. *Science* 254, 719-721.
89. Oberdick, J., Schilling, K., Smeyne, R.J., Corbin, J.G., Bocchiaro, C. and Morgan, J.I. (1993). A promoter that drives transgene expression in cerebellar Purkinje and retinal bipolar neurons. *Neuron* 10, 1007-1018.
90. Liss B. (2002) Improved Quantitative real-time RT-PCR for expression profiling of individual cells. *Nucleic Acids Res.* Sep 1;30 (17):e89.

91. Livak K. J. and Schmittgen T.D. (2001). Analysis of Relative Gene Expression Data using RealTime Quantitative PCR and the  $2^{-\Delta\Delta CT}$  Method. *Methods* 25, 402-408.
92. Beernink, P. T., and Tolan, D. R. (1992). Construction of a high-copy "ATG vector" for expression in *Escherichia coli*. *Prot. Expr. Purif.* 3, 332–336.
93. Morris, A. J., and Tolan, D. R. (1993) Site-directed mutagenesis identifies aspartate 33 as a previously unidentified critical residue in the catalytic mechanism of rabbit aldolase A, *J. Biol. Chem.* 268, 1095-1100.
94. Racker, E. (1947). Spectrophotometric measurement of hexokinase and phosphohexokinase activity, *J. Biol. Chem.* 167, 843-854.
95. Pezza, J., Stopa, J., Brunyak, E.M., Allen K. and Tolan D.R. (2007). Thermodynamic Analysis Shows Conformational Coupling and Dynamics Confer Substrate Specificity in Fructose-1,6-bisphosphate Aldolase. *Biochemistry* 46, 13010-13018.
96. Hedstrom, L., Szilagyi, L., and Rutter, W. J. (1992). Converting trypsin to chymotrypsin: the role of surface loops. *Science* 255, 1249–1253.
97. Holland, L. Z., McFall-Ngai, M., and Somero, G. N. (1997). Evolution of lactate dehydrogenase-A homologs of barracuda fishes (genus *Sphyræna*) from different thermal environments: differences in kinetic properties and thermal stability are due to amino acid substitutions outside the active site. *Biochemistry* 36, 3207–3215.
98. Sawadogo M. (1988). Multiple forms of human gene-specific transcription factor USF. *The Journal of Biological Chemistry* 263, 11994-12001.
99. Ferré-D'Amaré AR, Pognonec P, Roeder RG, Burley SK. (1994). Structure and function of the b/HLH/Z domain of USF. *EMBO J.* Jan 1;13(1):180-9.
100. Cheung E., Mayr P., Coda-Zabetta F., Woodman P.G., Boam D.S.W. (1999) DNA-binding activity of the transcription factor upstream stimulatory factor 1 (USF-1) is regulated by cyclin- dependent phosphorylation. *Biochem. J.* 344, 145-15



- 101.** Crusselle-Davis V.J., Vieira K.F., Zhou Z., Anantharaman A., and Bungert J. (2006). Antagonistic Regulation of  $\beta$ -Globin Gene Expression by Helix-Loop-Helix Proteins USF and TFII-I. *Mol. Cell. Biol.* 26(18): 6832-6843.
- 102.** Markkanen, M., Uvarov, P., and Airaksinen, M.S. (2008) Role of upstream stimulating factors in the transcriptional regulation of the neuron-specific K–Cl cotransporter KCC2. *Brain Res.* Oct 21;1236:8-15.
- 103.** Do Carmo Costa M., Gomes-da-Silva J., Miranda C. J, Sequeiros J., Santos M.M. and Maciel P. (2004) Genomic structure, promoter activity, and developmental expression of the mouse homologue of the Machado–Joseph disease (MJD) gene. *Genomics* 84 361–373.
- 104.** Steiger JL, Bandyopadhyay S, Farb DH, Russek SJ. J. (2004). cAMP response element-binding protein, activating transcription factor-4, and upstream stimulatory factor differentially control hippocampal GABABR1a and GABABR1b subunit gene expression through alternative promoters. *Neurosci.* Jul 7; 24(27):6115-26.
- 105.** Viney T.J., Schmidt T.W., Gierasch W., Sattar A.W., Yaggie R.E., Kuburas A., Quinn J.P., Coulson J.M. and Russo A.F. Regulation of the Cell-specific Calcitonin/Calcitonin Gene-related Peptide Enhancer by USF and the Foxa2 Forkhead Protein. (2004). *The Journal of Biological Chemistry*, November 26, 279, 49948-49955.
- 106.** Chen, W. G., West, A. E., Tao, X., Corfas, G., Szentirmay, M. N., Sawadogo, M., Vinson, C., and Greenberg, M. E. (2003). Upstream Stimulatory Factors are mediators of  $\text{Ca}^{2+}$ -Responsive Transcription in Neurons. *J. Neurosci.* 23, 2572–2581.
- 107.** Gerrard, L., Howard, M., Paterson, T., Thippeswamy, T., Quinn, J. P., and Haddley, K. (2005). A proximal E-box modulates NGF effects on rat PPT-A promoter activity in cultured dorsal root ganglia neurones. *Neuropeptides* 39, 475–483.

108. Tabuchi A, Sakaya H, Kisukeda T, Fushiki H, Tsuda M. (2002). Involvement of an upstream stimulatory factor as well as cAMP-responsive element-binding protein in the activation of brain-derived neurotrophic factor gene promoter I. *J Biol Chem* 277: 35920-35931.
109. Voogd J, Glickstein M. (1998). The anatomy of the cerebellum. *Trends Neurosci* 21:370–375.
110. Voogd J, Pardoe J, Ruigrok TJ, Apps R. (2003). The distribution of climbing and mossy fiber collateral branches from the copula pyramidis and the paramedian lobule: congruence of climbing fiber cortical zones and the pattern of zebrin banding within the rat cerebellum. *J Neurosci* 23:4645–4656.
111. Sugihara I, Quy PN. (2007). Identification of aldolase C compartments in the mouse cerebellar cortex by olivocerebellar labeling. *J Comp Neurol* 500:1076–1092.
112. Sugihara I, Shinoda Y. (2004). Molecular, topographic, and functional organization of the cerebellar cortex: a study with combined aldolase C and olivocerebellar labeling. *J Neurosci* 24:8771–8785.
113. Chockkan V, Hawkes R. (1994). Functional and antigenic maps in the rat cerebellum: zebrin compartmentation and vibrissal receptive fields in lobule IXa. *J Comp Neurol* 345:33–45.
114. Hallem JS, Thompson JH, Gundappa-Sulur G, Hawkes R, Bjaalie JG, Bower JM. (1999). Spatial correspondence between tactile projection patterns and the distribution of the antigenic Purkinje cell markers antizebrin I and anti-zebrin II in the cerebellar folium crus IIA of the rat. *Neuroscience* 93:1083–1094.
115. Chen G, Hanson CL, Ebner TJ. (1996). Functional parasagittal compartments in the rat cerebellar cortex: an *in vivo* optical imaging study using neutral red. *J Neurophysiol* 76:4169–4174.

116. Gao W, Chen G, Reinert KC, Ebner TJ. (2006). Cerebellar cortical molecular layer inhibition is organized in parasagittal zones. *J Neurosci* 26:8377–8387.
117. Furutama, D., Morita, N., Takano, R., Sekine, Y., Sadakata, T., Shinoda, Y., Hayashi, K., Mishima, Y., Mikoshiba, K., Hawkes, R. and Furuichi, T. (2010). Expression of the IP3R1 Promoter-Driven nls-LacZ Transgene in Purkinje Cell Parasagittal Arrays of Developing Mouse Cerebellum *Journal of Neuroscience Research* 88:2810–2825.
118. Wassef M, Sotelo C, Thomasset M, Granholm AC, Leclerc N, Raftafi J, Hawkes R. (1990). Expression of compartmentation antigen zebrin I in cerebellar transplants. *J Comp Neurol* 294:223–234.
119. Seil FJ, Johnson ML, Hawkes R. (1995). Molecular compartmentation expressed in cerebellar cultures in the absence of neuronal activity and neuron–glia interactions. *J Comp Neurol* 356:398–407.
120. Hashimoto M, Mikoshiba K. (2003). Mediolateral compartmentalization of the cerebellum is determined on the “birth date” of Purkinje cells. *J Neurosci* 23:11342–11351.
121. Arndt K, Redies D. (1998). Development of cadherin-defined parasagittal subdivisions in the embryonic chicken cerebellum. *J Comp Neurol* 401:367–381.
122. Karam SD, Burrows RC, Logan C, Koblar S, Pasquale EB, Bothwell M. (2000). Eph receptors and ephrins in the developing chicken cerebellum: relationships to sagittal patterning and granule cell migration. *J Neurosci* 20:488–6500.
123. Larouche M, Beffert U, Herz J, Hawkes R. (2008). The reelin receptors Apoer2 and Vldlr coordinate the patterning of Purkinje cell topography in the developing mouse cerebellum. *PLoS One* 3:e1653.

124. Sillitoe RV, Stephen D, Lao Z, Joyner AL. (2008). Engrailed homeobox genes determine the organization of Purkinje cell sagittal stripe gene expression in the adult cerebellum. *J Neurosci* 28:12150–12162.
125. Chung SH, Marzban H, Croci L, Consalez GG, Hawkes R. (2008). Purkinje cell subtype specification in the cerebellar cortex: EBF2 acts to repress the zebrin II-positive Purkinje cell phenotype. *Neuroscience* 153:721–732.
126. Terada N, Banno Y, Ohno N, Fujii Y, Murate T, Sarna JR, Hawkes R, Zea Z, Baba T, Ohno S (2004) Compartmentation of the mouse cerebellar cortex by sphingosine kinase. *J Comp Neurol* 469:119–127.
127. Fritschy JM, Meskenaite V, Weinmann O, Honer M, Benke D, Mohler H. (1999). GABAB-receptor splice variants GB1a and GB1b in rat brain: developmental regulation, cellular distribution and extrasynaptic location. *Eur J Neurosci* 11:761–768.
128. Chung SH, Kim CT, Hawkes R. (2007a). Compartmentation of GABAB receptor 2 in the mouse cerebellar cortex. *Cerebellum* 27:1–9.
129. Sarna JR, Marzban H, Watanabe M, Hawkes R. (2006). Complementary stripes of phospholipase C 3 and C 4 expression by Purkinje cell subsets in the mouse cerebellum. *J Comp Neurol* 496:303–313.
130. Smith EM, Akerblad P, Kadesch T, Axelson H, Sigvardsson M. (2005). Inhibition of EBF function by active Notch signaling reveals a novel regulatory pathway in early B-cell development. *Blood*. Sep 15;106(6):1995-2001.
131. Staugaitis SM, Zerlin M, Hawkes R, Levine JM, Goldman JE. (2001). Aldolase C/zebrin II expression in the neonatal rat forebrain reveals cellular heterogeneity within the subventricular zone and early astrocyte differentiation. *J Neurosci*. 21:6195–205.

132. Canete-Soler R, Shamim M, Zhai J, Lin H, Reddy KS (2003). The glycolytic enzymes aldolases A and C moonlight by binding the instability determinant of the NF-L mRNA. Paper presented at The RNA Society of North Carolina Symposium on RNA Biology V: RNA, Tool and Target, Research Triangle Park, NC, October.
133. Cañete-Soler, R., Reddy, K.S., Tolan, D.R., Zhai, J., (2005). Aldolases A and C are ribonucleolytic components of a neuronal complex that regulates the stability of the light-neurofilament mRNA. *J. Neurosci.* 25, 4353–4364.
134. Funari VA, Herrera VLM, Freeman D, Tolan DR. (2005). Genes required for fructose metabolism are expressed in purkinje cells in the cerebellum. *Molec Brain Res.* 142:115–22.
135. Funari V.A., Crandall J.E. Tolan D.R. (2007). Fructose metabolism in the cerebellum. *The Cerebellum.* 6: 130–140.
136. Welsh JP, Yuen G, Placantonakis DG, Vu TQ, Haiss F, O’Hearn E, et al. (2002). Why do Purkinje cells die so easily after global brain ischemia? Aldolase C, EAAT4, and the cerebellar contribution to posthypoxic myoclonus. *Adv Neurol.*; 89:331–59.
137. Jordan J, Simandle S, Tulbert C, Busija D, Miller A. (2003). Fructose-fed rats are protected against ischemia/reperfusion injury. *J Pharmacol Exp Ther.* 307:1007–11.
138. Joyeux-Faure M, Rossini E, Ribuoat C, Faure P. (2006). Fructose fed rat hearts are protected against ischemia-reperfusion injury. *Exp Biol Med (Maywood)*; 231:456–62.
139. Cavallaro, S., Agata, V., Manickam, P., Dufour, F., Alkon, D.L., 2002. Memory-specific temporal profiles of gene expression in the hippocampus. *Proc. Natl. Acad. Sci. U. S. A.* 99, 16279–16284.
140. Marsh, J.J., Lebherz, H.G., 1992. Fructose-bisphosphate aldolases: an evolutionary history. *Trends Biochem. Sci.* 17, 110–113.

141. Conaco, C., Otto, S., Han, J.J., Mandel, G., (2006). Reciprocal actions of REST and a microRNA promote neuronal identity. *Proc. Natl. Acad. Sci. U. S. A.* 103, 2422–2427.
142. Etcheberrigaray, E., Gibson, G.E., Alkon, D.L., (1994). Molecular mechanisms of memory and the pathophysiology of Alzheimer's disease. *Ann. N. Y. Acad. Sci.* 747, 245–255.
143. Leeds, P., Kren, B.T., Boylan, J.M., Betz, N.A., Steer, C.J., Gruppuso, P.A., Ross, J., (1997). Developmental regulation of CRD-BP, an RNA-binding protein that stabilizes c-myc mRNA *in vitro*. *Oncogene* 14, 1279–1286.
144. Liebhaber, S.A., Russell, J.E., (1998). Expression and developmental control of the human alpha-globin gene cluster. *Ann. N. Y. Acad. Sci.* 850, 54–63.
145. Stevens, A., Wang, Y., Bremer, K., Zhang, J., Hoepfner, R., Antoniou, M., Schoenberg, D.R., Maquat, L.E., (2002). Beta-Globin mRNA decay in erythroid cells: UG site-preferred endonucleolytic cleavage that is augmented by a premature termination codon. *Proc. Natl. Acad. Sci. U. S. A.* 99, 12741–12746.
146. Waggoner, S.A., Liebhaber, S.A., (2003). Regulation of alpha-globin mRNA stability. *Exp. Biol. Med. (Maywood)* 228, 387–395.
147. Stefanizzi I., Cañete-Soler R., (2007). Coregulation of light neurofilament mRNA by poly(A)-binding protein and aldolase C: Implications for neurodegeneration. *Brain Research.* 1139: 15–28.